TAMPEREEN TEKNILLINEN YLIOPISTO
TAMPERE UNIVERSITY OF TECHNOLOGY

MIKAEL VIRTA

# THE CAPABILITIES OF THE FUSED DEPOSITION MODELING MACHINE ULTIMAKER AND ITS ADJUSTING FOR THE BIO-MEDICAL RESEARCH PURPOSES

Master of Science Thesis

Examiner: Professor Minna Kellomäki
Examiner and topic approved in the
Faculty of Engineering Sciences
Council meeting on 4th of December
2013

# TIIVISTELMÄ

TAMPEREEN TEKNILLINEN YLIOPISTO
Materiaalitekniikan koulutusohjelma
**VIRTA, MIKAEL**: The capabilities of the fused deposition modeling machine Ultimaker and its adjusting for the biomedical research purposes
Diplomityö, 74 sivua, 26 liitesivua
Toukokuu 2014
Pääaine: Biomateriaalitekniikka
Tarkastaja: Professori Minna Kellomäki
Avainsanat: Materiaalia lisäävä valmistus, fused deposition modeling, Ultimaker

Ultimaker 3D-tulostin hyödyntää ekstruusioon perustuvaa materiaalia lisäävän valmistuksen tekniikkaa (fused depositon modeling, FDM). Tulostin kykenee muuttamaan tietokoneavusteisen suunnittelun (CAD) avulla luodun mallin fyysiseksi kappaleeksi automaattisesti kerros kerrokselta.

Diplomityön ensimmäisenä tavoitteena oli säätää ja kalibroida Ultimaker 3D-tulostin, jotta tulostettujen kappaleiden laatua saatiin parannettua. Tulostimeen asennettiin useita uusia osia, joista osa tulostettiin tulostimen avulla. Toisena tavoitteena oli arvioida, kuinka tulostusparametrit vaikuttavat tulostettujen kappaleiden ominaisuuksiin, sekä voidaanko tulostinta käyttää biolääketieteellisen tutkimuksen tarkoituksiin. Useita erilaisia näytteitä tulostettiin eri polymeerimateriaaleista karakterisointia varten. Näytteiden mekaaniset ominaisuudet määritettiin vetolujuustestillä. Muutokset materiaalien lämpöhistoriassa tutkittiin differentiaalipyyhkäisykalorimetrilla (DSC). Prosessoinnista johtuvaa materiaalin hajoamista tutkittiin määrittämällä materiaalin sisäinen viskositeetti (IV). Mittatarkkuus ja -pysyvyys määritettiin röntgenmikrotomografian (MicroCT) ja menetelmään liittyvien mittausten avulla. Myös silmämääräistä tarkastelua hyödynnettiin.

Tulostettujen kappaleiden laatu parani tulostimeen tehtyjen toimenpiteiden johdosta. Tulostuslämpötilan, suuttimen koon ja virtausnopeuden kasvattaminen yhdistettynä tulostusnopeuden laskemiseen kasvatti kappaleiden vetolujuutta. Tulostuksen aikana materiaaleissa tapahtui vähäistä hajoamista, joka alensi niiden sisäistä viskositeettiä. Kappaleet myös kutistuivat hieman verrattuna alkuperäisiin mittoihin. Kutistumalla oli negatiivinen poikkeama x- ja y-suunnassa, sekä positiivinen poikkeama z-suunnassa.

Yhteenvetona voidaan todeta, että tulostettaessa kappaleita kyseisellä tekniikalla on tärkeää valita optimaaliset asetukset ja parametrit kappaleelta vaadittujen ominaisuuksien perusteella. On kuitenkin huomioitava, että pyrkimys ainoastaan optimaalisiin materiaaliominaisuuksiin ei takaa, että lopullinen kappale olisi ulkoisesti hyväksyttävä ja soveltuva lopulliseen käyttötarkoitukseen. Kun otetaan huomioon tulostettujen kappaleiden mittatarkkuus ja -pysyvyys sekä tulostimen kyky valmistaa monimutkaisia geometrioita ja erittäin tarkkoja rakenteita, Ultimaker 3D-tulostin on potentiaalinen ehdokas biolääketieteellisen tutkimuksen tarkoituksiin. Lisäksi tulostimella voidaan tulostaa useita eri polymeerimateriaaleja.

# ABSTRACT

TAMPERE UNIVERSITY OF TECHNOLOGY
Master's Degree Programme in Materials Science and Engineering
**VIRTA, MIKAEL**: The capabilities of the fused deposition modeling machine Ultimaker and its adjusting for the biomedical research purposes
Master of Science Thesis, 74 pages, 26 appendix pages
May of 2014
Major: Biomaterials
Examiner: Professor Minna Kellomäki
Keywords: Additive manufacturing, fused deposition modeling, Ultimaker

The Ultimaker 3D printer utilizes the extrusion-based technique called fused deposition modeling (FDM), which is one of the additive manufacturing (AM) technologies. The printer is capable of translating a computer-aided design (CAD) model into a physical part automatically by using an additive approach.

The first objective of this thesis was to adjust and calibrate the Ultimaker 3D printer in order to enhance the quality of the printed parts. Several upgrade parts were installed in the printer, of which some were printed with the printer. The second objective was to evaluate how printing parameters affect the properties of the parts fabricated with the Ultimaker 3D printer and whether the printer can be applied for biomedical research purposes. Several different kinds of samples of different polymer materials were printed and characterized. The mechanical properties were determined by tensile testing. Changes in material thermal history were investigated by differential scanning calorimetry (DSC) analysis. Degradation due to processing was studied by inherent viscosity (IV) measurements. The dimensional accuracy and stability were investigated by x-ray microtomography (MicroCT) imaging and related measurements. Also visual inspection was exploited.

The quality of the printed parts enhanced due to improvements made to the printer. An increase in the printing temperature, nozzle size and flow rate combined with a decrease in printing speed increase the tensile strengths of the parts. Minor degradation took place during printing, decreasing the inherent viscosities of the materials. Printing also resulted in the minor shrinkage of the parts, having a negative deviation along x- and y-direction and a positive deviation along z-direction.

In conclusion, when fabricating parts by using the FDM technique, it is important to select the optimal settings and parameters according to the required properties of the part. However, obtaining only the optimal material properties does not ensure that the final part would be externally acceptable and suitable for the final application. When regarding the dimensional accuracy and stability of the printed parts as well as the ability of the printer to fabricate complex geometries and very fine structures, the Ultimaker 3D printer has potential to be utilized for biomedical research purposes. In addition, the printer can be adjusted to work with several different polymer materials.

# PREFACE

This thesis was made at the Tampere University of Technology (TUT), in the departments of Biomedical Engineering and Electronics and Communications Engineering.

I would like to thank my supervisor and examiner, professor Minna Kellomäki for offering me an interesting topic for my thesis. I would like to express my sincere gratitude to Tomas Cervinka and Ville Ellä. Without them, I would have not succeeded with my thesis. In addition, I am grateful to Pasi Kauppinen, with whom I had many fruitful conversations regarding my topic. I also owe my gratitude to Suvi Heinämäki for being very sweet and helpful every time I asked for help, and Raimo Peurakoski for helping me with the machinery issues.

Finally, I would like to thank my lovely spouse from my heart for encouraging me during the thesis project and my parents who have always supported and believed in me during my life.

Tampere, 14th of May, 2014

_____

Mikael Virta

# TABLE OF CONTENTS

## ABBREVIATIONS

| | |
|---|---|
| 2D | Two-dimensional |
| 3D | Three-dimensional |
| 3DP | Three-dimensional printing |
| AM | Additive manufacturing |
| AMF | Additive manufacturing file |
| ASTM | American society for testing and materials |
| BD | Beam deposition |
| CAD | Computer-aided design |
| $CO_2$ | Carbon dioxide |
| CS | Continuous stream |
| CT | Computed tomography |
| CVD | Chemical vapor deposition |
| DMD | Digital micromirror device |
| DOD | Drop-on-demand |
| DRM | Digital rights management |
| DW | Direct write |
| FDM | Fused deposition modeling |
| GB | Gigabyte |
| IR | Infrared |
| ISO | International organization for standardization |
| LCD | Liquid crystal display |
| LOM | Laminated object manufacturing |
| LPS | Liquid phase sintering |
| MPSL | Mask projection stereolithography |
| MRI | Magnetic resonance imaging |
| PBF | Powder bed fusion |
| PCB | Printed circuit board |
| PEEK | Polyether ether ketone |
| PLA | Polylactide |
| SD | Secure digital |
| SL | Stereolithography |
| SLS | Selective laser sintering |
| STL | Stereolithography file format |
| USB | Universal series bus |
| UV | Ultraviolet |

# 1 INTRODUCTION

Additive manufacturing (AM) includes all technologies that are capable of translating a computer-aided design (CAD) model into a physical part automatically by using an additive approach. A model is divided into horizontal layers of finite thicknesses and then combined together layer by layer with an AM machine in order to form a physical part. (Gibson et al. 2010, p. 1-2; Guo & Leu 2013, p. 215; Yan & Gu 1996, p. 307)

AM has several unique capabilities. Parts with almost any shapes can be produced due to a layer by layer approach (Gibson et al. 2010, p. 290; Guo & Leu 2013, p. 236). Designing and fabricating parts with different kinds of structures from nano- and microstructures to macrostructures is possible (Gibson et al. 2010, p. 291; Guo & Leu 2013, p. 223). In addition to individual part fabrication, also functional devices can be produced with AM (Gibson et al. 2010, p. 292; Upcraft & Fletcher 2003, p. 319). Material compositions of parts can be changed during fabrication, resulting in heterogeneous parts (Gibson et al. 2010, p. 295; Guo & Leu 2013, p. 223). Because of these unique capabilities, AM can be exploited in several ways also in the medical field, where complex customized solutions are required. With medical imaging machines, it is possible to build patient-specific models from both bone and soft tissue images and then fabricate precise and accurately fitting prosthetics devices and implants with a suitable AM machine. (Gibson et al. 2010, p. 388; Guo & Leu 2013, p. 231; Hutmacher et al. 2004, p. 354; Landers et al. 2002, p. 3108; Winder & Bibb 2005, p. 1006)

AM technologies include photopolymerization, powder bed fusion, printing, sheet lamination, beam deposition, direct write, and extrusion-based technologies. Depending on the technology, polymers, ceramics, metals and composites can be utilized for part fabrication. (Gibson et al. 2010, p. 32) In this thesis, the research was conducted by using the Ultimaker 3D printer, which utilizes the extrusion-based technique called fused deposition modeling (FDM). Ultimaker has won three prizes of being the most accurate, the fastest and the best open source hardware. As being the open source printer, experimenting possibilities are almost limitless. In addition, the printer can be adjusted to work with several different polymers. (Ultimaker Original [WWW]; Ultimaker specs and features [WWW])

In FDM, the polymer filament is fed into the extrusion head by the feeding mechanism including a gear and a wheel, which generates necessary pressure for the extrusion. During the extrusion, the polymer filament is extruded out from the nozzle in a semi-solid state. After the extrusion, material fuses with preceding material that has already been extruded and quickly solidifies in order to remain its shape. After the layer is completed, the build platform moves vertically downwards by one layer thickness

before the next layer is extruded. During the part fabrication, the extrusion head moves horizontally. (Gibson et al. 2010, p. 143, 157; Korpela et al. 2013, p. 1; Peltola et al. 2008, p. 13-14)

The first objective of this thesis was to adjust and calibrate the Ultimaker 3D printer in order to enhance the quality of the printed parts. Several upgrade parts were either printed or purchased and installed in the printer. The second objective was to evaluate how printing parameters affect the properties of the parts fabricated with the Ultimaker 3D printer and whether the printer can be applied for biomedical research purposes. Several different kinds of samples of different polymer materials were printed and characterized by mechanical, thermal and microscopical analysis. In addition, the device folder for the Ultimaker 3D printer was composed.

# THEORETICAL PART

# 2 ADDITIVE MANUFACTURING

In this chapter, a term additive manufacturing is explained as well as process steps of part fabrication when using additive manufacturing. Also the unique capabilities of additive manufacturing are discussed, including the capabilities for biomedical purposes. After that, all different additive manufacturing systems are reviewed, focusing more detailed on the extrusion based technique called fused deposition modeling due to its importance to this thesis.

## 2.1 Basics of additive manufacturing

Additive manufacturing (AM) is a standardized term approved by the International Organization for Standardization (ISO) and the American Society for Testing and Materials (ASTM) (What is Additive Manufacturing? [WWW]). By definition, AM includes all the technologies that are capable of translating a virtual solid model into a physical part automatically by using an additive approach (Gibson et al. 2010, p. 1; Guo & Leu 2013, p. 215). A virtual model is divided into a series of two-dimensional (2D) cross-sections of finite thicknesses. An AM machine combines these cross-sections together layer by layer in order to form a three-dimensional (3D) physical part. These basic principles apply to all AM machines. (Gibson et al. 2010, p. 2; Yan & Gu 1996, p. 307) Differences between the technologies derive from creating layers, bonding them together and what kind of materials can be utilized. These differences determine the accuracy of the final part and its mechanical and material properties. (Gibson et al. 2010, p. 2)

Conventional manufacturing usually requires a thorough and detailed analysis of the part geometry, required tools and processes as well as additional procedures in order to fabricate the part. In contrast, an AM machine is able to completely reproduce a geometry of a virtual model without having to adjust any manufacturing processes. Using AM requires only some basic dimensional details of the produced part and knowledge about the materials that are used. AM machines are the most valuable in situations where the geometry of the produced part is very complex. (Gibson et al. 2010, p. 2; Guo & Leu 2013, p. 215; Peltola et al. 2008, p. 5)

A virtual model is data from computer-aided design (CAD) information. This information is converted to the STL file format. The name of the format is derived from the oldest AM technology called stereolithography. The STL file format is known to be as the golden standard of the AM industry. After the STL file is created, additional software can be used for further modifying the file. Then the file is sliced into a series of cross-sectional layers. The slices are sent to the AM machine for the production of the final physical part. These slices are said to be in the x- and y-plane and the part is built

in the z-direction. The final physical part is however just an approximation of the virtual model since each layer has finite thickness. The thinner the layer thickness the closer the final part will be to the model (Figure 2.1). (Gibson et al. 2010, p. 2; Yan & Gu 1996, p. 312-313; What is Additive Manufacturing? [WWW])

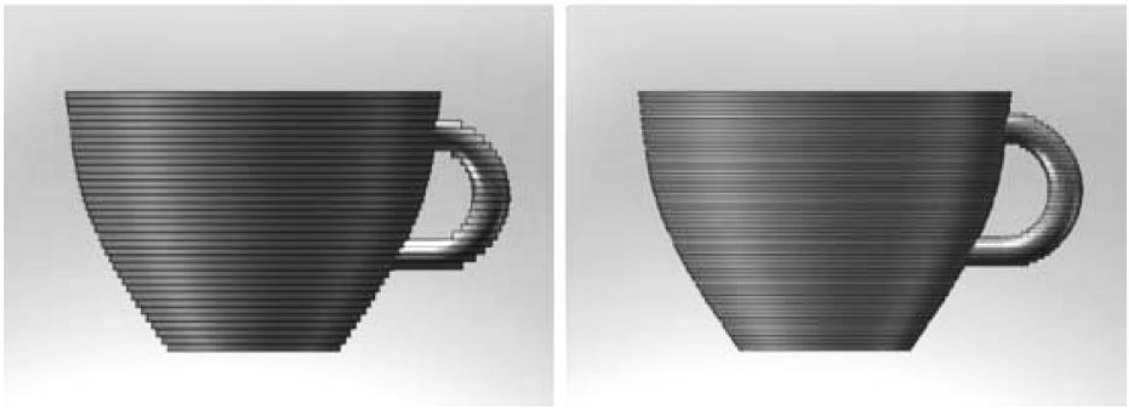

***Figure 2.1.*** *Two different layer thicknesses. The layer thickness is thinner on the right-hand resulting in the smoother surface.* (Gibson et al. 2010, p. 2)

The purpose of AM is to produce accurate 3D parts with complex geometries and very fine structures in a relatively short period of time and a little need for manual intervention. Originally, the purpose of AM was to manufacture prototypes rapidly and cost-effectively in order to check the functionality of an assembly and to inspect possible manufacturing issues. Hence, product development costs caused by design errors could be minimized. Nowadays, AM technologies have developed to the extent that manufacturers are using AM machines also to fabricate end-use products, such as dental restorations and medical implants. It is claimed that AM may cut new product costs by 70% and time to market by 90%. There is also a possibility of mass customization, where an end-product can be manufactured according to the needs of an individual consumer. This may be very beneficial especially in the medical field, where patient-specific products are required. (Gibson et al. 2010, p. 3; Pham & Gault 1998, p. 1257-1258; Yan & Gu 1996, p. 307; What is Additive Manufacturing? [WWW])

## 2.2 Additive manufacturing process steps

Fabricating parts with AM contains several steps from a virtual CAD model to a final physical part. Steps required depend on an AM technology being used and what kind of parts are fabricated. The AM process contains part modeling, STL file manipulation and machine setup, part building and post-processing. These steps are explained next.

### 2.2.1 Step 1: Modeling of the part

The first and the most important step, like in any product development process, is designing the part. When AM is used, the part must be designed in a way that the AM ma-

chine is able to fabricate it. The virtual model of the part is created with the CAD modeling software. The model must completely describe the external geometry of the part. After the part is modeled, it is translated to the STL file format. Almost all CAD software are able to output this kind of file format. The STL file describes the external surfaces of the CAD model by approximating the surfaces with a series of triangles (Figure 2.2). The minimum size of these triangles can be set with the CAD software. The size should be smaller than the resolution of the AM machine. The triangles must also point in a correct direction. However, creating triangles may be challenging for the CAD software, especially, if the part has very complex geometry. This may result in triangles that do not align correctly, causing gaps on the surface of the part. Several software tools have been developed to detect these kinds of errors and to repair them. (Ahn et al. 2002, p. 248; Gibson et al. 2010, p. 42-44; Yan & Gu 1996, p. 312-313)

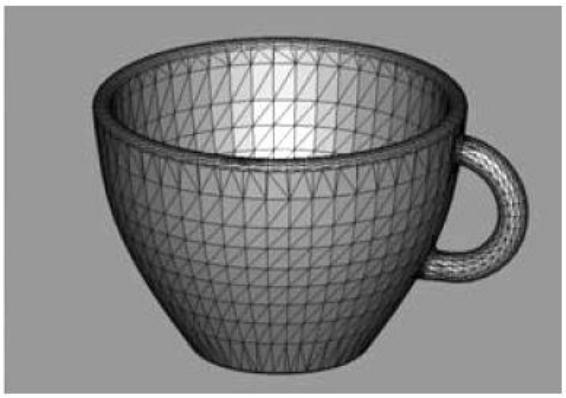

***Figure 2.2.*** *The external surfaces of the CAD model composed of triangles* (Gibson et al. 2010, p. 23).

At this point, it should be stated, that a new standardized file format is becoming into use. This file format is called AMF (Additive Manufacturing File). The AMF format should allow any CAD software to describe a shape and a composition of any 3D model in order to fabricate the part with any AM machine. (ASTM Additive Manufacturing File Format (AMF) [WWW])

### 2.2.2 Step 2: Model manipulation and machine setup

After the STL file is created, several actions are usually required before the part can be built. An AM system normally comes with a visualization software for STL files that allows the manipulation of the model. For instance the correct size, position, and orientation of the part can be determined. A possibility to scale the part is often required due to material properties since the final part may be slightly larger or smaller than the model. With the software it is also possible to properly set up the AM machine before the build process. For example, these settings and parameters include layer thickness, build speed and build temperature. All AM machines also have setup parameters that are machine-specific. Worth noticing is that often the part will be built even if the machine setup is not correct, resulting in the poor quality of the part. After model manipulation

and machine setup the STL file is translated to the file format which contains the operating instructions of the machine. (Ahn et al. 2002, p. 248-249; Gibson et al. 2010, p. 45)

### 2.2.3 Step 3: Building of the part

In this step the AM machine automatically builds the part layer by layer. Supervision is only required to ensure that errors, either hardware or software related, do not occur during building. After the AM machine has completed the build, the part must be removed from the machine. The interaction that the removal requires depends on the AM technology and the machine. Usually the part must be either separated from the build platform or removed from the excess build material that surrounds the part. (Gibson et al. 2010, p. 46)

### 2.2.4 Step 4: Post-processing of the part

After the part is removed from the AM machine, some post-processing may be required. This step is also dependent of the AM technology. The part may still be weak after the build, it may have support structures that must be removed, or it may need cleaning up. Post-processing often requires some manual manipulation and it may be time-consuming. Also additional treatments are often required, such as priming and painting in order to give a desirable surface texture and finished looks, abrasive finishing or coating. Required treatments in this step are very application-specific. (Gibson et al. 2010, p. 46-47)

## 2.3 Unique capabilities of additive manufacturing

The unique capabilities of the AM technologies bring new opportunities for customization, improve product performance, allow multifunctionality and decrease overall manufacturing costs (Gibson et al. 2010, p. 283; Levy et al. 2003, p. 591; Upcraft & Fletcher 2003, p. 319; Yan & Gu 1996, p. 308). These unique capabilities include shape complexity, structural complexity, functional complexity and material complexity.

### 2.3.1 Shape complexity

With AM it is possible to build a part with almost any shape due to the layer by layer approach since a capability of an AM machine to fabricate a layer is unrelated to a shape of a layer (Gibson et al. 2010, p. 290; Guo & Leu 2013, p. 236). When compared with two conventional manufacturing processes, machining and injection molding, that is a huge advantage. In machining, a limiting factor that determines shape complexity is tool accessibility. In injection molding, shape complexity is limited by a need to separate mold pieces from each other and remove parts from molds. (Gibson et al. 2010, p. 290) Shape complexity also makes possible to custom design part geometries. This is very beneficial especially in case of medical applications, where individually designed solutions are required. (Gibson et al. 2010, p. 290; Levy et al. 2003, p. 592)

### 2.3.2 Structural complexity

With AM it is possible to design and fabricate different kinds of structures from nano- and microstructures to macrostructures. Structures can also vary from point to point within a structure. These various types of structures can be achieved by carefully controlling the process parameters. (Gibson et al. 2010, p. 291-292; Guo & Leu 2013, p. 223) Especially beam deposition processes (Chapter 2.5.5) have been studied extensively regarding to structural complexity (Gibson et al. 2010, p. 291). Similar structural control is also possible with other AM processes either by changing materials during building or by processing materials beforehand. The ability to simultaneously control these various structures simply by changing the process parameters is something that is not possible to achieve when using conventional manufacturing methods. (Gibson et al. 2010, p. 292; Guo & Leu 2013, p. 223)

### 2.3.3 Functionality

In addition to individual part fabrication, also functional devices can be produced with AM processes. Since parts are built layer by layer, an inside of a part is always accessible. Operational mechanisms can be fabricated by carefully controlling the fabrication of each layer. Also different kinds of components can be inserted into fabricated parts during building. This makes post-fabrication assembly unnecessary. For instance, small metal parts, electric motors, printed circuit boards and sensors can be embedded in parts. (Gibson et al. 2010, p. 292-293; Upcraft & Fletcher 2003, p. 319)

### 2.3.4 Material composition

Since material can be deposited either one point or one layer at a time, it is possible to process material differently at different points or regions. This enables different material properties in different areas of the part. With many AM processes, it is also possible to change material composition either gradually or abruptly during building, resulting in heterogeneous parts. (Gibson et al. 2010, p. 295; Guo & Leu 2013, p. 223) When regarding fused deposition modeling (Chapter 2.6), it is possible to use multiple nozzles for multi-material deposition and thus create multi-material constructions. This can be very beneficial especially for biomedical materials research. One example is the fabrication of high-performance orthopedic implants which require excellent bone adhesion in certain regions, while other regions must be optimized for minimizing wearing. This can be achieved by changing the composition of the material at bone in-growth regions and on bearing surfaces. (Gibson et al. 2010, p. 295)

## 2.4 Additive manufacturing for biomedical purposes

AM can be used for biomedical purposes by fabricating complex customized solutions for patients (Gibson et al. 2010, p. 388; Guo & Leu 2013, p. 231; Hutmacher et al. 2004, p. 354). With medical imaging machines, it is possible to build a patient-specific

3D model from both bone and soft tissue images and then fabricate an implant with a suitable AM machine. Computed tomography (CT) imaging is typically used for imaging bone tissue and magnetic resonance imaging (MRI) is used for soft tissue imaging. Bone tissue models are used more often since fabricated implants resemble bone to some extent. Soft tissue models are typically used only for visualization purposes. (Gibson et al. 2010, p. 388; Landers et al. 2002, p. 3108; Winder & Bibb 2005, p. 1006)

AM can be exploited in several ways in the medical field. Parts fabricated with AM can help surgeons to understand a situation of a patient better and to plan procedures beforehand, and hence reduce time required for complex surgical operations. Precise and accurately fitting prosthetics devices and implants can be fabricated since the dimensional error of clinical CT imaging is only 0.2 mm. (Gibson et al. 2010, p. 387; Wang et al. 2009, p. 237). Furthermore, parts fabricated with AM machines have even higher accuracies. Thus, the limiting factor regaring accuracy is the imaging technique, not the AM technology. (Winder & Bibb 2005, p. 1010) In a model development phase it is possible to include additional features in models, such as tooling guidance and holes for screws. Models can also be used as templates. Flexible titanium meshes for instance, used in bone replacements, can be accurately bent to correct shape with a help of these templates. (Gibson et al. 2010, p. 389) With AM it is also possible to fabricate molds for other manufacturing processes. AM can also be used for tissue engineering approaches. Porous scaffolds resembling a shape and size of bone tissue, with the pores of a few hundred microns, can be fabricated from biocompatible and biodegradable materials (Antonov et al. 2005, p. 327; Gibson et al. 2006, p. 389-391; Guo & Leu 2013, p. 232) Living cells can be added into scaffolds afterwards. However, the challenge is to maintain the integrity of the scaffold long enough in order to form healthy and strong bone tissue. (Gibson et al. 2010, p. 391; Guo & Leu 2013, p. 233)

AM technologies were originally developed to serve a broad range of product manufacturing and not specifically for medical purposes. For that reason there are several deficiencies related to medical usage. Even though AM machines are designed for rapid manufacturing, build times may be several days and post-processing may be required. (Gibson et al. 2010, p. 393-394) Medical imaging data need to be processed before fabrication, which requires both software expertise as well as knowledge about human anatomy. Operating with AM machines requires technical expertise in order to produce good quality parts. In addition, setup options are often complex. For this reason, AM is not beneficial for fast diagnosis or emergency operations. (Gibson et al. 2010, p. 394-396; Winder & Bibb 2005, p. 1007) In addition, only a couple of polymer materials are classified as safe to be used into an operating room and even fewer polymers can be implanted into a body. These material limitations reduce a range of applications that can be used in the medical field. Metals however, particularly titanium, are being used regularly to fabricate implants. (Gibson et al. 2010, p. 395)

## 2.5 Additive manufacturing technologies

Classification between different AM technologies is based on the machine architecture and transformation physics of materials (Gibson et al. 2010, p. 32). AM technologies include photopolymerization, powder bed fusion, printing, sheet lamination, beam deposition, direct write, and extrusion-based technologies. The processing characteristics as well as advantages and disadvantages of these technologies are discussed next.

### 2.5.1 Photopolymerization processes

The photopolymerization processes use liquid radiation curable monomer resins as materials. Resins are mixtures composed of several types of ingredients including liquid monomers, photoinitiators, reactive diluents, flexibilizers and stabilizers. Resins become solid polymers when radiation causes chemical transformation in a photoinitiator and a photoinitiator reacts with liquid monomers. This chemical reaction is called photopolymerization. With different kinds of resin formulations it is possible to affect reaction rates and part properties so that those can be used with different kinds of applications. The solid part is fabricated layer by layer by exposing a liquid resin to a scanning laser. (Gibson et al. 2010, p. 65-67; Melchels et al. 2010, p. 6122-6124; Pham & Gault 1998, p. 1259-1264) Several types of radiation can be used to cure polymers. These include gamma and x-ray radiation, electron beam and ultraviolet light (UV), of which the UV is the most used. In some cases also visible light can be used. (Gibson et al. 2010, p. 61) The photopolymerization processes are known to be very accurate due to well-defined interactions between radiation and resins. (Gibson et al. 2010, p. 98; Pham & Gault 1998, p. 1259-1264)

Previously, resins used with photopolymerization processes were either acrylate or epoxy resins. (Gibson et al. 2010, p. 64; Melchels et al. 2010, p. 6122-6124; Pham & Gault 1998, p. 1259-1264) The advantage of the acrylate resins is quick reaction on radiation. The disadvantages are significant shrinkage, curling and warping, that leads to mechanically weak parts. The advantage of the epoxy resins is the low level of shrinkage, which leads to excellent adhesion and reduced curling. With epoxy resins, it is possible to build more accurate, harder, and stronger parts than with acrylate resins. However, the disadvantages of the epoxy resins are slow reaction on radiation, sensitivity to humidity and brittleness of the cured part. (Gibson et al. 2010, p. 64-65; Pham & Gault 1998, p. 1259-1264) Nowadays, usually the combinations of the acrylate and epoxy resins, called hybrid resins, are used. That way the advantages of both resins and curing types can be combined. Using the hybrid resins leads to the more rapid part building, which strengthens the part. Also the brittleness of the part is reduced. (Gibson et al. 2010, p. 64-65) In addition to common polymer parts, complex ceramic or metal parts can be fabricated using photopolymerization by mixing ceramic or metal particles and polymer resins together. Afterwards, the polymer resin, acting as binder, is removed and the part sintered in order to strengthen the part. (Brady & Halloran 1997, p. 61; Chartier et al. 2002, p. 3141-3142; Levy et al. 2003, p. 597)

There are three photopolymerization process configurations, which all utilize the stereolithography (SL) technology and the curing process takes place in a vat of liquid resin. These configurations are vector scan SL, mask projection SL and two-photon SL. (Gibson et al. 2010, p. 62) These three configurations are discussed next.

### Vector scan stereolithography

Vector scan SL is the most typical approach of the commercial SL machines. In vector scan SL, solid parts are cured with a scanning UV laser which selectively solidifies a liquid photocurable resin in a vat. The part is built on the platform that is dipped into the vat of resin. After each layer, the platform is lowered and the surface of the vat is re-coated. (Gibson et al. 2010, p. 71; Melchels et al. 2010, p. 6122; Peltola et al. 2008, p. 9; Pham & Gault 1998, p. 1259) The vector scan process is shown in Figure 2.3.

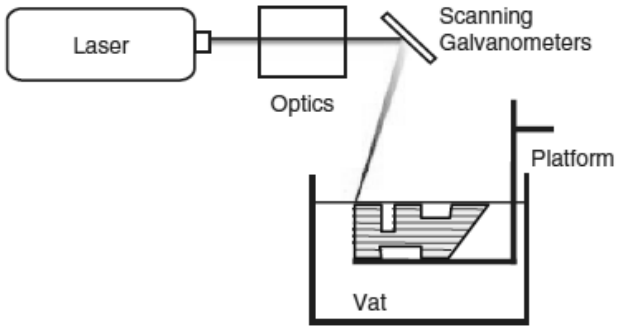


***Figure 2.3.*** *A schematic figure of vector scan SL* (Gibson et al. 2010, p. 62).

The subsystem hierarchy of a typical vector scan SL machine can be seen in Figure 2.4. Five main subsystems are the recoating system, platform system, vat system, laser and optics system, and control system. In recoating, the build platform moves down after each layer according to the layer thickness and a new layer of resin is deposited with a blade. The platform system consists of a build platform and elevator. The elevator moves the platform up and down. The vat system consists of a vat that encloses the resin and resin level adjustment device. The laser and optics system includes a laser, focusing and adjustment optics, and two galvanometers which scan the laser beam across the vat surface. The control system consists of three main subsystems. First, the environment controller adjusts the resin vat temperature, environment temperature and humidity. Second, the beam controller adjusts the beam spot size, focus depth, and scan speed. Third, the process controller controls the machine operations that are described in the build file. (Gibson et al. 2010, p. 72-73)

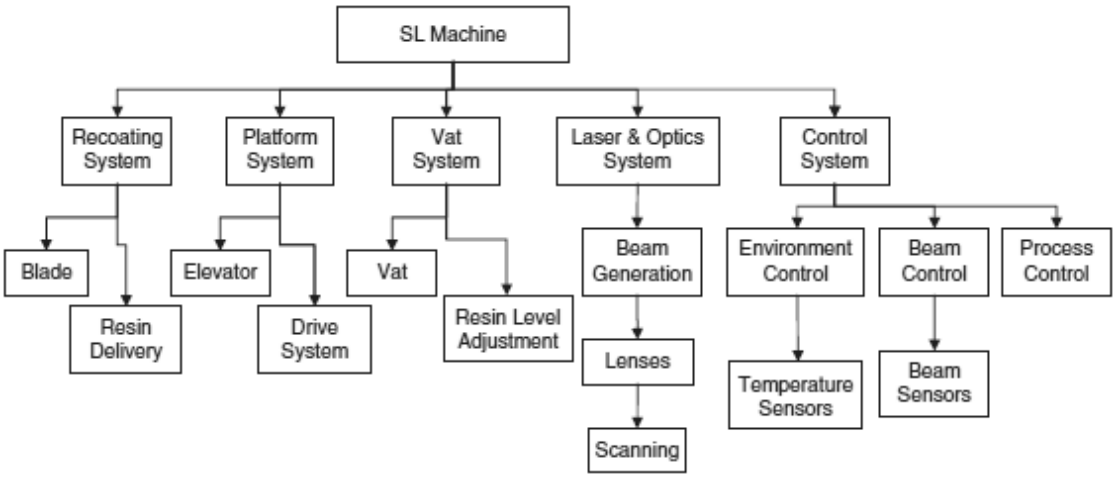


***Figure 2.4.*** *The subsystem hierarchy of vector scan SL* (Gibson et al. 2010, p. 72).

Two main advantages of vector scan SL are the part accuracy and surface finish when compared with other AM technologies. The feature size of 80 µm can be achieved with vector scan SL. However, the mechanical properties of the parts are moderate. (Gibson et al. 2010, p. 73-74; Pham & Gault 1998, p. 1263) Also three phenomena that affect all radiation processes as well as other layer-based AM processes should be noted. First, layer by layer curing causes discretization. This means that layers cause steps on the slanted or curved surfaces and make the edges of layers visible. Second, when the laser scans a cross section, the material solidifies and shrinks. After photopolymerization, the volume occupied by the monomer molecules is larger than the volume of the reacted polymer. The shrinkage pulls on the previous layers and causes residual stresses. Those stresses can also cause part edges to warp. Third, extra energy that lies below the current layer may result in thicker part sections. This phenomenon is called a print-through error. (Gibson et al. 2010, p. 83)

### Mask projection stereolithography

In mask projection SL (Figure 2.5), an entire cross section can be cured at once. This is the main advantage of this method when compared with vector scan SL and two-photon SL since curing happens much faster than scanning with a single laser beam. In mask projection, a large radiation beam is generated by another device, usually with Digital Micromirror Device (DMD). Each slice cross section is saved as bitmaps, which are projected onto a resin surface by DMD. An UV lamp acts as a light source. (Gibson et al. 2010, p. 92-93; Guo & Leu 2013, p. 216-217; Sun et al. 2005, p. 114-115) The minimum feature size of mask projection SL is around 20 µm (Melchels et al. 2010, p. 6122; Sun et al. 2005, p. 114).

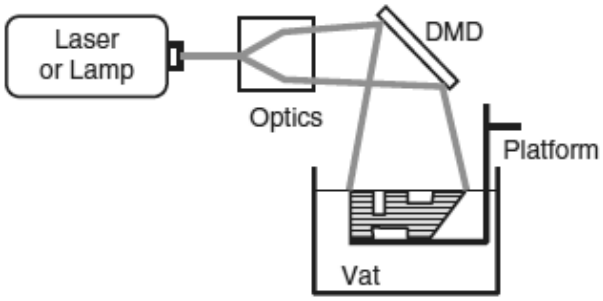


***Figure 2.5.*** *A schematic figure of mask projection SL* (Gibson et al. 2010, p. 62).

A solid part can also be built upside down. With this kind of approach, the vat is illuminated vertically upwards through a window. A cured resin layer sticks to the window and cures into the previous layer. The build platform moves away from the window and leaves a slight gap between the resin and the window. This kind of approach leads to two advantages. First, a recoating mechanism comes unnecessary since gravity forces the resin to fill in the area below the cured part. Second, the top vat surface is a flat plane instead of a free surface, which enables more accurate layer fabrication. The disadvantage of this approach is that detailed features may be damaged when the cured layer is separated from the window. (Gibson et al. 2010, p. 94-95; Melchels et al. 2010, p. 6122-6123)

### Two-photon stereolithography

In two-photon SL (Figure 2.6), two scanning lasers are used for polymerization. Photopolymerization occurs at the intersection of two scanning laser beams when two photons hit to a photoinitiator, initiating polymerization. For this reason it is possible to reach high resolution with this approach since only the center of the laser has high enough irradiance to make two photons strike at the same photoinitiator molecule. The advantage of this approach is that complicated parts can be produced quickly and accurately. Even 0.2 μm feature sizes have been achieved. (Gibson et al. 2010, p. 96-97; Lee et al. 2008, p. 633; Spangenberg et al. 2013, p. 36-38) The advantage compared with vector scan SL and mask projection SL is that the part is fabricated below the resin surface, which makes recoating unnecessary (Gibson et al. 2010, p. 63). However, the viscosity of the resin in the vat has to be high enough so that the cured part cannot float away during the build (Gibson et al. 2010, p. 97).

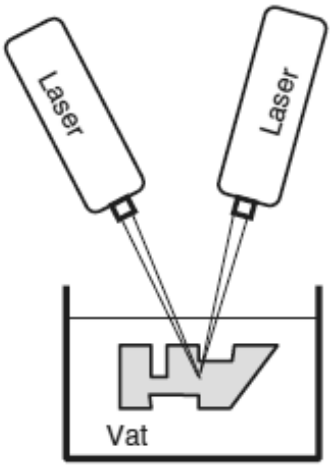


***Figure 2.6.*** *A schematic figure of two-photon SL* (Gibson et al. 2010, p. 62).

It is possible to use typical polymer resins in the two-photon approach. However, the photoinitiators used in these resins have small two-photon absorption cross sections. The absorption cross section describes the capacity of the intiator to absorb two photons (Spangenberg et al. 2013, p. 39). Therefore these initiators require high laser-power and long exposure times. Due to these reasons, also other materials have been studied for the two-photon approach, especially long molecule photoinitiators which have larger absorption cross sections. (Gibson et al. 2010, p. 98)

### 2.5.2 Powder bed fusion processes

All powder bed fusion (PBF) processes are based on selective laser sintering (SLS) which was the first commercialized PBF process. A basic SLS process is shown in Figure 2.7. Other PBF processes modify this basic process in different ways either to enhance productivity or to enable the usage of different materials. All PBF processes have some common characteristics, including a thermal source for inducing fusion between powder particles, method for controlling powder fusion, and mechanism for adding and smoothing powder layers. The SLS process can be either a point-wise laser scanning or a layer-wise fusion technique. (Gibson et al. 2010, p. 103) Polymer, ceramic and metal powders and composites can be used depending on the approach. The final part properties are comparable to the properties achieved by many conventional manufacturing methods. For these reasons the PBF processes are widely used all over the world. (Gibson et al. 2010, p. 103; Kruth et al. 2005, p. 58; Pham & Gault 1998, p. 1272)

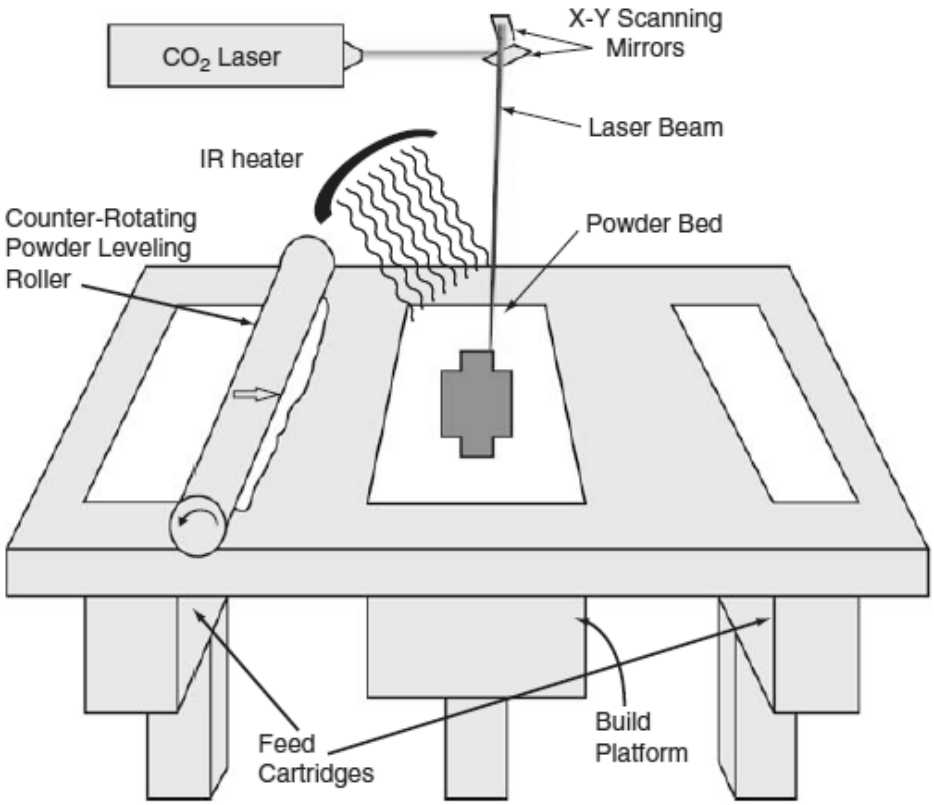


***Figure 2.7.*** *A schematic figure of the Selective Laser Sintering process* (Gibson et al. 2010, p. 104).

SLS fuses thin layers of powder which are typically 0.1 mm thick. Layers are spread across the build platform by using a counter-rotating powder leveling roller. The part is built inside a chamber that is filled with nitrogen gas. Nitrogen gas minimizes the oxidation and degradation of the powder material. The powder temperature is kept just below the melting point or glass transition temperature. Infrared (IR) heaters are placed above the build platform to maintain an elevated temperature of the powder to prevent the warping of the part during the build. After the powder layer is spread and preheated, a focused carbon dioxide ($CO_2$) laser beam is directed onto the powder bed. The beam is moved by using galvanometers. The scanning laser beam fuses the powder material to form the layer cross section. Surrounding powder remains loose and acts as support material for following layers. This also makes the secondary supports unnecessary. After the layer is complete, the build platform is lowered by one layer thickness. The process repeats until the part is complete. After that the part is cooled down to prevent the part both from degrading in the presence of oxygen and warping due to uneven thermal contraction. Finally, the part is removed from the powder bed and loose powder is cleaned off. If necessary, post-processing operations are performed. (Gibson et al. 2010, p. 104-105; Pham & Gault 1998, p. 1272; Yan & Gu 1996, p. 310)

There are four different binding mechanisms which are used in the PBF processes: diffusion-induced solid-state sintering, chemically-induced sintering, liquid-phase sin-

tering, and full melting. Most commercial processes use mainly liquid-phase sintering and melting. (Gibson et al. 2010, p. 105; Kruth et al. 2005, p. 44)

Generally, sintering means the fusion of powder particles in their solid state, without melting, at elevated temperatures. The sintering mechanism is primarily diffusion between the powder particles. When the particles are fused, the total surface area decreases. To achieve very low porosity, long sintering times or high sintering temperatures are required. Smaller particles sinter more rapidly and require lower temperatures than larger particles. Nevertheless, diffusion-induced solid-state sintering is the slowest mechanism within the PBF processes. However, there are also a couple of advantages. The powder bed gains relatively good tensile and compressive strengths, which reduces part curling. Also a wide variety of materials can be processed with solid-state sintering. (Gibson et al. 2010, p. 105-106; Kruth et al. 2005, p. 45-46)

Chemically-induced sintering is primarily used for ceramic materials. In this process, powder particles are bound together by a by-product, which is formed with thermally-activated chemical reactions. These reactions can occur between two types of powders or between powders and atmospheric gases. Chemically-induced sintering leads to part porosity. For that reason, post-process infiltration or high-temperature furnace sintering is usually required to gain higher densities and better properties. This expensive and time-consuming post-processing has limited the usage of chemically-induced sintering in commercial machines. (Gibson et al. 2010, p. 108; Kruth et al. 2005, p. 47)

Liquid-phase sintering (LPS) is the most diverse process within the PBF processes. LPS means that powder particles which include binding material and structural material are fused so that a portion of powder particles become molten while other portions remain solid. The molten particles act as glue binding the solid particles together. For that reason, high-temperature particles can be bound together without needing to melt or sinter particles directly. In many situations, there is a clear distinction between the binding material and the structural material. These materials can be combined as separate particles, as composite particles or as coated particles. In many cases, a well-mixed combination of binder and structural powder particles is enough. However, structures formed from separate particles are typically quite porous and need post-processing in a furnace to achieve the required properties. Parts that are held together by binders and require post-processing are called green parts. Because of this high porosity, it is often beneficial to bind structural and binder particles together into larger particles to gain composite powder particles. Composite particles contain both the binder and structural material within each powder particle. Portions of these particles are distinct from each other. By doing so, higher density green parts are obtained. Also the resulting surface quality is better than with separate particles. In some cases, it is more effective to use coated particles than composite particles. In coated particles, structural particles are coated with the binder material. The advantages of these coated particles are the more effective binding of the structural particles and better flow properties. In some cases, it is also possible to use indistinct mixtures. This means that microstructural alloying

eliminates the distinct binder and structural regions. (Gibson et al. 2010, p. 108-112; Kruth et al. 2005, p. 48-52)

Full melting is the most commonly used with metal alloys and semi-crystalline polymers. In these materials, the entire region of material is melted to a depth exceeding the layer thickness. In that way it is possible to re-melt a portion of the previously solidified structure. For that reason, full melting is very effective when creating well-bonded, high-density structures from metals and polymers. (Gibson et al. 2010, p. 112; Kruth et al. 2005, p. 55)

There are some advantages and limitations. The PBF processes are especially competitive when it comes to geometrically complex parts. In case of polymers, the support structures are not needed since the loose powder bed acts as support material. This enables advanced geometries and complex features. (Gibson et al. 2010, p. 140; Yan & Gu 1996, p. 310) For metals, support structures are needed to prevent the part from warping due to high residual stresses. However, metal parts have excellent material properties when compared with conventional manufacturing methods. Many parts can also be produced in a single build, which improves the productivity. The build accuracy and surface quality is worse than with liquid-based processes. However, both properties depend on the operating conditions and powder particle size. The part build time may take longer than with other AM processes due to heating and cooling cycles. (Gibson et al. 2010, p. 140) With PBF processes, producing satisfactory parts requires optimal process parameters. These parameters include laser-related, scan-related, powder-related and temperature-related parameters, which are also strongly interdependent. Therefore, operating with PBF processes require the expertise of many fields. (Gibson et al. 2010, p. 133; Pham & Gault 1998, p. 1273)

### 2.5.3 Printing processes

The printing processes divide in two different printing technologies: direct printing and binder printing. In direct printing, all of the part material is dispensed by a print head. In binder printing, a binder is printed onto a powder bed to form a part cross section. (Gibson et al. 2010, p. 171) The most commonly used printing process is 3D printing (3DP) which utilizes the binder printing technology (Gibson et al. 2010, p. 195). For this reason the 3DP process is described in this context. It should be noted that commonly the term 3D printing is incorrectly assumed to refer to any additive manufacturing technology, especially to the commercial fused deposition modeling technique (Chapter 2.6). A schematic of the 3DP process is shown in Figure 2.7.

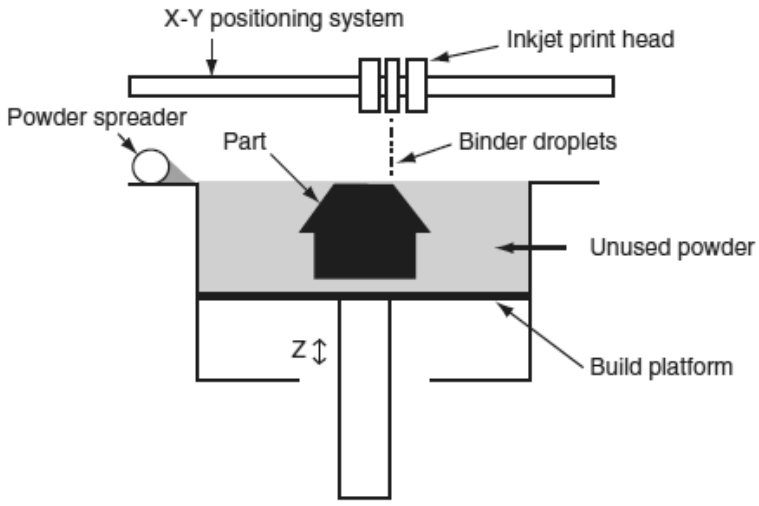


***Figure 2.7.*** *A schematic figure of the 3D Printing process* (Gibson et al. 2010, p. 196).

In 3DP, which is based on the binder printing technology, only a small portion of the part material is delivered through the print head while most of the part material is in powder form in the powder bed. Binder droplets bond binder liquid and powder particles together and at the same time enable bonding to the previously printed layer. After the layer is printed, the powder bed is lowered and a new layer of powder is spread. The spreading mechanism is very similar to the PBF processes. After the part is completed, it is left in the powder bed to gain strength and in order for the binder to fully settle. Finally, the part is post-processed by removing excess powder with pressurized air and the part is filled with an infiltrant to make it stronger. The 3DP process has many same advantages as the PBF processes. Parts are self-supporting due to the powder bed and hence support structures are not needed. (Gibson et al. 2010, p. 195-196; Pham & Gault 1998, p. 1274-1275; Yan & Gu 1996, p. 311) Also the assemblies of several parts can be fabricated since excess powder can be removed between the parts after printing. (Gibson et al. 2010, p. 196; Yan & Gu 1996, p. 312)

Liquid material can exit the nozzle as either a continuous column of liquid, called continuous stream (CS), or as discrete droplets, called drop-on-demand (DOD) (de Gans et al. 2004, p. 204; Dimitrov et al. 2006, p. 137; Gibson et al. 2010, p. 184). The advantage of the CS deposition is the high throughput rate. The disadvantage is that the materials must be able to carry a charge. DOD is the more preferable method for all applications due to its smaller droplet size and higher placement accuracy. All commercial printing machines use the DOD print heads. (de Gans et al. 2004, p. 204-205; Gibson et al. 2010, p. 184-187)

The primary advantages of both direct and binder printing are the low cost, high speed, scalability, use of multiple materials, and capability of printing colors. The reason for the relatively low cost is that printing machines are assembled from standard components. Printing machines have print heads with hundreds or even thousands of nozzles, which enables depositing a lot of material quickly and over a large area. The scalability means that printing speed can pretty easily be increased by adding another

print head to a machine. By adding several print heads it is also possible to print multiple materials and different colors. (Dimitrov et al. 2006, p. 144-145; Gibson et al. 2010, p. 174) Binder printing also has some distinct advantages when compared with direct printing. It is faster since only a small fraction of the total part volume is dispensed through the print heads. Powder materials and additives in binders can be combined, which makes possible to use material compositions that cannot be used with direct printing. Ceramic and metal parts can be produced with better quality since slurries with higher solid loadings are possible to achieve. (Gibson et al. 2010, p. 201) There are also some disadvantages with both direct and binder printing. The part accuracy is not as good as with some other AM processes. The choice of materials is also limited. (Dimitrov et al. 2006, p. 145; Gibson et al. 2010, p. 174) Only waxes and photopolymers are available for direct printing. For binder printing, some polymer-ceramic composites and metals are available, but with many limitations. However, research groups have done successful experiments with several polymer, ceramic and metal materials. (Gibson et al. 2010, p. 174)

Printing also has several technical and operational challenges. The first challenge is the formulation of the liquid material. The printed material has to be in a liquid form and possess acceptable characteristics. The second challenge is the droplet formation. The liquid material must be converted into small discrete droplets. Furthermore, even very small changes to the material, process parameters or physical setup may dramatically change the droplet forming behavior. (de Gans et al. 2004, p. 205; Gibson et al. 2010, p. 182) The third challenge is the droplet deposition controlling. In the printing processes, either the print head or the build platform is moving. This has to be taken into account when calculating the trajectory of the droplets. In addition, the droplet velocity and size will also affect the deposition characteristics. The fourth challenge is to prevent very small nozzles from blocking up. Most machines go through cleaning cycles during builds to keep as many nozzles open as possible. The fifth challenge is to gain the best possible print resolution. Many small droplets should be produced very close to each other. This requires the high nozzle density in the print head, which is not always possible. Another method is to make multiple passes over the same area. However, this often leads in the overlapping problem because of the thermal or pressure differentials. (Gibson et al. 2010, p. 182-183)

### 2.5.4 Sheet lamination processes

There are several sheet lamination processes that are developed for different materials and cutting strategies. In sheet lamination, only the outlines of the part is cut. Sheets can be either cut and then stacked or stacked and then cut. The sheet lamination processes can be categorized based on the layer bonding mechanism: gluing or adhesive bonding, thermal bonding or clamping. (Gibson et al. 2010, p. 207; Levy et al. 2003, p. 599)

In gluing or adhesive bonding, build material is usually paper which is coated with a thermoplastic polymer on one side. Basically any material that is in a form of sheet and can be precisely bonded and cut can be used (Yan & Gu 1996, p. 311). Sheet material is

precisely cut using either a laser or a mechanical cutter. The lamination process is either bond-then-form or form-then-bond. In the former process, the part building consists of three steps, including placing the laminate, bonding it to the substrate, and cutting it according to the slice contour. In the latter process, sheet material is cut to shape first and then bonded to the substrate. The first commercialized sheet lamination process was Laminated Object Manufacturing (LOM) which uses the bond-then-form process. This process can be seen in Figure 2.8. (Gibson et al. 2010, p. 207-212; Wimpenny et al. 2003, p. 215)

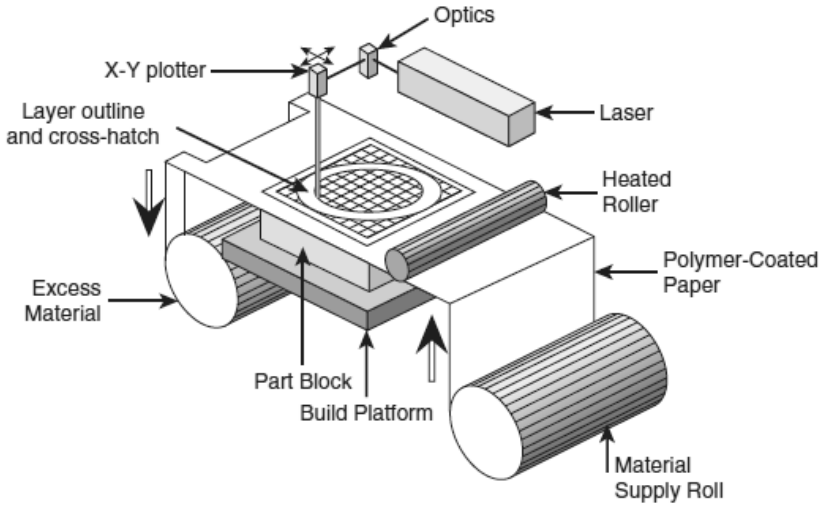


***Figure 2.8.*** *A schematic figure of the Laminated Object Manufacturing (LOM) process* (Gibson et al. 2010, p. 208).

In LOM, the heated roller melts the adhesive plastic coating causing the adhesion between the sheets. The sheets are cut using $CO_2$ laser to a depth of one layer thickness. Each paper sheet acts as one cross-sectional layer of the part. The excess sheet material is diced into small cubes and it acts as support material. The process is repeated until the part is complete. Finally the part is post-processed by removing the excess material using carving tools. (Chua et al. 1998, p. 148; Gibson et al. 2010, p. 208; Wimpenny et al. 2003, p. 215) With bond-then-form processes, also metal, ceramic, and composite materials can be used (Gibson et al. 2010, p. 209; Yan & Gu 1996, p. 311). Instead of paper sheets, ceramic or metal tapes are used as the build material and post-processing involves high-temperature sintering. The advantages of the bond-then-form processes include a little shrinkage, residual stresses, and distortion. Large parts can be fabricated quickly (Gibson et al. 2010, p. 209; Guo & Leu 2013, p. 218). Material, machine, and process costs are low when compared with other AM systems. There are also limitations. Parts made of paper require coating to prevent moisture absorption and excessive wear. The mechanical and thermal properties of the parts are inhomogeneous due to the usage of adhesive. Small features may be destroyed during the excess material removal. (Gibson et al. 2010, p. 208-210)

The form-then-bond processes are used for fabricating metallic or ceramic parts. There are some advantages using this approach compared with the bond-then-form approach. The parts with internal features and channels can be fabricated. With bond-then-

form process these features are impossible to obtain since excess material inside the part cannot be removed after bonding the layers (Gibson et al. 2010, p. 210; Yang et al. 2002, p. 2). Previous layers will stay unharmed during cutting since cutting happens before stacking. Also time-consuming dicing step is eliminated. The disadvantages include the need of external support structures in case of overhangs, and alignment system for placing the cut layer accurately on top of the previous layer. (Gibson et al. 2010, p. 210-212)

Thermal bonding is used for metal sheets and it is an effective method for fabricating complex metal parts and tools which have internal cavities. With metals, the form-then-bond approach is used since an excess metal material is difficult to remove if using the bond-then-form approach. (Gibson et al. 2010, p. 212) Clamping is used for assembling metal sheets into simple parts. Sheets are clamped together with bolts. The benefits are that clamping is quick and cheap and there is no need for an adhesive or thermal bonding method. The drawback is that sheets may separate from each other under certain conditions leaving gaps. (Gibson et al. 2010, p. 214; Wimpenny et al. 2003, p. 214)

### 2.5.5 Beam deposition processes

The beam deposition (BD) processes use a focused high-power laser beam to melt deposited material. Also an electron beam or plasma arc can be used as an energy source. Material can be either in a form of powder or wire. Otherwise the BD method is quite similar to the extrusion-based processes (Chapter 2.5.7). (Gibson et al. 2010, p. 237; Levy et al. 2003, p. 598-600) BD can be used for ceramics and metals that are stable in a molten state. Also the mixtures of those can be used. However, usually metal powders are used since ceramic materials need much higher temperatures and cracking may occur during solidification. (Gibson et al. 2010, p. 248-249) A schematic of the BD process can be seen in Figure 2.9.

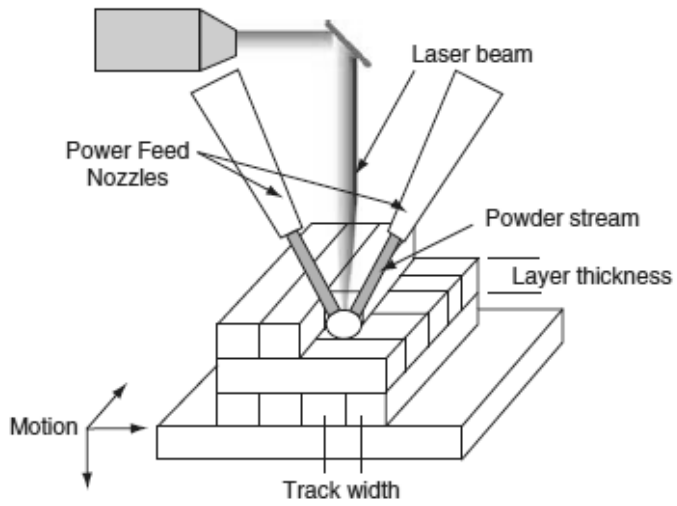


***Figure 2.9.*** *A schematic figure of the beam deposition process* (Gibson et al. 2010, p. 238).

Generally, the method is similar in all BD machines. Differences include changes in laser power, laser spot size, laser type, powder delivery method, inert gas delivery, feedback control and motion control. Compared with most commercialized AM machines that are sold pre-programmed and with optimized process parameters, BD machines are sold as flexible platforms. (Gibson et al. 2010, p. 248) BD is the most beneficial in situations where features or coatings are added on existing components (Gibson et al. 2010, p. 257).

The parts made with BD have high densities (Gibson et al. 2010, p. 238; Kruth et al. 2005, p. 536). The microstructure of the part can be controlled between layers and even within layers. The material composition and solidification rate can be changed. With BD it is possible to produce directionally solidified and single crystal structures. The surface quality and resolution are not very good. The part surface usually has some porosity due to partially adhered molten powder particles. Also the post-processing using machining is usually needed due to the poor part accuracy. Parts with complex geometries also need support structures or multi-axis deposition. Also the slow build speed is a limitation. (Gibson et al. 2010, p. 257; Levy et al. 2003, p. 600)

### 2.5.6 Direct write technologies

The direct write (DW) technologies within the AM processes refer to the technologies that are designed to fabricate structures in meso-, micro-, and nano-scale (Gibson et al. 2010, p. 259; Lewis & Gratson 2004, p. 32). Materials that can be used with DW are for instance dielectric polymers, conductive metals and biological materials. Deposition can be made onto several substrate materials including plastic, metal, ceramic, glass, and even textiles. The possibility to combine several types of materials and substrates expands the range of applications. (Gibson et al. 2010, p. 278; Lewis & Gratson 2004, p. 32) The DW technologies include ink based, laser transfer, thermal spray, beam deposition, liquid-phase and beam tracing processes (Gibson et al. 2010, p. 260).

The ink based processes are the simplest to use and least expensive of the DW technologies (Gibson et al. 2010, p. 260). There are several different ink types available which are either extruded as a continuous liquid filament through a nozzle or deposited as droplets through a printing head. Nozzle dispensing and quill processes use continuous deposition while printing and aerosol processes use droplets. In the nozzle dispensing, inks are pushed through an orifice by using a syringe mechanism. (Gibson et al. 2010, p. 260-261; Lewis & Gratson 2004, p. 33-34) Some machines have a scanning system that scans the topology of the substrate before material deposition. The scanning system makes possible to deposit fine line traces on non-planar substrates. Another benefit is that a wide variety of inks can be used. The disadvantage is that inks must be thermally post-processed to achieve the desired properties. (Gibson et al. 2010, p. 262-263) In the quill process, a pen is dipped into an ink which adheres to the surface of the pen, from which the ink is transferred to the substrate. By controlling the pen motion, accurate patterns can be created. The quill processes are typically used for creating nano-scale features on flat surfaces. (Bullen et al. 2004, p. 789; Gibson et al. 2010, p.

264) In the printing process, the method is similar to the direct printing (Chapter 2.5.3). The difference is that the process is optimized for printing complex electronic circuitries with high accuracy onto flat substrates. (Gibson et al. 2010, p. 265) The aerosol process deposits inks through a nozzle in a form of aerosol mist using a carrier gas (Gibson et al. 2010, p. 266; Mette et al. 2007, p. 622-623). With this process it is possible to produce features as small as 5 μm. The process is also gentle enough to deposit living cells. (Gibson et al. 2010, p. 266)

The laser transfer processes utilize two different material deposition mechanisms. In the first mechanism, a transparent carrier (a foil or a plate) is coated with a layer of transfer material and a layer of build material. The laser penetrates the transparent carrier and ablates the transfer material, which pushes the build material toward the substrate. The build material impacts with the substrate and adheres onto it forming a coating onto the substrate. In the second mechanism, a laser pulse is directed onto the surface of the build material causing the ablation. This ablation creates thermal waves and shock waves which transmit through the material on the opposite surface causing a surface fracture. This fractured material impacts with the substrate forming a coating onto the substrate. Usually deposited material does not need further post-processing. With laser transfer processes it is possible to use metal, ceramic, and polymer materials, as well as living tissue. (Gibson et al. 2010, p. 267-270; Lewis & Gratson 2004, p. 36)

In the thermal spray process, powder or wire form material is melted and sprayed at high velocity onto the substrate in a form of droplets. Metal, ceramic, polymer and composite materials can be used. Droplets can be deposited in a solid or semi-solid state, enabling the deposition also at the room temperature. This enables the wider material property adjustment as well as the usage of many different substrates. Also multilayer devices can be produced from different materials. (Ahn et al. 2005, p. 342; Gibson et al. 2010, p. 270-272)

The beam deposition process is based on chemical vapor deposition (CVD), where a reactant gas is converted to a solid material at a substrate by using thermal energy. The solid material is formed on the regions where the temperature rises above a certain value. The heat source can be a laser, focused ion beam, or electron beam. Also multimaterial structures can be formed by using multiple gases. Post-processing is not needed since the density of the final part is 100%. The disadvantages of the CVD are the very low deposition rate and relatively high complexity. The process also uses high temperatures. (Gibson et al. 2010, p. 272-275; Kadekar et al. 2004, p. 790-791)

In the liquid phase process, liquid materials are converted into solid materials by using thermal or electrical energy. These thermo- and electrochemical techniques can be used with any metal or ceramic materials that are compatible with mentioned techniques. The disadvantages of the thermochemical process include possibly toxic or corrosive chemical substances and the need for a heated substrate. The disadvantages of the electrochemical process include the slow deposition rate and the need for post-processing due to the porosity of the final part. (Gibson et al. 2010, p. 275-276; He et al. 2000, p. 4-7)

The beam tracing process combines layer-wise additive approaches with beam subtractive approaches. A thin coating layer is added to the surface of the substrate by an additive manner and then this layer is trimmed according to the desired cross-sectional geometry by a subtractive manner. The process is similar to the bond-then-form sheet lamination processes described in Chapter 2.5.4. The coating techniques include physical or chemical vapor deposition and thermo- or electrochemical deposition. (Gibson et al. 2010, p. 276-278)

### 2.5.7 Extrusion-based systems

The extrusion-based systems fabricate parts by extrusion. The extrusion means that the build material is forced out through the nozzle in a semi-solid state by using pressure. After the extrusion, the material fully solidifies in order to remain its shape. In addition, the material bonds with the preceding material that has already been extruded. During the part fabrication, material flow is stopped while scanning across the build platform and started again after that. After the layer is completed, either the extruder system moves upwards or the build platform moves downwards before the next layer is built. (Gibson et al. 2010, p. 143; Kruth et al. 2005, p. 533; Peltola et al. 2008, p. 13-14) A schematic of the extrusion-based system can be seen in Figure 2.10. The most common extrusion-based system is fused deposition modeling (FDM). In FDM, the polymer material is fed into the extruder system as a filament by using a gear. The force applied from the gear generates the necessary pressure for the extrusion. (Agarwala et al. 1996, p. 5-6; Gibson et al. 2010, p. 157) The FDM technique is explained in more detail in Chapter 2.6 due to its importance to this thesis.

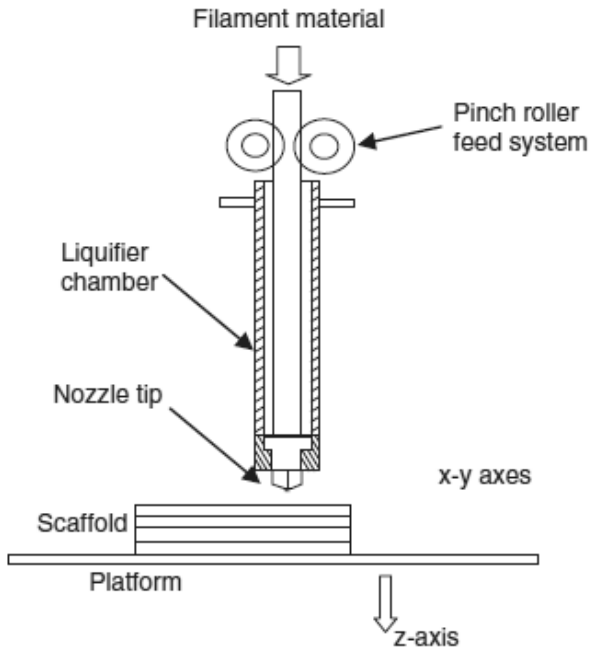


***Figure 2.10.*** *A schematic figure of the extrusion-based system* (Gibson et al. 2010, p. 145).

There are two different ways of controlling the material state with the extrusion-based systems; temperature and chemical change (Gibson et al. 2010, p. 143). The most commonly used approach is to use temperature. In this approach, the build material is melted inside the reservoir so that it can flow out through the nozzle and bond with already extruded material before solidifying. The extruder is vertically mounted on the extruder system. (Agarwala et al. 1996, p. 6; Gibson et al. 2010, p. 143) An alternative approach is to use a chemical change to cause solidification. This approach is used more in biochemical applications where a choice of material is very restricted and material must be biocompatible with living cells. (Gibson et al. 2010, p. 143)

There are a number of key features that are common to all extrusion-based systems. These include the loading of material, liquefaction of material, extrusion, solidification, positional control, bonding, and support generation. (Gibson et al. 2010, p. 144) These are discussed next.

### Loading of material

When the extrusion is used, there is some kind of a reservoir chamber where the liquefaction process happens and from which the material is being extruded. The chamber can be either preloaded with material or the material is fed into the chamber continuously as a filament. The material can be either in a liquid form or in a solid form. The best way to feed the liquid material into the reservoir chamber is to pump it. The solid material can be in a pellet form, powder form, or a continuous filament. Pellets and powders are fed through the chamber either under gravity or by using a screw. When using gravity, a plunger or compressed gas is needed to force the material through the nozzle. A continuous filament can be pushed into the reservoir chamber and that way provide high enough input pressure for the material to extrude through the nozzle. (Gibson et al. 2010, p. 144-145)

### Liquefaction of material

As already mentioned, the build material can be in a liquid form inside the reservoir chamber. However, usually the input material is in a solid form and liquified by using the elevated temperatures. Heat is usually applied by the heater coils wrapped around the reservoir chamber. The material inside the chamber is kept in a semi-solid state. However, the temperature should be kept as low as possible. The reason for that is that some polymers degrade quickly at high temperatures and they could also burn, leaving a residue inside the chamber. This residue may contaminate the upcoming materials. The high temperature inside the chamber also requires additional cooling after the extrusion to ensure the quick enough solidification. (Gibson et al. 2010, p. 145-146)

### Extrusion

The shape and size of the extruded material depend on the extrusion nozzle. Usually, the nozzle is conical. A larger nozzle diameter makes the material flow more rapidly. However, the part extruded with a larger nozzle has lower precision than the part extruded with a smaller nozzle. The diameter of the nozzle also determines the minimum feature size, in other words the x- and y-resolution. The feature size cannot be smaller than the nozzle diameter. In fact, features should be larger than the nozzle diameter in order to guarantee that the part has sufficient strength. Hence, the extrusion-based processes are more suitable for parts that have features and wall thicknesses at least twice the diameter of the nozzle. Material flow through the nozzle is related to the pressure drop between the chamber and the surrounding atmosphere, nozzle geometry, and material viscosity. The viscosity is primarily a function of the extrusion temperature. (Gibson et al. 2010, p. 146)

### Solidification

After the material is extruded, it should maintain its shape and size. However, the shape may change due to gravity and surface tension and the size may vary due to cooling and drying effects. A molten state material may also shrink when cooling. This cooling is also nonlinear, resulting in the distorted part. This effect can be minimized by ensuring that the temperature differential between the liquifier chamber and the surrounding atmosphere is as minimal as possible. For that purpose a build chamber with the controlled environment should be used and the cooling process should be carried out gradually and slowly. However, with all machines this is not possible. (Gibson et al. 2010, p. 149)

### Positional control

The formation of individual layers is controlled by moving the build platform vertically. The part geometry is controlled by moving the extrusion head in the horizontal plane. When the pressure is kept constant, the extruded material will flow at a constant rate and constant cross-sectional diameter. The diameter will also remain constant if the nozzle travels across the build surface at a constant speed that corresponds to the flow rate. Horizontal movement must be in sync with the extrusion rate to ensure the smooth and consistent deposition. When the extrusion head changes the direction, deceleration must be followed by acceleration. The material flow rate must correspond to this change in speed or otherwise too much or too little material is deposited. Horizontal movement is carried out with a planar plotting system containing two orthogonally mounted linear drive mechanisms. Cheaper systems often use belts driven by stepper motors and more expensive systems use servo drives with lead-screws. These drive mechanisms need to be powerful enough in order to move the extrusion system at required velocity and to

respond to rapid changes in direction without backlash effects. The drive mechanism must also be able to move constantly many hours. Because the material flow control during rapid direction changes is challenging, the outline of the layer is usually extruded before the infill by using a slower speed to ensure a consistent material flow. (Gibson et al. 2010, p. 150)

The outer shell also acts as a constraining region for the filler material and prevents it from affecting the overall precision. The extrusion head must be capable of depositing the fill material without damaging the material that has already been extruded. On the other hand, the material must be laid down close enough to the preceding material to enable effective bonding since the strength of the part may be reduced due to the gaps between the paths. (Ahn et al. 2002, p. 249; Gibson et al. 2010, p. 154) The software determines a start location and a trajectory for the fill. Creating the optimal fill pattern is difficult for the software. Usually, the fill pattern cannot be a single continuous path due to the part complexity and even in the case of a seemingly simple geometry that may not be possible, as presented in Figure 2.11. On principle, there should be as few individual paths as possible since a discontinuity in the fill pattern may reduce the mechanical strength of the final part. (Gibson et al. 2010, p. 154-156)

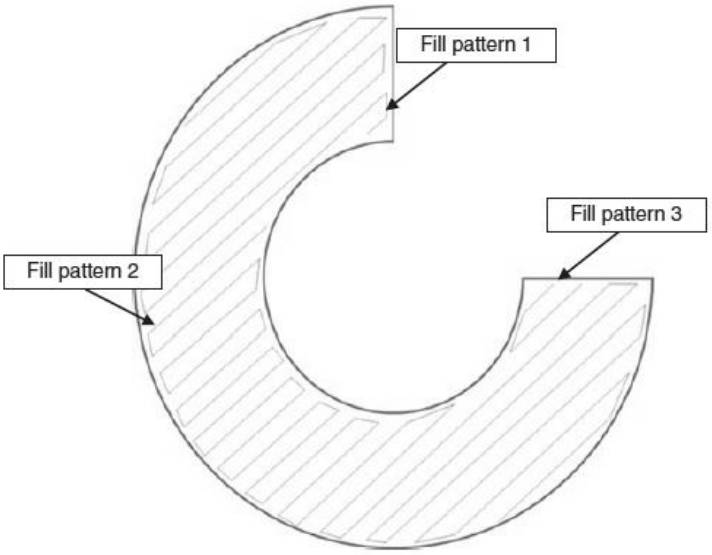


***Figure 2.11.*** *Three individual fill patterns of a cross section* (Gibson et al. 2010, p. 151).

The strength of the part may also be reduced due to the gaps between the outer shell and the infill. These gaps are located in areas where path direction changes when the infill reaches the outer shell (Figure 2.12). For this reason minor overlapping can be used in these regions to ensure that the final part has sufficient mechanical strength. However, overfill also results in some swelling in overlapping areas. Another option is to leave these gaps to ensure the optimal part accuracy with no swelling. (Ahn et al. 2002, p. 249; Gibson et al. 2010, p. 155-156)

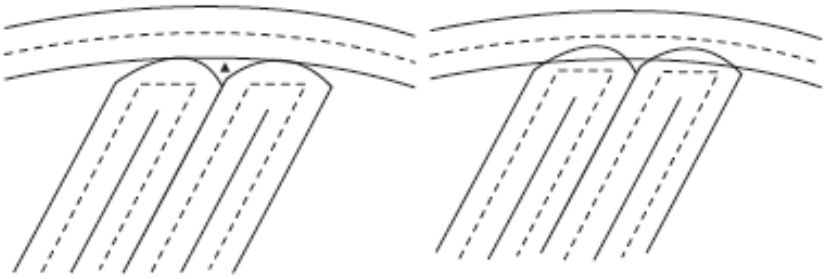

***Figure 2.12.*** *The fill patterns for the optimal part accuracy (left) and optimal part strength* (Gibson et al. 2010, p. 155).

The precise control of the extrusion depends on several parameters. A change in the material input pressure affects the output flow rate. The temperature inside the hot end and the build chamber should be kept constant. The viscosity of the material affects the material flow through the nozzle. Different materials as well as parts with different sizes and geometries cool down at different rates. These and some other factors should be taken account of when fabricating the parts in order to be able to control the material flow and to achieve the optimal part accuracy and strength. (Gibson et al. 2010, p. 156)

### Bonding

During the extrusion and solidification, the material must bond with the previously extruded material. The extrusion head must supply enough heat energy to activate the surfaces of the previous layers to enable bonding. If there is not enough energy, distinct boundaries exist between new and previously deposited layers. This results in a fracture surface where the layers can be easily separated. If there is too much energy, the previously deposited material starts to flow, which results in a poorly defined part. (Gibson et al. 2010, p. 151)

### Support generation

With extrusion-based systems, it may be necessary in some cases to keep the part features in place during the build by using the additional supports. These supports can be fabricated either from the material similar to the build material or from another material. If the machine has only one extruder, the supports must be made using the same material as for the part. (Agarwala et al. 1996, p. 10; Gibson et al. 2010, p. 152; Kruth et al. 2005, p. 533) In this case, the part and supports have to be designed and placed so that they can be separated from each other. One option is to use different temperature for the support structure. Then the resulting fracture surface can be used for separating the support material from the part material. Another option is to leave a tiny gap between the deposited material and the support material. This gap affects the energy transfer between the layers and leads in the fracture phenomenon. In both cases, separating the support material from the part material is always challenging when using similar materials. (Gibson et al. 2010, p. 152-153)

If the machine has two separate extruders, the most effective way to remove the support structure from the part is to fabricate them from a different material. Different material properties make it possible to easily separate the support material from the part material either mechanically or chemically. For the mechanical removal, the support structure is made of weaker material than the part. For the chemical removal, the support structure is removed by using a solvent that does not affect the part material. Also a different color can be used for the support material to visually distinguish it from the part itself. (Gibson et al. 2010, p. 153; Winder & Bibb 2005, p. 1009)

## 2.6 Fused deposition modeling technique

FDM is the most common extrusion-based AM technology (Gibson et al. 2010, p. 157). The part fabrication process includes several steps. At first, the part has to be modeled using a CAD software and the model file translated to the STL file format. Then the STL file is horizontally sliced into thin cross-sectional layers by the slicing software. Usually, these software are machine-specific, but there are also universal software that can be used with all FDM machines. During the slicing process, the software generates the file that includes all the information the FDM machine needs for the part fabrication. Then the part is fabricated layer by layer from bottom to top. Lastly, the part is post-processed by removing the excess support material and by giving additional treatments. (Bansal 2011, p. 7)

During the extrusion, the polymer filament is fed into the nozzle through the heating element which heats the polymer into a semi-solid state. The filament is pushed into the chamber through the feeding mechanism including a gear and a wheel, which generates the necessary pressure for the extrusion. The filament is continuously deposited through the nozzle in order to fabricate the part. During the deposition, the material fuses with already deposited material. The extrusion head moves in the x- and y-plane while the build platform moves vertically in the z-plane. (Gibson et al. 2010, p. 157; Korpela et al. 2013, p. 1; Peltola et al. 2008, p. 13-14)

One of the benefits of FDM is a wide range of build materials that can be used for the part fabrication (Pham & Gault 1998, p. 1270). Materials that are used with FDM machines should be polymers that are rather amorphous than crystalline. Amorphous polymers can be extruded as a viscous paste since there is not an exact melting point, leading to a semi-solid material that softens when the temperature is gradually increased. In other words, the material viscosity is suitable for the extrusion since the extruded material maintains its shape and size and solidifies fast enough. This also enables the bonding of the newly extruded material and previously extruded material. Another important benefit is the mechanical properties of the fabricated parts. The parts fabricated with FDM are the strongest inside the polymer-based AM processes. (Gibson et al. 2010, p. 157-160)

There are several aspects that should be noted when using FDM for part fabrication. In FDM, the build material is extruded point-wise and thus building requires several

changes in direction. The size of the nozzle diameter can be changed by using nozzles of different kinds. Also the road width depends on the nozzle diameter. With a larger nozzle, the part fabrication is faster, but also the precision is lower. (Gibson et al. 2010, p. 157-158) It may be necessary to use support structures in order to prevent horizontal overhangs from falling (Upcraft & Fletcher 2003, p. 324). Since the printing software creates the support structures automatically, part orientation has a significant impact on the amount of supports required as well as on the build time and surface quality (Pham & Gault 1998, p. 1259). After the extrusion, the polymer material shrinks during rapid cooling. For this reason the dimensions of the fabricated part do not match with the dimensions of the modeled part. The shrinkage has a negative deviation along width and length, and a positive deviation along thickness. (Bansal 2011, p. 7) Holes of the nozzles are circular and thus it is not possible to fabricate sharp corners or edges. the sharpness depends on the diameter of the nozzle hole as well as on the movement characteristics and viscoelastic behavior of the filament material. (Gibson et al. 2010, p. 160-161) The properties of the parts fabricated with FDM are anisotropic. Hence, different layering strategies result in different part properties. (Upcraft & Fletcher 2003, p. 324) The parts fabricated by FDM may have small voids and bubbles inside them, leading to possible failure when mechanical stress is applied to them (Gibson et al. 2010, p. 159-160). Degradation of the material is also possible due to the elevated temperatures during the extrusion. (Gibson et al. 2010, p. 146)

### 2.6.1 Fused deposition modeling for biomedical purposes

FDM can be utilized also for biomedical purposes. Scaffolds with fully interconnected pores and controlled architecture have been successfully produced from biocompatible and biodegradable materials. (Chim et al. 2006, p. 933; Zein et al. 2002, p. 1176) FDM may also be useful for fabricating strong scaffolds for bone applications (Peltola et al. 2008, p. 14-15). When fabricating scaffolds, the purpose is to produce as strong scaffolds as possible. In addition, scaffolds should be as porous as possible in order to provide enough space for cells to grow and cell adhesion to happen. The pores are created by setting a specific distance between the extruded lines. Strength can be achieved by using nozzles with wider hole diameters and hence reduce the amount of individual lines. (Gibson et al. 2010, p. 162-164)

Even though FDM can be applied to produce scaffolds for biomedical purposes, there are still issues to be studied. Since the extruded material is in a form of a filament and usually mixed with ceramic particles, some difficulties may arise. Pressure generated by the feeding mechanism may be insufficient for pushing a semi-solid material through the nozzle due to ceramic particles in the polymer matrix. The pore distribution and filler geometry should be investigated, as well as how different parameters affect on those. Also the influence of mixing and processing on the degradation behavior should be investigated, since both affect the crystallinity and thus the degradation behavior and time. Knowledge over these may help to create scaffolds with both amorphous and

semi-crystalline areas that have the optimal mechanical properties and degradation behavior. (Drummer et al. 2012, p. 506; Gibson et al. 2010, p. 163)

### 2.6.2 Ultimaker 3D printer

The Ultimaker 3D printer (Figure 2.13) utilizes the FDM technique. The printer has won three prizes of being the most accurate, fastest and best open source hardware. It also has the fastest horizontal acceleration in the market as well as large build volume compared with many other open source printers. (Ultimaker Original [WWW]; Ultimaker wiki [WWW]) Some specifications and features of Ultimaker are stated in Table 2.1.


***Figure 2.13.*** *The Ultimaker 3D printer* (Ultimaker Original [WWW]).

***Table 2.1.*** *Ultimaker specifications and features* (Ultimaker Original [WWW]; Ultimaker specs and features [WWW]).

| | |
|---|---|
| **Technology** | Fused deposition modeling (FDM) |
| **Build material** | Polymer filament |
| **Weight** | 9 kg |
| **Frame size** | 358x338x389 mm |
| **Build volume** | 210x210x205 mm |
| **Print speed** | < 150 mm/s |
| **Theoretical resolution** | 0.0125 mm |

Ultimaker has several important advantages. It has a special kind of a print head design, which minimizes the weight and allows the print head to move very fast. Electronics are integrated and wires are plugged into one printed circuit board (PCB). Ultimaker is totally portable and it can be connected directly to an USB port of the comput-

er. Ultimaker is light-weight, relatively small in size and robust. In spite of size, build volume to frame volume ratio is 20%, which enables printing relatively large parts. The ratio is also very good when compared with other popular 3D printers of which have ratios of 3.2% and 1.4%. With Ultimaker it is possible to achieve the printing speed as fast as 150 mm/s, while the common printing speeds of many other 3D printers are around 30 mm/s. Even faster speeds can be achieved by the correct settings and calibration. The hot-end heats up to the printing temperature within two minutes and it can be assembled in under a minute. The geared material filament feeding mechanism is innovative since the filament can be changed during printing. This comes handy for example when printing multi-colored parts or if the printer runs out of the filament during a large print. The feature also reduces the excess material. Ultimaker is not limited to use a certain polymer material. Hence, it is possible to adjust the printer to work with several polymers as long as the material can be processed in a form of a filament. (Ultimaker Original [WWW]; Ultimaker specs and features [WWW])

As being the open source printer, experimenting and tuning possibilities with Ultimaker are almost limitless. In addition, the printer does not contain the digital rights management (DRM) technology. Hence, physical part upgrades are released online for free and they can be printed with Ultimaker. Also mechanical designs, software upgrades and electronics files are released online. (Ultimaker specs and features [WWW])

The printer casing is made of birch plywood and the build platform is made of acrylic glass. Several extruder parts are made of Delrin® acetal resin (polyoxymethylene) which has a unique combination of creep resistance, strength, stiffness, hardness, dimensional stability, toughness, fatigue resistance, abrasion resistance, low wear and low friction (Delrin acetal resin [WWW]). The print head design uses the special ceramic heater cartridge which is reliable, durable and easy to install. The print head also has the glass filled injection moulded polyether ether ketone (PEEK) thermal barrier which stays stable at high temperatures. (Ultimaker Original [WWW])

# EXPERIMENTAL PART

# 3 ULTIMAKER ASSEMBLY AND MODIFICATIONS

The complete Ultimaker kit was purchased from the Ultimaker online store (Ultimaker Original [WWW]). The kit included all the parts needed for assembling an appropriately functioning Ultimaker. Ultimaker was assembled by Pasi Kauppinen, since the electronics and correct assembly required advanced technical skills and knowledge.

After Ultimaker was assembled, the adjusting and calibration of the machine began. The purpose of that was to improve the printing quality. For those improvements, several upgrade parts were either printed or purchased. The modifications that were made to Ultimaker are discussed next in a form of a work report. Figures are used to clarify the functions and locations of the installed upgrade parts.

### Belt tensioners

Eight belt tensioners were installed in the both sides of all four x- and y-axis slider blocks (Figure 3.1). The STL file for printing the belt tensioners was downloaded from Thingiverse (Ultimaker Belt Tensioner [WWW]). The belt tensioners are created for tightening the long timing belts. Reserve in the original tightening clamps of the slider blocks was not enough to tighten the long timing belts properly. Too loose timing belts cause backlash error, which reduces the printing quality either by leaving gaps between the extruded lines or by leveling layers poorly on top of each other. On the other hand, too tight timing belts create too much friction for the stepper motors to provide enough torque to overcome the friction.

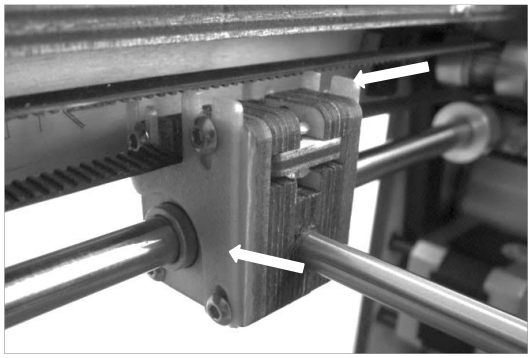

***Figure 3.1.*** *Two belt tensioners (indicated with white arrows) installed in the both sides of the slider block.*

There were some difficulties in tightening the belts evenly due to the manual adjustment of the belt tensioners. The tensioning of the belts is based on the pitch of the sound coming from the belts when vibrating them by hand. After trial and error the correct tension was found. There was an obvious improvement in the printing quality after the belt tensioners were successfully adjusted. Extruded lines aligned correctly and small features became more accurate.

### Feet for Ultimaker

Four strong feet with rubber dampers were installed in the bottom corners of Ultimaker. The STL files for printing the feet were downloaded from Thingiverse (Ultimaker Strong Foot [WWW]). Originally, Ultimaker stands on the table on its wooden frame, which causes the movement and vibration of the printer while printing. The feet are designed for stabilizing the printer. The rubber dampers were glued at the bottom of the feet in order to reduce the vibration and sound during printing. The feet also have openings in upper parts of them for wires located at the bottom of the printer. Figure 3.2 shows the foot from two different angles.

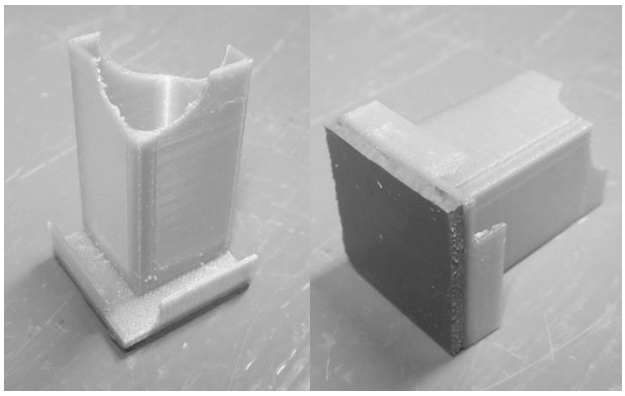

***Figure 3.2.*** *The foot for Ultimaker. An opening for wires can be seen on the left and a rubber damper on the right.*

The installation was easy to accomplish. Installing the feet clearly stopped the printer from moving at the table during printing. Also the vibration reduced. There was not a significant change in loudness. The foot has however a minor design error. Even though the feet themselves are very strong, the walls keeping the feet in their place are very thin and fragile (Figure 3.2). A couple of walls snapped when the printer was moved. Nevertheless, the feet are worth using. Another option could be either designing the better feet or bolting the printer onto the table.

### Cooling fan duct

The new cooling fan duct was installed (Figure 3.3) to replace the original foldable polypropylene fan duct. The STL file for printing the new fan duct was downloaded from

Thingiverse (Ultimaker Fan-Duct [WWW]). The new fan duct should direct the airflow more efficiently onto the part while printing and thus cool down the extruded material more rapidly. This should improve the printing quality, especially in the case of small features.

***Figure 3.3.*** *The cooling fan duct installed*.

The new fan duct is undoubtedly better than the original one. Air flows more accurately onto the newly extruded area. The fan duct is also much robuster than the old one. However, one problem still remained. The printed part was slightly distorted due to the airflow that came only from the other side of the part. For that reason a better cooling system should be designed in which the air flows more evenly around the part. One option could be another fan duct on the opposite side of the existing fan duct.

### Heat sinks for stepper motors

The aluminium heat sinks were attached to the x- and y-motors as well as on the material feeder motor in order to prevent the motors from overheating during printing. The stepper motors became very hot after printing a while. The heat sinks used for this purpose were originally meant for cooling computer processors. The bottoms of the heat sinks were sanded flat and attached to the motors with the double-sided thermal adhesive tape (Figure 3.4).

***Figure 3.4.*** *The heat sink attached to the material feeder motor*.

After attaching the heat sinks to the stepper motors, the maximum temperatures of the motors during printing clearly decreased. However, the material feeder motor still

became rather hot after printing a while. This can probably be explained by the fact that feeding the filament into the extrusion head requires quite much pressure which is generated by the feeder motor. A more efficient option could be coolers that include heat sinks, fans and thermally conductive adhesive pads.

### Quick connect shim for material feeder

The quick connect shim was installed around the inner part of the quick fit coupling which locates on the material feeder (Figure 3.5). The STL file for printing the quick connect shim was downloaded from Thingiverse (Ultimaker Quick Connect Shim [WWW]). The quick fit coupling is supposed to keep the bowden tube in place during printing. However, there was some leeway in the coupling that caused the bowden tube to move back and forth every time the retraction occurred. For this reason the retraction did not work as it should, causing scruffy prints. The quick connect shim should prevent the movement of the bowden tube.

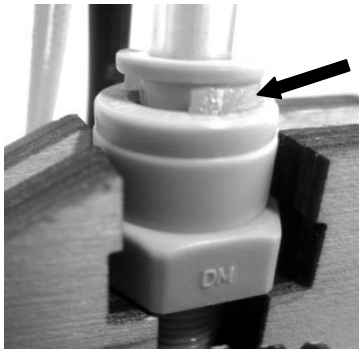

***Figure 3.5.*** *The quick connect shim (indicated with a black arrow) installed around the quick fit coupling.*

Even though the quick connect shim is a very simple design and easy to install, the effect on the printing quality was significant. After the installation, the retraction started to work flawlessly.

### Axis end caps

Eight new axis end caps were installed to replace the original wooden end caps. The STL files for printing the axis end caps were downloaded from Thingiverse (Ultimaker Axis End Cap [WWW]). The original end caps were replaced due to the slight longitudinal movement back and forth in the axis when the slider blocks changed their direction during printing. This movement may cause accuracy problems in the printed parts. Differences in the new cap compared with the old one were a hole in the middle of the cap for the M3 bolt and a hole inside the cap for a M3 hex nut. Before the installation, M3 hex nuts were embedded inside the end caps. Then the caps were screwed in place with M3 bolts which were first ground in a conical shape. The grinding was performed

in order to reduce the friction between the bolts and the axis. Next, M3 bolts were tightened until there was no more longitudinal movement in the axis when moving the axis back and forth by hand. The installed axis end cap is shown in Figure 3.6.

***Figure 3.6****. The axis end cap installed.*

The improvement on the printing quality is hard to prove since there were not a clear causation between the rod movement and printing quality before the installation. Nevertheless, the installation of the new end caps ensures that the printing quality will not be affected by the unnecessary movement in future.

### Reel holder

The new reel holder was installed to replace the original wooden reel holder (Figure 3.7). The STL files for printing the new reel holder were downloaded from Thingiverse (Ultimaker Reel Holder [WWW]). The old reel holder was otherwise strong and workable but semicircle plates visible in Figure 3.7 were too far from each other. That caused the reel to slip between the plates creating unnecessary friction while the reel revolved around the holder during printing.

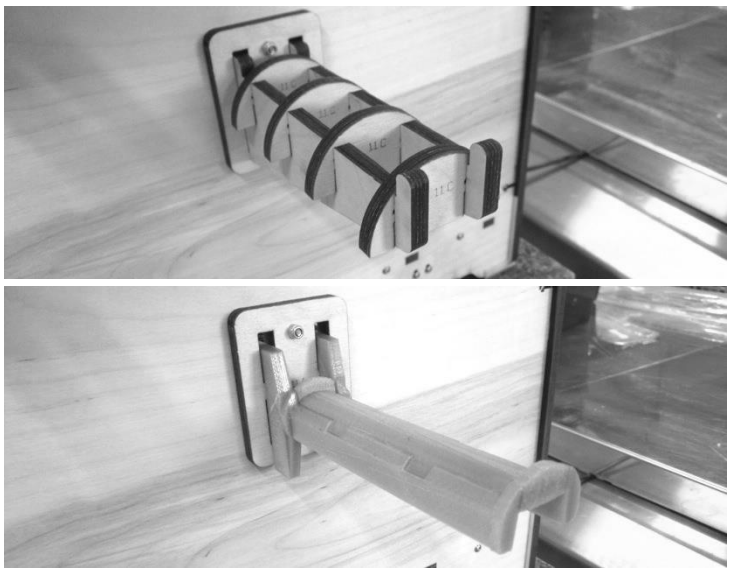

***Figure 3.7.*** *The old reel holder (above) and the new reel holder (below).*

The solid structure of the new reel holder fixed the problem. Also the polymeric surface of the holder is smoother than the old wooden one, reducing friction between the reel and the holder.

### UltiController LCD interface

UltiController is intended for controlling Ultimaker before, during and after printing. UltiController enables more possibilities to affect the printing parameters during printing than the printing software does. It is also possible to print stand-alone with UltiController. Therefore there is no need for having a computer attached to Ultimaker.

UltiController is developed by Bernhard Kubicek and it was ordered from the Ultimaker online store (UltiController Kit [WWW]). UltiController is made of laser cut birch plywood. It has a LCD screen which was pre-mounted to the UltiController electronics. Also the electronics were pre-assembled. UltiController can be directly connected with the Ultimaker electronics and it is self-powered. UltiController came with a 2 GB SD memory card.

The assembly of UltiController was very fast and easy. The electronics were put inside the laser cut birch plywood parts which were put together with nuts and bolts. The push-and-turn button was put in its place on top of UltiController. The wooden cover at the bottom of Ultimaker had to be removed in order to access the PCB and to connect UltiController with the Ultimaker electronics. After that, UltiController was ready for use. Assembled UltiController can be seen in Figure 3.8.


***Figure 3.8.*** *UltiController.*

UltiController is very easy to use. It is controlled with a single button which can be turned and pushed in order to navigate through the menus. The LCD screen is very clear and the menus are logical. A printable GCODE file can be chosen from the SD card after the file is saved in the card from the computer. The print status can be monitored and almost any parameter can be changed during printing. It is possible to affect the printing quality and find the optimal settings for different sections of the part while printing.

### Optional nozzles

The nozzle with the hole diameter of 0.25 mm was ordered from the QU-BD online store (V9 Brass Extruder Nozzle .25 mm [WWW]). Ultimaker came with the nozzle that has the hole diameter of 0.4 mm. The size of the nozzle defines the minimum feature size that can be printed. With a smaller nozzle it is possible to print more accurate parts.

The 0.25 mm nozzle is not originally developed for Ultimaker. Nonetheless, the nozzle is compatible with it. However, the inner diameter of the nozzle neck is thinner than the inner diameter of the hot end isolator tube. These two components are directly connected to each other and a semi-solid polymer flows through them during printing. The differences in the inner diameters may have an effect on the polymer flow properties and possibly cause clog formation in the hot end during printing. Thus far there have not been any problems in spite of several hours of printing. There are also other nozzle sizes available, the 0.25 mm nozzle being the smallest.

### Heating printing bed

The removable heating printing bed was assembled by Tomas Cervinka. The bed can be inserted onto the existing acrylic build platform and removed if necessary. The bed itself was order from the RepRap webpage (PCB Heatbed [WWW]). The electronics components were purchased either from the Farnell online store (Farnell [WWW]) or from a local electronics store. The instructions and schematics for assembling the first version of the bed can be found online (Heated Bed [WWW]). The first version consists of the cork plate as thermal insulator, PCB heatbed, aluminium build platform, power supply, other necessary electronics components, and foldback clips for mounting the bed onto the existing build platform. The first version is shown in Figure 3.9. After attaching the heating printing bed, it was necessary to update the Ultimaker firmware in order to be able to control the bed temperature. The necessary HEX file was downloaded from internet (UM 1.5.7 Heatbed Firmware [WWW]).

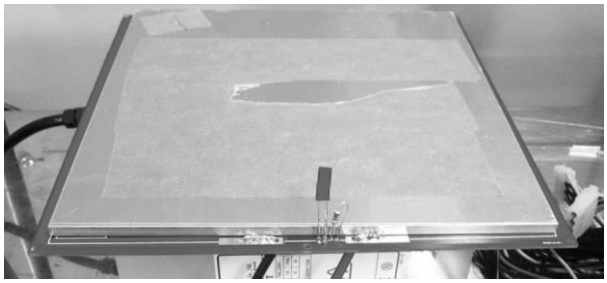

***Figure 3.9.*** *The heating printing bed with the taped aluminium plate*.

There were some issues with the heating printing bed. Heating the bed up to 65°C took about 15 minutes and slowed down towards the end. During printing the bed temperature decreased to 50°C, even though the temperature was supposed to remain at

65°C. A possible reason for this heating problem was identified to be a lack of a relay, since the Ultimaker electronics was not powerful enough for keeping the bed temperature stable during printing.

While heating up the bed, the tapes on the aluminium bed detached from each other due to heating effect, leaving visible gaps between the tapes. Also the removal of the printed part from the taped platform was very difficult since those were strongly attached to each other. A solution may be to print without the tape. However, the surface roughness of the aluminium plate is so high that the part would adhere very strongly with the plate, making the removal of the part at least as much difficult as with the tape. A better solution may be replacing the aluminium plate with a smoother one.

The foldback clips were somewhat too high. The cooling fan duct slightly hit on the clips while sliding over them during printing and thus lowering the bed at certain regions. This affects the first layers of the part by distorting them. The problem can be avoided by printing small enough parts and placing them correctly on the build platform in a way that the fan duct does not reach the clips during printing. However, this solution significantly downsizes the printing area. Another solution may be either attaching the heating printing bed onto the original build platform with screws or replacing it entirely in order to get rid of the clips. However, the downside would be the loss of the removability of the heating printing bed. Also some other temporary attaching mechanism may be a good idea.

Because of these problems, some improvements were performed to the bed. A relay was purchased. The instructions for assembling the upgraded version of the heating printing bed with the relay were found in internet (Heated Build Platform for Ultimaker [WWW]). Also the aluminium plate was replaced by the glass plate. The improved heating printing bed can be seen in Figure 3.10.


***Figure 3.10.*** *The improved heating printing bed inserted onto the original acrylic build platform by the foldback clips.*

The improvements were useful. Heating up time decreased. Heating the bed up to 70°C took about 5 minutes. The bed temperature also remained at that value during printing. Therefore, the bed started to work as it should and the temperature could be accurately controlled. The usage of the glass plate made it possible to get rid of the

tapes. The printed part also detached easily from the glass after the bed was cooled down. The problem with the foldback clips still remained.

### Direct drive upgrade

The direct drive upgrade is developed by Calum Douglas. The assemly instructions were downloaded from the website of the developer (Direct Drive Upgrade [WWW]). The purpose of the direct drive upgrade is to improve the extrusion head drive system. This can be achieved by relocating the x- and y-motor. Originally, the motors were located inside the main case and connected to the short belts (Figure 3.11). By placing the motors outside the main case on the ends of the shafts (Figure 3.12) the short belts can be disposed. This results in having only one long belt for each axis instead of having the short belt and the long belt in series. Thus the backlash error should be reduced, bringing improvement in layer-to-layer repeatability. Also the noise coming from the x- and y-motor should be reduced since the motor brackets, flexible shaft couplers and spacers are placed between the main case and the motors (Figure 3.13). Some of the parts required for the upgrade were the original Ultimaker parts that were reused, such as motors, spacers, bolts and nuts. However, a few parts needed to be acquired. The original shafts were too short for the upgrade. For that reason a silver steel shaft was purchased from Rollco Oy (Hardened Precision Shaft W). Since the shaft was two meters long, it was cut according to the instructions. The flexible shaft couplers were ordered from eBay (Flexible Shaft Coupler [WWW]). The motor brackets were printed with Ultimaker and the STL file for those was downloaded from the website of the developer.

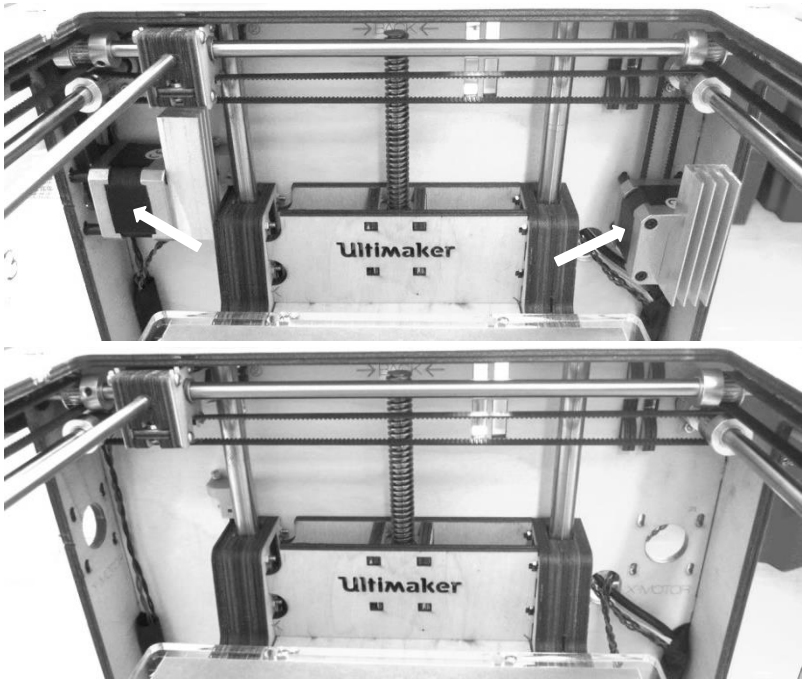


***Figure 3.11.*** *The x- and y-motors (indicated with white arrows) inside the main case connected to the short belts (above) and being removed (below).*

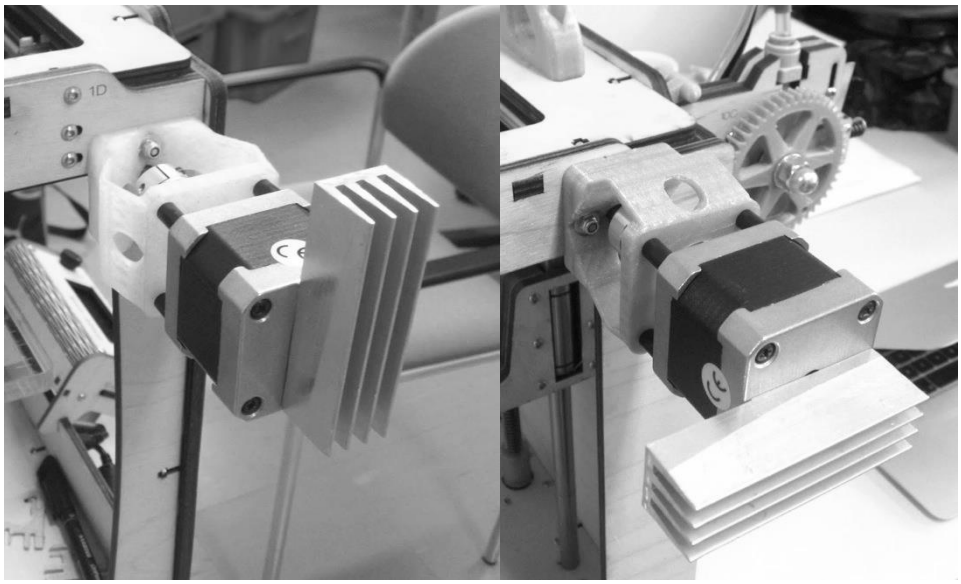

***Figure 3.12.*** *The x-motor (left) and y-motor (right) mounted outside the main case.*

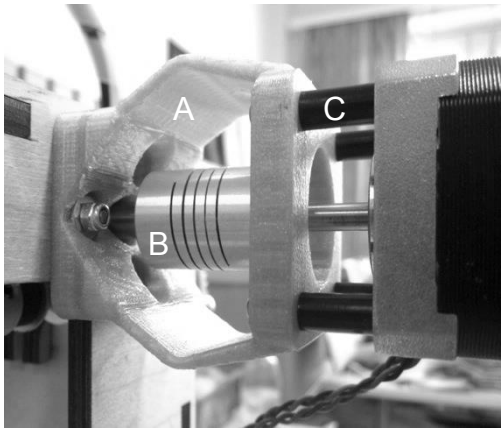


***Figure 3.13.*** *The stepper motor mounting. The motor bracket (A), flexible shaft coupler (B) and spacer (C).*

Before starting the assembly, the belt tensioners were loosened and the necessary axis end caps were removed. In order to keep the x- and y-axis aligned, the original shafts were removed and new ones installed one by one. Since the tolerances of the new shafts were tighter than the tolerances of the original ones, some oil was required in order to slide the shafts through the bearings. Next, the motor bracket was mounted onto the main case with M3 bolts and M3 self-locking nuts. Then the flexible shaft coupler was put inside the motor bracket and the end of the shaft was slid into the 8 mm hole of the coupler. After that the stepper motor was mounted on the bracket with M3 bolts. Also the spacers were put between the bracket and the motor. Simultaneously, the motor axle was slid into the 5 mm hole of the coupler. Finally, the nuts of the coupler were tightened in order to keep the shaft and the motor axle in place.

Before the direct drive upgrade, the short and long belts were already well tightened and the printing quality was rather good. Therefore the effect on the backlash error is hard to prove. The extrusion head began to move more effortless. This may be due to

the decrease in force required from the motors while moving the extrusion head, resulting from disposing of the short belts. Also the noise coming from the motors was reduced slightly.

### Bowden tube clamp for extrusion head

The new strong bowden tube clamp mechanism was installed to replace the original weak clamp mechanism (Figure 3.14). The STL files for printing the new clamp mechanism were downloaded from Thingiverse (Bowden Clamp for Ultimaker [WWW]). The original clamp mechanism contains the white bowden tube clamp and blue horseshoe. Those are supposed to keep the bowden tube at its place while printing and prevent the tube from popping out. However, after a few months of active printing the clamp mechanism failed during printing. For that reason the new bowden tube clamp mechanism was printed and installed. In order to do so, the amplifier circuit board assembly had to be mounted at a different position to get the new clamp to fit in its place. Fortunately there were ready-made holes for that in the top wooden part of the extrusion head. Otherwise the installation was quick and easy. The new clamp mechanism contains three components; a riser, tightening cone and nut. The riser was mounted onto the extrusion head with three existing mounting screws. The tightening cone was put around the bowden tube and into the riser. The bowden tube was firmly tightened at its place by screwing the nut around the riser.

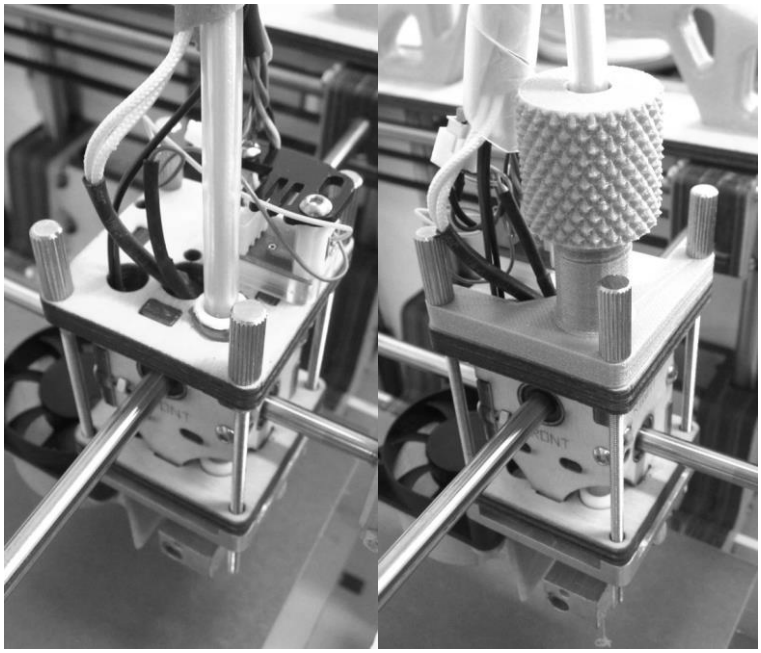

***Figure 3.14.*** *The original (left) and new (right) bowden tube clamp mechanism.*

The new bowden tube clamp mechanism has worked flawlessly after the installation. It feels very strong compared with the original one and the bowden tube stays very

firmly at its place. The tube can also be released quickly and easily, which is useful in cases of cleaning the tube or removing the blockage.

### Filament feeder upgrade

The STL files for printing the filament feeder upgrade were downloaded from Thingiverse (Ultimaker Extruder Gear Upgrade [WWW]; Ultimaker Quiet Retraction [WWW]). The original feeder and the upgraded feeder can be seen in Figure 3.15. The main reason for the upgrade was the original wooden extruded gear that was bend for some reason, which caused the gear to grind against the filament feeder clamp while printing. The upgrade should also bring other benefits compared with the original one. The hook mechanism, that fastens the feeder on the frame, should reduce the noise generated by the material feeder motor. The more flexible structure of the feeder should enable the feeder to follow the movements of the extrusion head, relieving some tension from the bowden tube. Also the bowden tube coupling holder mechanism should be more reliable.

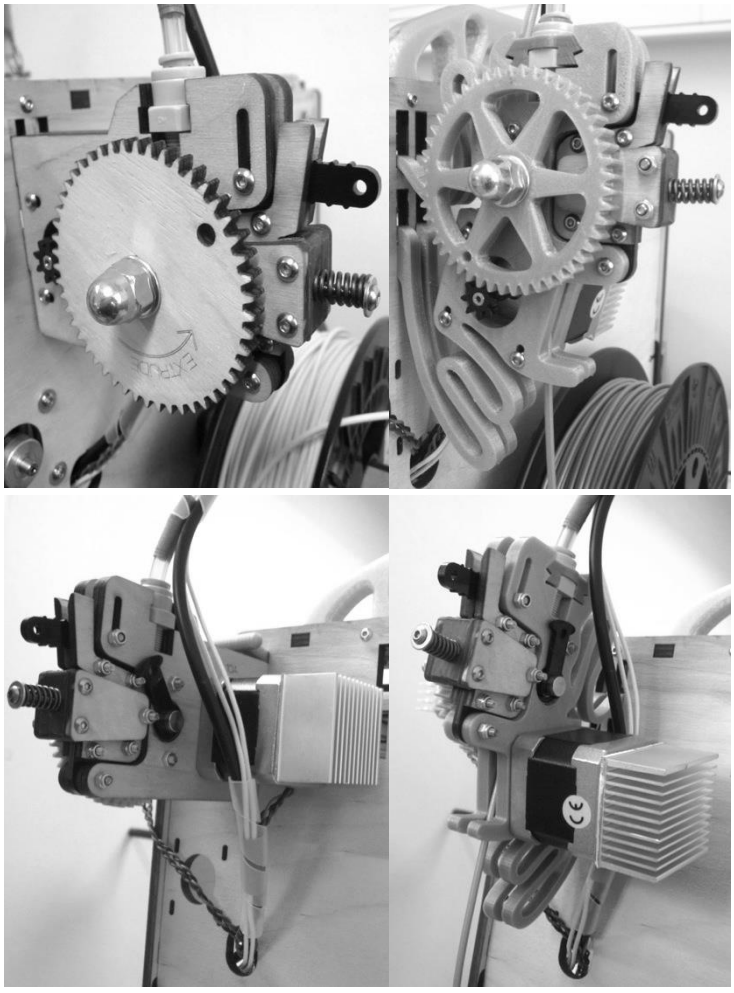

***Figure 3.15.*** *A front view of the original (upper left) and the upgraded (upper right) filament feeder. A back view of the original (lower left) and the upgraded (lower right) filament feeder.*

The installation required some time since several original components were used in the upgraded version again. Therefore the original feeder had to be disassembled before being able to assemble the upgraded one. Otherwise the installation worked out well and all the old and new components fit together flawlessly. The grinding problem disappeared after the upgrade. Also the noise reduced a bit. The tension relieving effect is hard to prove. At least the feeder follows the movements of the extrusion head. It is also hard to prove whether or not the coupling holder mechanism is better than the original one since there were no problems related to it beforehand.

# 4 RESEARCH MATERIALS AND METHODS

In this chapter it is evaluated how the processing conditions and parameters affect the performance of parts fabricated by the FDM technique. Materials as well as methods used for fabricating the samples are introduced. The samples were characterized by mechanical, thermal and microscopic analysis. The mechanical properties were investigated by tensile testing. Thermal analysis was done by DSC analysis. Possible changes in the molecular weights due to processing were studied by the inherent viscosity (IV) measurements. The surface quality as well as dimensional accuracy and stability of the samples were investigated by x-ray microtomography (MicroCT) imaging, necessary measurements and visual inspection.

## 4.1 Materials

Five different biodegradable polymer filaments were studied in this thesis:

- Polylactide, PLA silver grey, diameter 2.85 mm, filament manufacturer: Ultimaking Ltd. (PLA Silver-Grey [WWW])
- Poly(L-lactide-co-D,L-lactide) (70/30), PLA 70/30, medical grade, diameter 2.80 mm, raw polymer manufacturer: Corbion Purac, filament manufactured in-house
- Poly(L-lactide-co-D-lactide) (96/4), PLA 96/4, medical grade, diameter 2.94 mm, third party material, filament manufacturer: N/A
- Polybutylene succinate (PBS), Bionolle 1020 MD, injection molding grade, diameter ~3 mm, raw polymer manufacturer: Showa Denko K.K., filament manufactured in-house
- Cyclo Olefin Copolymer (COC), Topas 5013, extrusion grade, diameter 2.50 mm, raw polymer manufacturer: Topas Advanced Polymers, filament manufactured in-house

## 4.2 Filament manufacturing

PLA 70/30, Bionolle 1020 MD and Topas 5013 granules were extruded in-house to a form of a filament, diameters being under 3 mm in order to be able to print the materials with the Ultimaker 3D printer. After the extrusion, the filaments were wound on reels by hand, except during the PLA 70/30 filament manufacturing, where the filament was wound on a reel automatically by placing the reel at the extrusion line (Figure 4.1).

However, this procedure was not very successful since the filament was too loose around the reel.

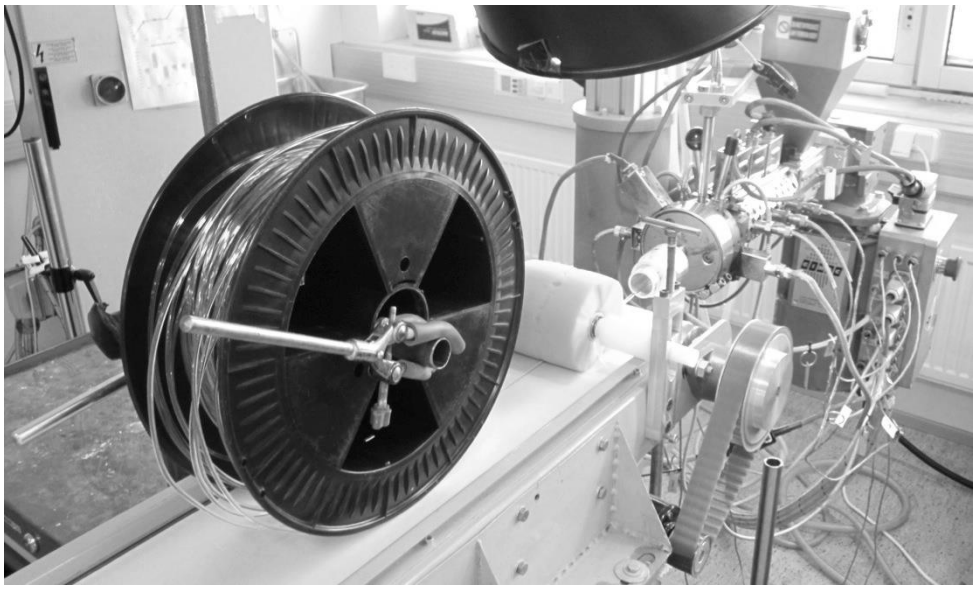

***Figure 4.1.*** *The extrusion line and the experimental winding mechanism.*

Prior to the filament manufacturing, PLA 70/30 granules were dried in the vacuum chamber for seven hours. Then the temperature of the vacuum chamber was set up to 80°C for sixteen hours. Bionolle 1020 MD granules were dried in the vacuum chamber in 80°C for seven hours. Topas 5013 granules were dried in the vacuum chamber for approximately twenty four hours without heating. The filaments were manufactured by using the Gimac single screw microextruder (Gimac, Castronno, Italy) with 12 mm screw diameter, 4 mm nozzle and big-holed breaker plate. The temperatures of the heating zones, screw speeds and drawing speeds are shown in Table 4.1.

***Table 4.1.*** *The screw speeds, drawing speeds and temperatures of the heating zones used in the filament manufacturing.*

| **Material** | **Screw speed (rpm)** | **Drawing speed (m/min)** | **Temperature (°C)** | | | | | |
|---|---|---|---|---|---|---|---|---|
| | | | **Zone 1** | **Zone 2** | **Zone 3** | **Zone 4** | **Zone 5** | **Zone 6** |
| **PLA 70/30** | 15 | 3.7 | 170 | 80 | 90 | 200 | 220 | 240 |
| **Bionolle 1020 MD** | 15 | N/A | 90 | 100 | 120 | 100 | 110 | 135 |
| **Topas 5013** | 20 | N/A | 230 | 235 | 240 | 245 | 250 | 250 |

## 4.3 Sample models

The models of the printed samples that were characterized in this thesis were modeled with Solidworks 3D CAD software and saved in the STL file format. The modeling was performed by Tomas Cervinka. The summary of the sample models, materials used for fabricating the samples and characterization methods are shown in Appendix 1. Sample A was designed for tensile testing purposes. Sample B was designed for determining the circularity of the round and hexagonal holes in the printed plate. The surface quality of different sizes of hemispheres printed on the plate was examined from Sample C. Sample D was designed for studying the dimensional accuracy of the thin walls. The dimensional stability measurements were performed on Sample E, F and G.

## 4.4 Model preparation and sample printing

The Cura slicing software versions 13.04 and 13.06.5 were used for preparing the models created with Solidworks 3D CAD software. Cura is an open-source slicing software developed for the Ultimaker 3D printer. Cura includes everything that is needed for preparing the model for printing. The prepared models were saved in the GCODE file format which includes all information the printer requires for fabricating the samples. The Cura settings used for sample printing are shown in Appendix 2. All other settings were kept as default. The Ultimaker 3D printer was used for printing the samples. The device folder for Ultimaker is in Appendix 3.

## 4.5 Tensile testing

The influence of the printing parameters on the mechanical properties of the printed samples was investigated by tensile testing. Samples were made of different materials and printed at different temperatures. The dimensions of the tensile testing sample do not comply with any standard. However, the sample size and shape comply with an internal standard of the department. Thus, the results are comparable within the department. The dimensions of the testing sample are shown in Figure 4.2.

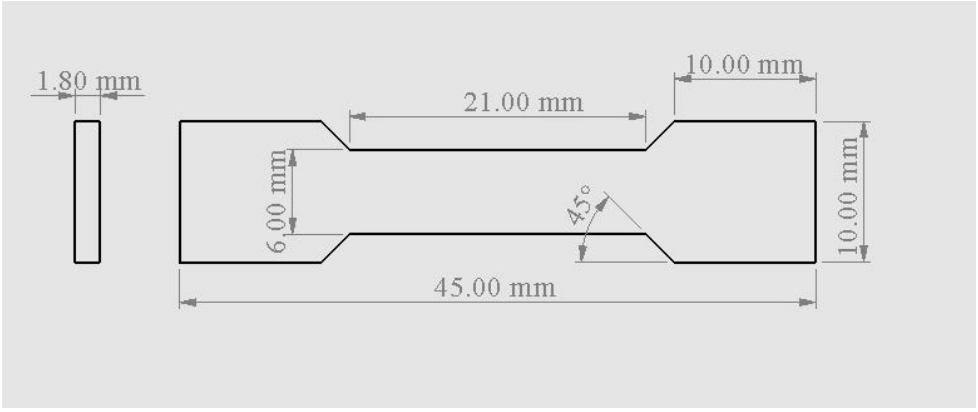


***Figure 4.2.*** *The dimensions of the tensile testing sample.*

The machine used for testing was Instron 4411 material testing machine (Instron Ltd., High Wycombe, England). The testing parameters were: grip distance of 25 mm, gauge length of 20.44 mm, load cell of 5 kN, crosshead speed of 20 mm/min. Tests were carried out at the room temperature and the samples were dry. Five parallel samples were tested, except in case of Bionolle 1020 MD only two samples were tested. The average maximum load, displacement, stress and strain, as well as Young's modulus were automatically calculated by the Instron IX software (Intron Series IX, version 8.31).

## 4.6 Differential scanning calorimetry analysis

Differential scanning calorimetry (DSC) analysis was performed in order to investigate changes in a thermal history of the different materials. The DSC TA Q1000 machine (TA Instruments, New Castle, USA) was used. The starting temperature of the cycle was 0°C and ending temperature 200°C. The heating speed was 20°C/min and cooling rate 50°C/mm. Two heating cycles and one cooling cycle were performed for two parallel samples. The resulting DSC curves were analyzed with the Universal Analysis software. The melting temperatures ($T_m$) and melting enthalpies ($\Delta H_m$) were determined from the first cycles and the glass transition temperatures ($T_g$) from the second cycles. Granules, filaments and printed samples of different materials were analyzed.

## 4.7 Inherent viscosity measurements

The inherent viscosities (IV) were measured by viscometric analysis with the Lauda PVS equipment (Lauda-Königshofen, Germany) and Ubbelohde 0c capillars (Schott-Instrument, Mainz, Germany) in chloroform solvent at 25°C. The measuring equipment and measurements comply with ISO 1628-1:1998 (E) and ISO 3105:1994 standards. The weights of the polymer samples were 20 $\pm$ 1 g. The samples were dissolved in chloroform overnight. Two parallel samples were used. The inherent viscosities of raw materials, filaments and samples were determined. The IV was determined from the flow time of the polymer solution through the capillary relative to the flow time of the solvent through the capillary. The inherent viscosities were calculated from the equation below.

$$\eta_{inh} = \frac{ln\frac{\eta_{sample}}{\eta_{solvent}}}{c}, \tag{4.1}$$

where $\eta_{sample}$ and $\eta_{solvent}$ are kinematic viscosities and $c$ is the concentration of the polymer solution. $\eta_{inh}$ is reported in deciliters per gram (dl/g). The inherent viscosity values were automatically calculated by the Lauda PVS software.

## 4.8 Surface quality inspection

The surface quality of the hemispheres printed on the plate was inspected visually from Sample C. The purpose of the surface quality inspection was two-folded. The first aim was to determine how well the printer is able to print all the hemispheres. The second aim was to determine whether the retraction has an effect on the surface quality or not. The retraction means that the filament is pulled back into the nozzle when the extrusion head is moving over a gap while printing. The retraction reduces the amount of thin lines, called strings, within a printed part. However, using the retraction may also result in scruffy prints and hence reduced surface quality. For this reason Sample C was printed twice with and without using the retraction.

## 4.9 Dimensional accuracy and stability measurements

The dimensional accuracy was determined from Sample B and D. Both samples were imaged with the MicroCT imaging system (Zeiss X-Radia MicroXCT-400). The imaging was performed by Kalle Lehto. The MicroCT parameters for Sample B were: pixel size of 37.3366 µm, acceleration voltage of 80 kV, 0.4x objective lens, shutter speed of 0.7 s. The MicroCT image of Sample B was analyzed with the Avizo Fire 3D analysis software for materials science in order to determine the circularity of the round and hexagonal holes of Sample B. With Avizo Fire it is possible to visualize and analyze qualitative and quantitative information about material structure images (Avizo Fire [WWW]). The actual diameters, perimeters and areas of the holes were measured from the MicroCT image. From those values the circularity of the holes was calculated using a formula below.

$$f_{circ} = \frac{4\pi A}{p^2}, \tag{4.2}$$

where $f_{circ}$ is the circularity, $A$ is area, and $p$ is perimeter. The circularity was calculated automatically by the analysis software. Also comparison between the initial modeled diameters and actual diameters of the holes was performed.

The thicknesses of the thin walls were determined from Sample D by MicroCT imaging and related measurements. The MicroCT parameters for Sample D were: pixel size of 33.9458 µm, acceleration voltage of 90 kV, 0.4x objective lens, shutter speed of 0.6 s. The initial modeled wall thicknesses were compared with the actual wall thicknesses of the printed sample in order to determine how accurately the dimensions of the printed sample correspond to the dimensions of the model.

The dimensional stability measurements were performed on Sample E, F and G to find out how accurately the dimensions of the samples remain constant along x, y- and z-directions. The actual thicknesses of the Sample E and F were measured from multiple points with a digital slide gauge and compared with the initial modeled thicknesses. Figure 4.3 shows the measuring points of Sample E and F.

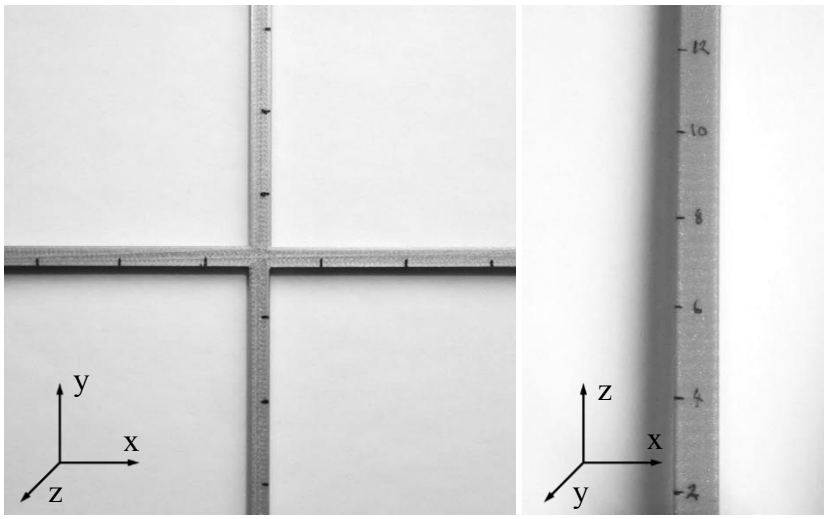


***Figure 4.3.*** *Partial Sample E (left) and F (right). The measuring points are marked with black.*

Sample G was imaged with MicroCT in order to determine the dimensional stability along z-direction on the outer surface. The MicroCT parameters for Sample G were: pixel size of 23.4109 µm, acceleration voltage of 140 kV, 0.4x objective lens, shutter speed of 0.6 s. The dimensional stability was determined only by visual inspection from the MicroCT image, further measurements were not used.

# 5 RESULTS AND DISCUSSION

## 5.1 Filament manufacturing and sample printing

The quality of the produced PLA 70/30 filament was excellent with constant diameter. The diameter of the Bionolle 1020 MD filament varied during the filament manufacturing, being slightly below and above 3.0 mm. The Topas 5013 filament became a bit grainy, but the diameter was constant.

Printing the samples with the commercial PLA silver grey filament was trouble-free, probably because it was meant for the Ultimaker 3D printer. With other materials printing was more challenging. When printing the tensile samples from the PLA 70/30 filament at 220°C and 230°C, the infill did not bond adequately with the outline and the printing quality on the corners was mediocre (Figure 5.1). Reason for that was probably too low printing temperature. As Gibson et al. (2010, p. 151) stated, enough heat energy must be supplied in order to activate the surfaces of the previous layers to enable bonding. Otherwise, distinct boundaries exist between the new and previously deposited lines or layers. After the printing temperature was increased to 240°C and 250°C, bonding improved and the printing quality enhanced. However, the outline/infill effect could still be detected (Figure 5.1). At 260°C the polymer started to become liquid, preventing printing. The same outline/infill effect was observed when printing with the PLA 96/4 filament. The effect was partially corrected by increasing the printing temperature.

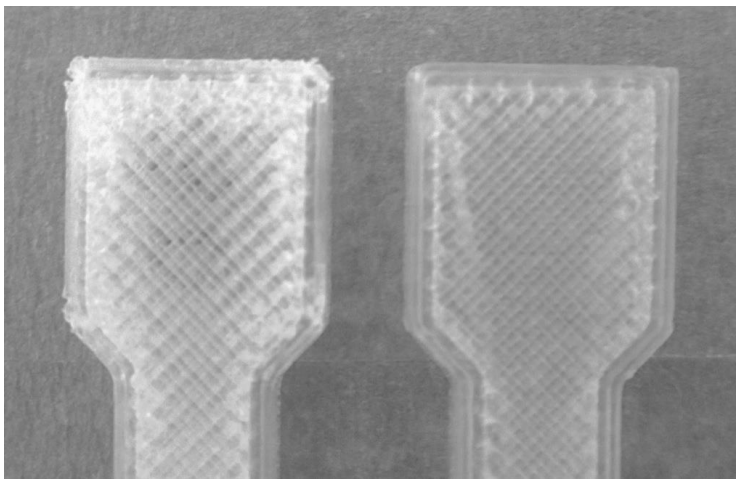

***Figure 5.1.*** *The PLA 70/30 tensile samples printed at 220°C (left) and at 250°C (right).*

The Bionolle 1020 MD filament did not come out from the nozzle very easily. The reason for that may be the varying diameter of the filament, as mentioned earlier. The filament diameter should be below 3.0 mm since the bowden tube of the printer is 3.0

mm wide. The filament is supposed to move effortlessly through the bowden tube. However, it was possible to print with Bionolle 1020 MD filament since it was soft enough in order to come out from the nozzle despite the varying diameter of the filament. The Bionolle 1020 MD filament also extruded out from the nozzle helically, as it remembered the screw extrusion process during the filament manufacturing. In addition, some warping occurred, meaning that samples adhered poorly to the build platform. The usage of the removable heating printing bed did not fix the warping problem. However, two parallel tensile samples were successfully printed at 200°C and 220°C. With Topas 5013 filament, printing was not successful at all since the extruded lines were popping up from the build platform instantly after the extrusion and the material did not adhere with previously printed material. Changing the printing temperature or using the removable heating printing bed did not fix the problem. In the case of the Binolle 1020 MD and Topas 5013 filament, a closed build chamber with controlled environment could be used to ensure that the temperature differential between the extruded material and surrounding atmosphere remains as minimal as possible, as Gibson et al. (2010, p. 149) has suggested. In addition, the cooling process should be carried out gradually and slowly. However, with Ultimaker this is not possible.

## 5.2 Mechanical properties

The average tensile strength values of the PLA silver grey samples printed at four different temperatures with two different nozzles and printing speeds are shown in Figure 5.2.

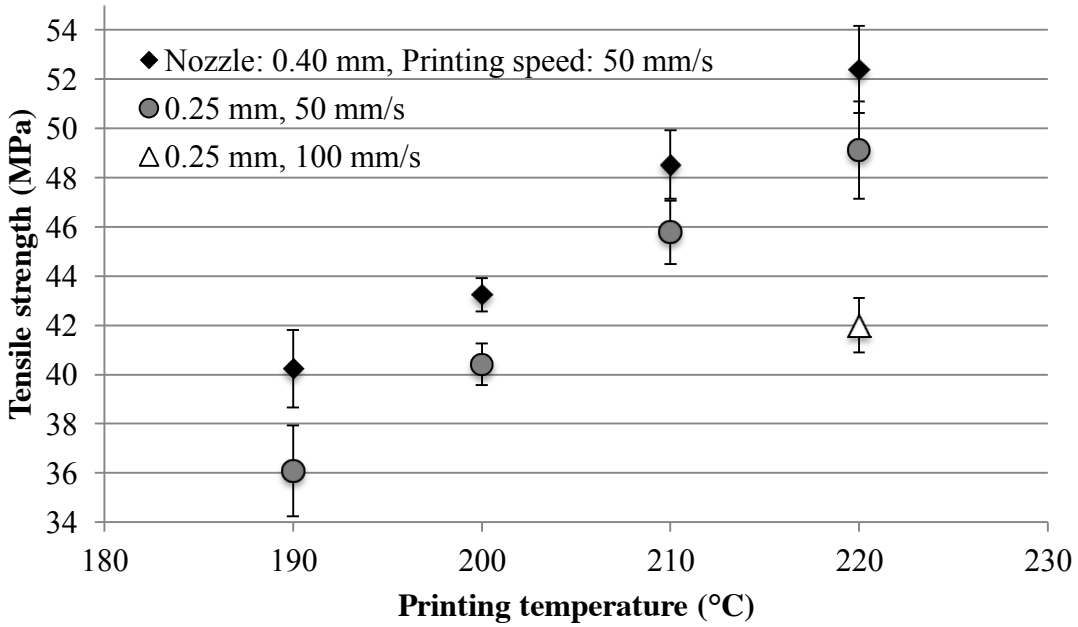


***Figure 5.2.*** *The average tensile strength values of the PLA silver grey samples printed at four different temperatures with two different nozzles and printing speeds. Also standard deviations are shown. Five parallel samples were tested.*

As can be seen from the Figure 5.2, the tensile strength increases when the printing temperature is increased. The tensile strength also increases when the bigger nozzle is used. Increasing the printing speed affects the tensile strength by decreasing it. Hence, it can be assumed that printing at higher temperatures with bigger nozzles and lower speeds increases the tensile strength of the sample. The Young's modulus of the samples varied from 1220 MPa to 1400 MPa, standard deviation being between 30 MPa and 140 MPa. The maximum strain varied from 4.3% to 4.8%. There was nothing notable in those values, except the fact, that the strain values indicate that the PLA silver grey samples fabricated by FDM are brittle in nature. Hence, the fracture occurs rapidly without deformation under load.

The average tensile strength values of the PLA 70/30 samples printed at four different temperatures with 0.4 mm nozzle and printing speed of 50 mm/s are shown in Figure 5.3.

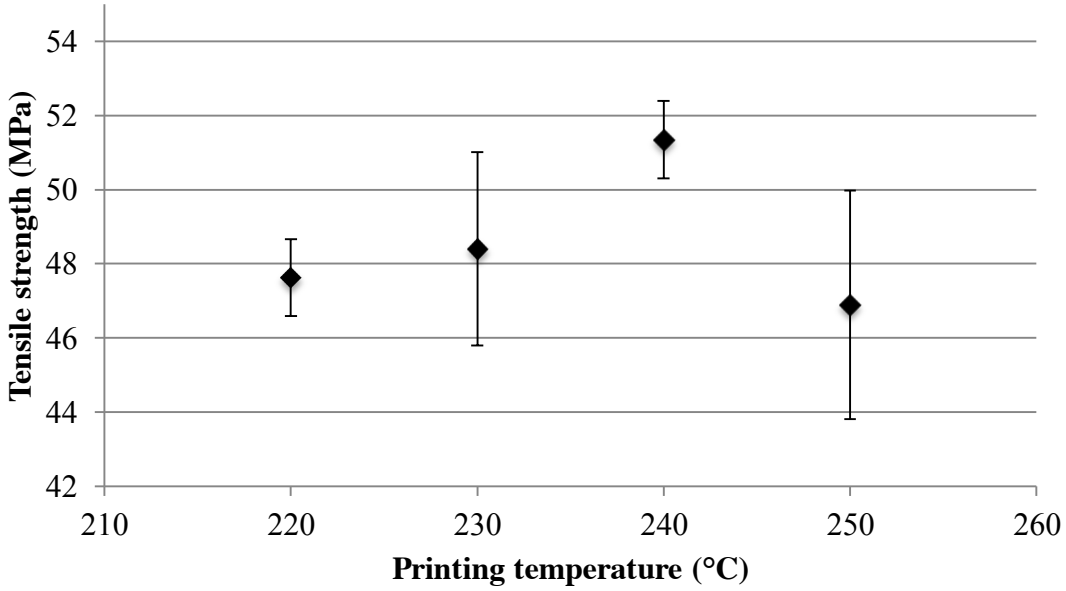


***Figure 5.3.*** *The average tensile strength values of the PLA 70/30 samples printed at four different temperatures with 0.4 mm nozzle and printing speed of 50 mm/s. Also standard deviations are shown. Five parallel samples were tested.*

As can be seen from Figure 5.3, the tensile strength increases along the printing temperature, except at 250°C. Therefore it can be assumed that at a certain point when increasing the printing temperature, the tensile strength begins to decrease. The Young's modulus of the samples varied from 1340 MPa to 1470 MPa, standard deviation being between 60 MPa and 120 MPa. The maximum strain varied from 4.4% to 5.2%. From the strain values, it can be concluded that the PLA 70/30 samples fabricated by FDM are brittle in nature.

The average tensile strength values of the PLA 96/4 samples printed at two different temperatures with 0.4 mm nozzle and printing speed of 50 mm/s are shown in Figure 5.4. Also the flow rate was changed when printing the samples, 100% being the standard flow rate.

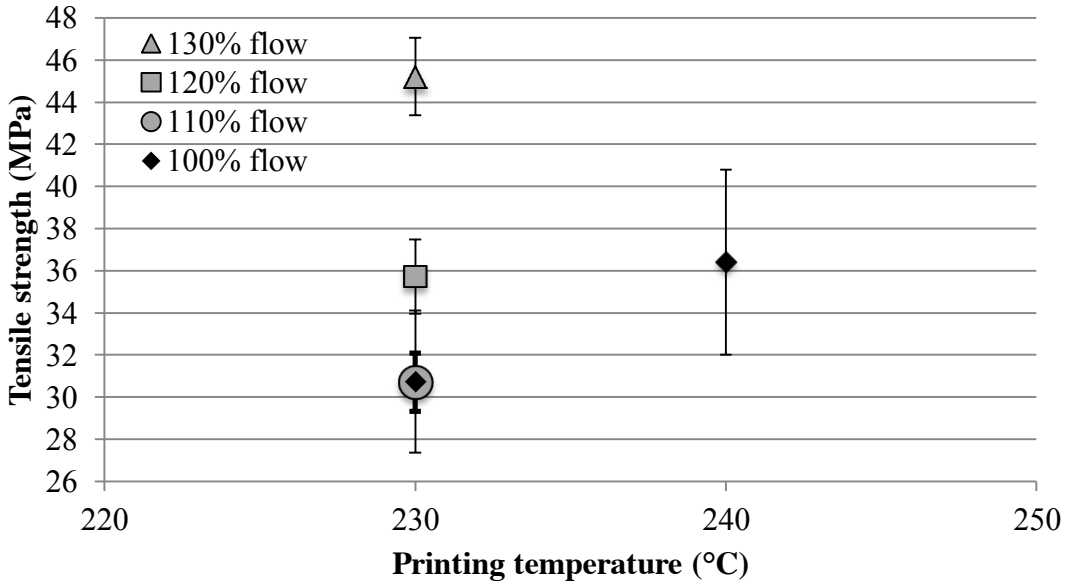


***Figure 5.4.*** *The average tensile strength values of the PLA 96/4 samples printed at two different temperatures with 0.4 mm nozzle, printing speed of 50 mm/s and four different flow rates. Also standard deviations are shown. Five parallel samples were tested.*

Increasing the flow rate increases the amount of filament that is being extruded from the nozzle. An increase of 10% did not affect the tensile strength. Increases by 20% and 30% increased the tensile strength in a clear manner. The reason for that may be the overextrusion, causing the extruded lines to overlap and bond more efficiently to each other. However, the overextrusion usually distorts the shape and size of the part. Hence, the optimal settings between the strength and external properties of the part must be considered carefully by the terms of the final application. Similar aspects are also stated by Gibson et al. (2010, p. 154-156).

The average Young's modulus values of the PLA 96/4 samples printed at 230°C and with four different flow rates are shown in Figure 5.5.

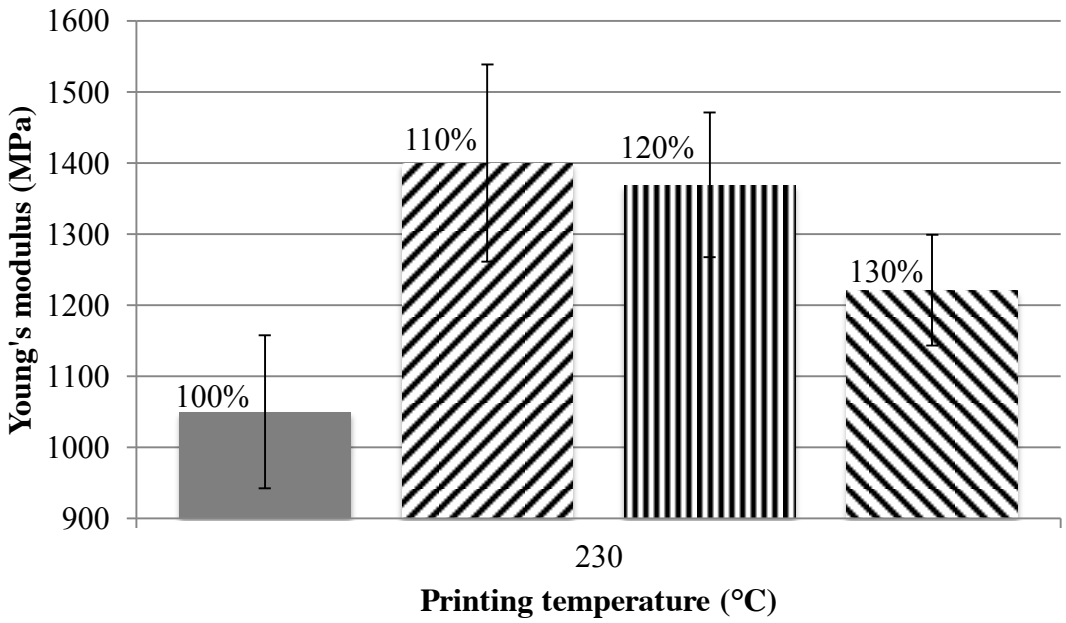


***Figure 5.5.*** *The average Young's modulus values of PLA 96/4 samples printed at 230°C with 0.4 mm nozzle, printing speed of 50 mm/s and four different flow rates. The flow rates are marked above the bars. Also standard deviations are shown. Five parallel samples were tested.*

The Young's modulus of the PLA 96/4 samples behaved in an opposite way compared with tensile strength when the flow rate was increased, as can be seen from Figure 5.5. The highest modulus was obtained with an increase of 10%. The modulus decreased steadily when increasing the flow rate. For comparison, the Young's modulus of the samples printed at 240°C with the standard flow rate was 1140 MPa, standard deviation being 70 MPa. The value was lower than the one obtained with a 30% increase. Hence, changing the flow rate gives further possibilities when selecting the optimal parameters for printing. The maximum strain of all PLA 96/4 samples varied from 4.6% to 4.8%. From strain values, it can be concluded that the PLA 96/4 samples fabricated by FDM are brittle in nature.

The mechanical properties of PLA can vary from soft and elastic materials to stiff and high-strength materials, depending for instance on crystallinity, structure, molecular weight, material formulation and orientation (Sin et al. 2012, p. 177). For comparison, the maximum tensile strength, Young's modulus and strain values of the tested PLA samples along with the corresponding literature values, reported by different sources, are shown in Table 5.1 (Auras et al. 2004, p. 851; Jamshidian et al. 2010, p. 560; Sin et al. 2012, p. 180).

***Table 5.1.*** *The maximum tensile strength, Young's modulus and strain values of the tested PLA samples along with the corresponding literature values reported by different sources.*

| | **Auras et al.**[(1)] | **Jamshidian et al.** | **Sin et al.** | **PLA silver grey** | **PLA 70/30** | **PLA 96/4** |
|---|---|---|---|---|---|---|
| **Tensile strength (MPa)** | 44-59 | 48-53 | 55-59 | 52 | 51 | 36 |
| **Young's modulus (MPa)** | 3750-4150 | 3500 | 3550-3750 | 1400 | 1470 | 1140 |
| **Strain (%)** | 4-7 | 30-240 | 1.5-7 | 4.8 | 5.2 | 4.8 |

[(1)] Samples were injection molded.

The tensile strengths of the PLA silver grey and PLA 70/30 samples were inside the reported literature values. The tensile strengths of the PLA 96/4 samples were slightly lower. The Young's modulus of all PLA samples were clearly lower than the corresponding literature values. The strains of all PLA samples corresponded with values reported by Auras et al (2004, p. 851) and Sin et al. (2012, p. 180).

The average tensile strength values of the Bionolle 1020 MD samples printed at two different temperatures with 0.4 mm nozzle and printing speed of 50 mm/s are shown in Figure 5.6.

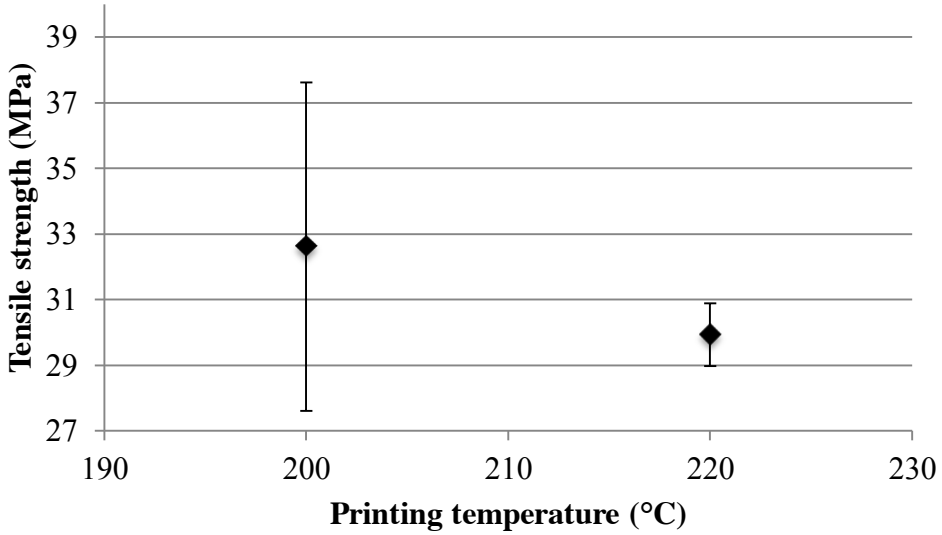


***Figure 5.6.*** *The average tensile strength values of the Bionolle 1020 MD samples printed at different temperatures with 0.4 mm nozzle and printing speed of 50 mm/s. Also standard deviations are shown. Two parallel samples were tested.*

It should be noted that since only two parallel samples were tested, the reliability of the results probably suffered. According to Figure 5.6, the tensile strength is higher with samples printed at 200°C than at 220°C, being 33 MPa. For Bionolle 1020 MD, the lit-

erature value of the tensile strength is 62 MPa according to the manufacturer (Showa Denko K.K. [WWW]). Hence, the tensile strengths of the samples are clearly lower in comparison with the literature value. The Young's modulus of the Bionolle 1020 MD samples varied from 310 MPa to 340 MPa, standard deviation being between 14 MPa and 24 MPa. The values are lower than the literature value 470 MPa (Showa Denko K.K. [WWW]). The maximum strain of two parallel samples printed at 200°C varied significantly, the values being 20% and 460%. The average maximum strain of other two parallel samples printed at 220°C was 20%, standard deviation being 1.7%. The actual reason for the high strain value of one sample remained unknown since all the printing parameters were kept the same between the parallel samples. The literature value of the maximum strain is reported being 660% (Showa Denko K.K. [WWW]).

## 5.3 Thermal properties

The melting temperatures ($T_m$), melting enthalpies ($\Delta H_m$) and glass transition temperatures ($T_g$) of the granules, filaments and printed samples were determined by DSC analysis. The results are shown in Table 5.2, where "-" indicates that the sample in question does not exist, and "x" indicates that the particular property does not exist.

***Table 5.2.*** *The average $T_m$, $\Delta H_m$ and $T_g$ values of the different materials. Two parallel samples were analyzed.*

| Material | Melting temperature $T_m$ (°C) | Melting enthalpy $\Delta H_m$ (J/g) | Glass transition temperature $T_g$ (°C) |
|---|---|---|---|
| **PLA silver grey** | | | |
| Granule | – | – | – |
| Filament | 154.4 | 10.7 | 58.5 |
| Sample (190°C) | 154.9 | 3.0 | 58.7 |
| Sample (220°C) | 152.8 | 4.7 | 58.4 |
| **PLA 70/30** | | | |
| Granule | 121.8 | 12.9 | 57.3 |
| Filament | x | x | 57.7 |
| Sample (220°C) | x | x | 56.0 |
| Sample (250°C) | x | x | 54.5 |
| **PLA 96/4** | | | |
| Granule | – | – | – |
| Filament | 153.9 | 4.9 | 59.9 |
| Sample (230°C) | 155.4 | 4.5 | 58.0 |
| **Bionolle 1020 MD** | | | |
| Granule | 117.0 | 67.8 | x |
| Filament | 116.9 | 73.0 | x |
| Sample (200°C) | 116.7 | 69.2 | x |
| Sample (220°C) | 115.8 | 62.8 | x |

The $T_m$ and $T_g$ of the PLA silver grey samples remained virtually constant compared with corresponding values of the filament. The energy required for melting PLA silver grey decreased during printing. The $T_g$ of PLA 70/30 remained virtually constant after the filament manufacturing and printing. The $T_m$ and hence the energies required for melting the PLA 70/30 filament and samples could not be determined from the DSC curves since those did not exist. The reason may be the amorphousness of the material due to the filament fabrication and printing. Gibson et al. (2010, p. 160) has claimed that rather amorphous than crystalline polymers should be used with the FDM technique. Amorphous polymers can be extruded as a viscous paste since there is not an exact melting point. This leads to a semi-solid material that softens when the temperature is gradually increased. The $T_m$, $T_g$ and $\Delta H_m$ of the PLA 96/4 samples remained virtually constant compared with corresponding values of the filament.

For comparison, in literature it is reported that the $T_m$ of PLA is 130-180°C and $T_g$ 40-70°C, depending on the grade (Auras et al. 2004, p. 845; Jamshidian et al. 2010, p. 560). The melting temperatures of analyzed PLA silver grey and PLA 70/30 were inside the reported literature values. The melting temperatures of PLA 96/4 were slightly lower than the literature values. The glass transition tempereatures of all analyzed PLA grades were inside the reported values.

The $T_m$ of Bionolle 1020 MD remained virtually constant after the filament manufacturing and printing. The energy required for melting Bionolle 1020 MD increased during the filament fabrication and decreased during sample printing compared with raw material value. The $T_m$ of Bionolle 1020 MD is reported being 114°C and $T_g$ -32°C (Showa Denko K.K. [WWW]). The $T_m$ of analyzed Bionolle 1020 MD seems to be close to the literature value. It was not possible to determine the $T_g$ by thermal analysis since the starting temperature of the analysis cycle was 0°C and the $T_g$ is reported being as low as -32°C.

Analysis of the Topas 5013 filament was not successful since the DSC curves were abnormal for both parallel samples and the thermal properties could not be determined from the curves. Analysis was conducted twice but the problem remained.

## 5.4 Inherent viscosity

The inherent viscosities were measured from the raw materials, filaments and samples. The average IV values are shown in Table 5.3.

***Table 5.3.*** *The average inherent viscositiy values of the different polymer materials. Two parallel samples were measured.*

| Sample | Viscosity (dl/g) | Sample | Viscosity (dl/g) |
|---|---|---|---|
| PLA silver grey filament | 1.77 | PLA 96/4 filament | 3.92 |
| PLA silver grey sample Printing temp. 190°C | 1.68 | PLA 96/4 sample Printing temp. 230°C | 3.29 |
| PLA silver grey sample Printing temp. 220°C | 1.61 | Bionolle 1020 MD granules | 1.05 |
| PLA 70/30 granules | 2.93 | Bionolle 1020 MD filament | 0.98 |
| PLA 70/30 filament | 2.86 | Bionolle 1020 MD sample Printing temp. 200°C | 0.97 |
| PLA 70/30 sample Printing temp. 220°C | 2.32 | Bionolle 1020 MD sample Printing temp. 220°C | 0.89 |
| PLA 70/30 sample Printing temp. 250°C | 2.13 | | |

The IV of the commercial PLA silver grey samples printed at 190°C and 220°C decreased 5% and 9% compared with IV of the filament. Hence, the decrease is not very notable and it is safe to assume that printing commercial PLA silver grey does not affect the molecular weight of the polymer very much. Although it must be noted that the complete composition of the commercial PLA silver grey is not known.

The IV of the PLA 70/30 filament decreased only 2% compared with IV of the granules, from which the filament was fabricated by melt extrusion. Hence, the filament fabrication process does not greatly affect the IV of the polymer. However, the IV of the PLA 70/30 samples decreased significantly when compared with filament. At the printing temperature of 220°C the decrease was 19% and at 250°C it was 26%. Hence, there was a notable decrease in molecular weight and it can be concluded that some degradation took place during printing.

The IV of the PLA 96/4 sample decreased 16% compared with IV of the filament. Hence, some degradation occurred during printing. The inherent viscosity of PLA 96/4 was the highest in comparison with inherent viscosities of other materials measured for this thesis. In addition, the PLA 96/4 filament did not come out from the nozzle very easily at any temperature. The reason for that may be the high IV value since the viscosity partially affects the printability of the material.

The IV of the Bionolle 1020 MD filament decreased 7% compared with granules. When printing at 200°C the decrease was only 1% and at 220°C it was 9%. Hence, the

decrease in molecular weight during printing was only minor. As too high viscosity, also too low viscosity makes the printing troublesome. The inherent viscosity of the Bionolle 1020 MD filament was undoubtedly too low, since printing was not that successful with it. Even changing the printing temperature or printing speed did not help.

In conclusion, the decrease in viscosity was very minor during the filament fabrication. The molecular weight and hence the material properties related to the molecular weight are very similar before and after the filament fabrication. However, some degradation occurred during printing since the viscosity decreased in a clearer manner.

## 5.5 Surface quality

The surface quality of the hemispheres printed on the plate was inspected visually from Sample C. The diameters of the hemispheres were 1.0, 2.0, 3.0 and 4.0 mm. The printer was able to print all the hemispheres. The hemispheres printed with and without retraction are shown in Figure 5.7. The hemispheres that were printed without retraction were formed better and had better surface quality than hemispheres printed with retraction. The biggest difference was scruffy peaks of those hemispheres printed with retraction. However, a stringing effect was seemingly greater in the part printed without retraction. This is self-explanatory since the retraction setting is created to prevent stringing. It should also be noted that strings must be removed afterwards in order to clean the part from the excess material. The removal may harm the part and affect the final quality.

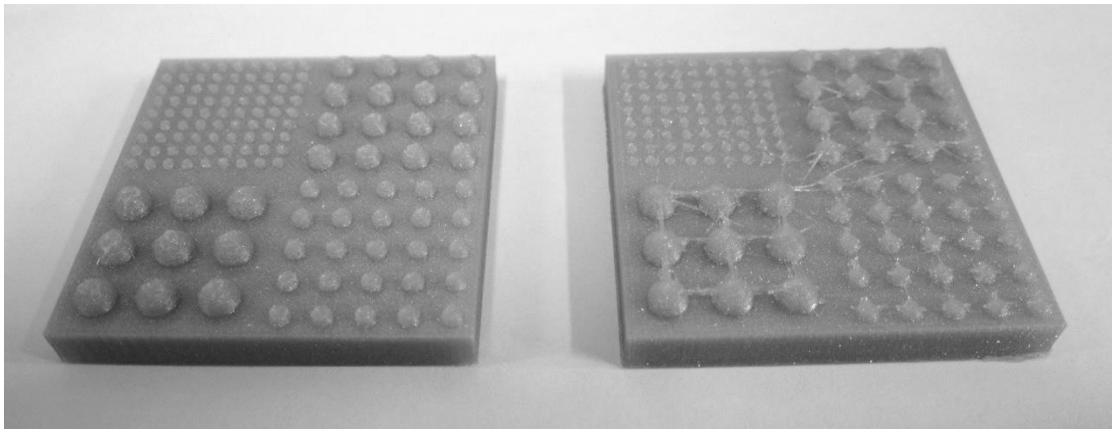

***Figure 5.7.*** *The image of the hemispheres printed on the plate with (left) and without (right) retraction.*

Using the retraction is a two-folded decision. On the other hand, the better surface quality and shape of small features can be obtained without retraction. Then, the removal of the excess material may be challenging without harming the delicate features of the part. The optimal solution may be to aim at modeling of parts that do not have several individual small features close to each other (Armillotta 2006, p. 39).

## 5.6 Dimensional accuracy and stability

### Circularity of holes

The circularity of the round and hexagonal holes of Sample B was determined from the MicroCT image of Sample B by analyzing the image with the Avizo Fire 3D analysis software. The initial diameters of the round holes were from 2.0 mm to 16.0 mm with 2.0 mm intervals. The initial inner diameters of the hexagonal holes were 2.0, 4.0, 6.0, 8.0 and 12.0 mm. The initial diameters along with the actual diameters, perimeters, areas and circularities of the holes are shown in Table 5.4.

***Table 5.4.*** *The circularities of the round and hexagonal holes*.

| | **Initial diameter (mm)** | **Diameter (mm)** | **Perimeter (mm)** | **Area ($mm^2$)** | **Circularity** |
|---|---|---|---|---|---|
| **Circle** | 2.0 | 2.12 | 6.07 | 2.91 | 0.99 |
| | 4.0 | 4.23 | 12.58 | 12.61 | 1.00 |
| | 6.0 | 6.25 | 18.86 | 28.11 | 0.99 |
| | 8.0 | 8.21 | 25.14 | 49.57 | 0.99 |
| | 10.0 | 10.17 | 31.23 | 77.22 | 1.00 |
| | 12.0 | 12.21 | 37.87 | 112.52 | 0.99 |
| | 14.0 | 14.16 | 44.07 | 152.02 | 0.98 |
| | 16.0 | 16.36 | 50.59 | 199.00 | 0.98 |
| **Hexagon** | 2.0 | 2.60 | 7.47 | 4.29 | 0.97 |
| | 4.0 | 4.72 | 14.12 | 14.93 | 0.94 |
| | 6.0 | 6.88 | 20.57 | 31.65 | 0.94 |
| | 8.0 | 9.09 | 27.42 | 55.77 | 0.93 |
| | 12.0 | 13.74 | 41.65 | 126.44 | 0.92 |

The circularity of the round holes is close to one, which presents the perfect circularity. Hence, it is safe to assume that round holes actually are circular. In case of the hexagonal holes, the circularity varies more the lowest value being 0.92. It also seems that the circularity is less while the hexagonal holes get bigger. This may result in problems if precise compatibility or fit between two components is required.

The actual diameters of the round and hexagonal holes seem to be bigger than the initial diameters. In case of the round holes, the average increase in diameter is close to 0.2 mm, standard deviation being only 0.07 mm. For the hexagonal holes, the increase in diameter varies from 0.6 mm to 1.7 mm. The increase in the hole diameter results from rapid cooling after the extrusion when the material shrinks. The shrinkage should have a negative deviation along x- and y-direction (Bansal 2011, p. 5). This holds true according to the results in question. The interesting fact concerning the round holes is that the increase in diameter and hence the shrinkage effect is not proportional to the hole size, but is rather constant. The reason for that may be the FDM technique, where

every layer consists of thin individual lines. The previously deposited lines have time to cool down before the next lines are deposited and bonded together. Hence, the amount of shrinkage is material dependent and probably affected by the line width. However, when concerning the hexagonal holes, the increase in diameter is not constant but neither proportional. The difference between the initial and actual diameters increases along the increasing diameter.

Due to the constant difference in diameter between the initial and actual diameters and almost the perfect circularity of the round holes, it can be concluded, that printing of round holes is accurate as long as the increase in diameter is taken account of in the modeling phase. The same conclusions cannot be made for hexagonal holes. More measurements should be done for hexagonal holes in order to be able to make more precise reasoning.

### Dimensional accuracy of thin walls

The thicknesses of the thin walls were determined from Sample D by MicroCT imaging and related measurements. The initial modeled wall thicknesses were from 0.4 mm to 1.4 mm with 0.1 mm intervals. The initial and actual wall thicknesses are shown in Figure 5.8.

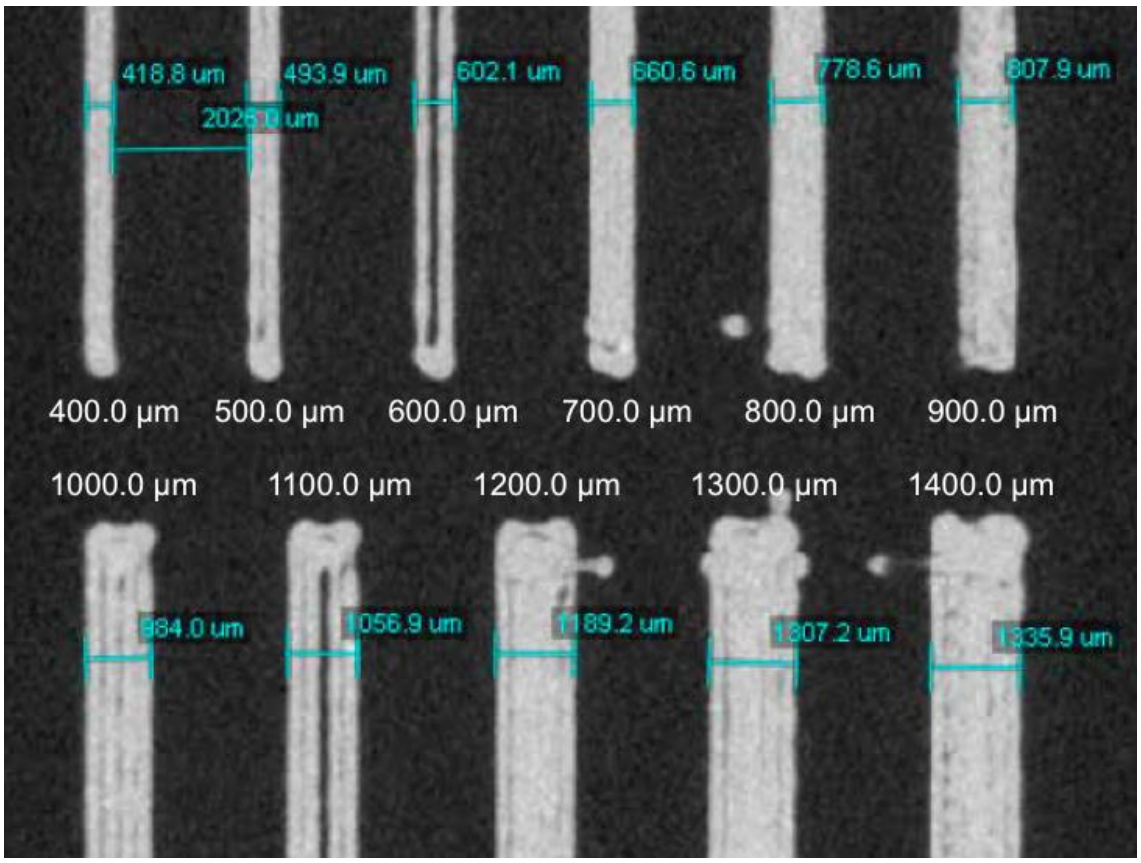


***Figure 5.8.*** *The microCT image of the printed walls (top view). The initial wall thicknesses are marked in white and actual wall thicknesses are marked in blue. Pixel size 33.9458 µm, acceleration voltage 90 kV, 0.4x objective lens, shutter speed 0.6 s.*

The minimum difference between the initial and actual thickness was 0.002 mm, maximum difference 0.092 mm and average difference 0.029 mm, standard deviation being 0.028 mm. In principle, the minimum features of the modeled part should be a multiple of the nozzle size and at least twice of the nozzle size (Gibson et al. 2010, p. 146). In this case, the wall thicknesses should be a multiple of 0.25 mm since the nozzle size of 0.25 mm was used. Considering that fact, the dimensional accuracy was remarkably good. The results were also very promising regarding biomedical applications, where features cannot always be a multiple of the nozzle size.

However, as can be seen from Figure 5.8, the printer had trouble printing fully filled walls with the thicknesses of 0.6 mm and 1.1 mm. It seems that printer does not print lines of 0.1 mm width. This is somewhat odd since lines of 0.05 mm width are printed well. The reason may be the printing software which slices the model files.

When considering printing thin walls, there are several factors that should be taken account of. The most important ones are the nozzle size and software, including both printing software and modeling software. Cura is the open-source software, optimized for the universal usage of the printer and developed by one individual. The Solidworks 3D CAD software used for modeling samples is not optimized for 3D printing purposes. The nozzle size should be chosen according to the part and desired feature size. At the moment, the nozzle size of 0.25 mm is the smallest commercially available.

### Dimensional stability

The thickness of Sample E was measured from multiple points along x-, y- and z-directions. The initial thickness of Sample E was 5.0 mm in all directions. The initial and average actual thicknesses, average differences between initial and actual thicknesses along with standard deviations are shown in Table 5.5.

***Table 5.5.*** *The initial thicknesses, average actual thicknesses and average differences between initial and actual thicknesses of Sample E. Also standard deviations (SD) are shown.*

| | **x** | **y** | **x-z** | **y-z** |
|---|---|---|---|---|
| **Initial thickness (mm)** | 5.00 | 5.00 | 5.00 | 5.00 |
| **Actual thickness (mm)** | 4.75 | 4.78 | 5.14 | 5.10 |
| **Difference (mm)** | -0.25 | -0.22 | +0.14 | +0.10 |
| **SD (mm)** | 0.04 | 0.07 | 0.02 | 0.03 |

As can be seen from Table 5.5, the average difference in thickness along x-direction was 0.25 mm and along y-direction 0.22 mm below the initial 5.00 mm thickness. The average difference in thickness along x-z-direction was 0.14 mm and along y-z-direction 0.10 mm above the initial 5.00 mm thickness. The results correspond with the previously conducted study, where the shrinkage had a negative deviation along x- and y-directions and a positive deviation along z-direction (Bansal 2011, p. 5).

The thickness of Sample F was measured from multiple points along x- and y-direction. The initial thickness of Sample F was 10.00 mm in both directions. The initial and average actual thicknesses, average differences between initial and actual thicknesses along with standard deviations are shown in Table 5.6.

***Table 5.6*** *The initial thicknesses, average actual thicknesses and average differences between initial and actual thicknesses of Sample F. Also standard deviations (SD) are shown.*

| | **x** | **y** |
|---|---|---|
| **Initial thickness (mm)** | 10.00 | 10.00 |
| **Actual thickness (mm)** | 10.00 | 9.96 |
| **Difference (mm)** | 0.00 | -0.04 |
| **SD (mm)** | 0.01 | 0.01 |

As can be seen from Table 5.6, the average difference in thickness along x-direction was zero and in y-direction 0.04 mm below the initial 10.00 mm thickness. The results do not fully correspond with the previous study (Bansal 2011, p. 5). The one reason for the divergent results may be the measuring accuracy of the digital gauge used for determining the thicknesses. The accuracy is supposed to be 0.02 mm. Also the measuring practice can be questioned. However, all thicknesses were measured in the same way with the same gauge. In the future, a more accurate measuring device could be used, for instance a thickness gauge based on ultrasound. Anyhow, the preceding results can be exploited when defining the dimensions of the parts during the modeling phase, at least for this particular PLA silver grey material.

Also the dimensional stability of the outer surface of sample G was inspected. Figure 5.9 shows that the sides of the sample are wobbling. It should be noted that the sample is upside down in the figure when concerning the build direction.

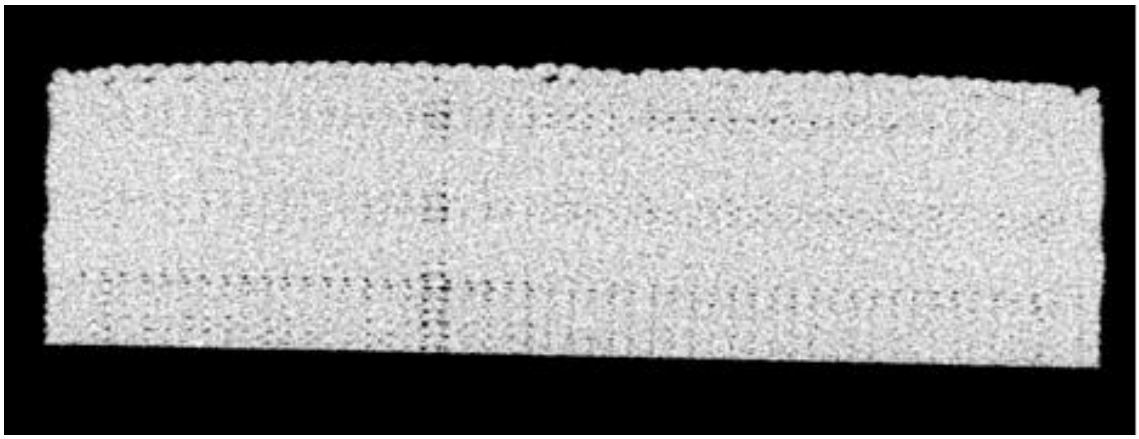

***Figure 5.9.*** *The MicroCT image of Sample G (side view). Repeating wobbling is visible on the sides of the sample. Pixel size 23.4109 µm, acceleration voltage 140 kV, 0.4x objective lens, shutter speed 0.6 s.*

Wobbling seems to be repeating at constant intervals. The reason for this may be hardware related and happened during the Ultimaker assembly. The M8 threaded rod which moves the printing bed upwards and downwards, may not be aligned correctly with the z-coupler located at the bottom of Ultimaker (Figure 5.10). During the assembly, the rod is put through the brass nut which should have a bit of play in order to get it adjusted correctly afterwards (Figure 5.10).

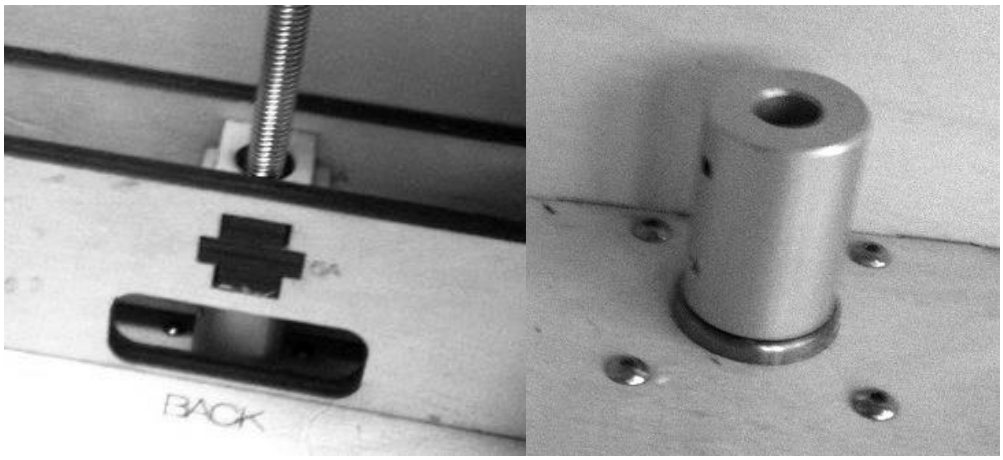


***Figure 5.10.*** *The M8 threaded rod goes through the brass nut (left) and inside the z-coupler (right)* (Ultimaker rev.4 assembly: Z-stage [WWW]).

Also few other observations can be made from the MicroCT image. The bottom of the sample is not completely flat. This is due to the cooling effect which makes the bottom layers of the part to warp at the edges. A solution to reducing the warpage may be the usage of the heating printing bed which enables the material to cool down slower. The top surface is however incredibly flat and even. This information can be utilized when selecting the part orientation before fabricating the part.

# 6 CONCLUSION AND PROPOSITIONS

The first objective was to adjust and calibrate the Ultimaker 3D printer in order to enhance the quality of the printed parts. Several upgrade parts were installed in the printer. The quality of the printed parts enhanced due to the improvements made to the printer. After installing the belt tensioners and tightening the timing belts, extruded lines aligned correctly and small features became more accurate. However, there are also better timing belts and pulleys available which would enhance the printing quality even more by reducing the backlash error. In addition, better slider blocks would enable the more even tensioning of the timing belts. The new cooling system was undoubtedly better than the original one and air flew more efficiently onto the extruded area. However, since air flew only to the other side of the part, the part slightly distorted. For that reason a better cooling system should be designed, from which air flows more evenly around the part. One option could be another fan duct on the opposite side of the existing one. The new axis end caps prevented the long shafts from moving back and forth during printing and hence affected the horizontal printing accuracy. Usefulness of the heating printing bed is questionable, at least without the controlled build chamber. The bed should prevent the part from warping during printing. However, when the bed was required in sample printing for the sake of this thesis, it did not fulfill its purpose. Also the correct calibration of the printer is crucial and has a huge effect on the printing quality. When considering the Ultimaker 3D printer, the axis should be perfectly aligned, timing belts correctly and evenly tensioned, and build platform accurately leveled. The calibration is however conducted by hand and thus requires experience.

The second objective was to evaluate how the printing parameters affect the properties of the parts fabricated with the Ultimaker 3D printer and whether the printer can be applied for biomedical research purposes. Several different kinds of samples of different polymer materials were printed and characterized. Besides one commercial printing filament, the filaments used in the research were manufactured in-house from the raw materials. Printing the samples with the commercial PLA silver grey filament was trouble-free since it was meant for printing purposes. With other filaments printing was more challenging, and finding the correct settings and parameters was time-consuming. With the Topas 5013 filament, printing was not successful at all. Therefore, filament manufacturing as well as material selection affects the printing quality and printability.

An increase in the printing temperature, nozzle size and flow rate combined with a decrease in the printing speed increases the tensile strengths of the parts. However, the bigger nozzle size increases the minimum feature size of the part, lowering the part accuracy. Increasing the flow rate results in overextrusion, distorting the shape and size of

the part. The lower printing speed increases the time required for printing. The samples fabricated by FDM for this theses were brittle in nature resulting in the rapid fracture without deformation. The molecular weights of the samples slightly decreased during printing since the inherent viscosities decreased. Hence, minor degradation took place. The material viscosity affects the printability. Both too high viscosity and too low viscosity makes the printing troublesome. Printing resulted in minor part shrinkage, having a negative deviation along x- and y-direction and a positive deviation along z-direction. The interesting fact is that the shrinkage effect is not proportional to the part size. It is rather constant. The reason for that may be the FDM technique, where every layer consists of thin individual lines. Previously deposited lines have enough time to cool down before next lines are deposited. Hence, the amount of shrinkage is material dependent and affected probably by the line width, in other words by the nozzle size. Therefore, the dimensional accuracy of the printer is rather good. The preceding results can be exploited when defining the dimensions of the parts during the modeling phase. When considering of printing very small features, the dimensional accuracy is even better. In principle, the minimum features of the modeled part should be a multiple of the nozzle size. However, the results showed that the part accuracy stayed remarkably good even when the feature size was not a multiple of the nozzle size. These results are also very promising when regarding biomedical applications.

It should be noted that the results of this thesis are limited only to the specific printer and related to the chosen settings and parameters. Also more advanced printers are constantly being developed, resulting in enhanced printing quality, affecting in particular on the printing accuracy and the dimensional stability of the printed parts. In addition to the hardware, also the software affects the printing quality. The modeling phase should be conducted carefully by the terms of the FDM technique and final application. The modeling phase may also reduce the amount of post-processing when conducted properly. The modeling software has an effect on how well the slicing software is able to handle the external geometry of the part. The Solidworks 3D CAD software used for modeling the samples is not optimized for printing purposes. Also the printing software has differences in creating layers and fill patterns. The Cura printing software used for slicing the sample models is the open-source software, optimized for the universal usage of the printer and developed by one individual. With commercial printing software better results may be obtained.

In conclusion, when fabricating parts with the FDM technique, it is important to select the optimal settings and parameters according to the required properties of the part. However, obtaining only the optimal material properties does not ensure that the final part would be externally acceptable and suitable for the final application. When regarding the dimensional accuracy and stability of the printed parts as well as the ability of the printer to fabricate complex geometries and very fine structures, the Ultimaker 3D printer has potential to be utilized for biomedical research purposes. In addition, the printer can be adjusted to work with several different polymer materials.

# REFERENCES

ASTM Additive Manufacturing File Format (AMF) [WWW]. [Cited 24.06.2013]. Available at: http://amf.wikispaces.com.

Avizo Fire [WWW]. [Cited 15.10.2013]. Available at: http://www.vsg3d.com/avizo/fire.

Bowden Clamp for Ultimaker [WWW]. [Cited 28.01.2014]. Available at: http://www.thingiverse.com/thing:11864.

Delrin acetal resin [WWW]. [Cited 25.06.2013]. Available at: http://www2.dupont.com/Plastics/en_US/Products/Delrin/Delrin.html.

Direct Drive Upgrade [WWW]. [Cited 28.01.2014]. Available at: http://www.calumdouglas.ch/ultimaker-3d-printer/direct-drive-upgrade/.

Farnell [WWW]. [Cited 24.02.2014]. Available at: http://www.farnell.com.

Flexible Shaft Coupler [WWW]. [Cited 09.02.2014]. Available at: http://www.ebay.com/itm/1PCS-5x8mm-Shaft-Coupling-5mm-to-8mm-Flexible-Shaft-Coupler-Connector-/220877879583.

Heated Bed [WWW]. [Cited 24.02.2014]. Available at: http://wiki.ultimaker.com/Heated_Bed.

Heated Build Platform for Ultimaker [WWW]. [Cited 24.02.2014]. Available at: http://flashgamer.com/arduino/comments/adding-a-heated-build-platform-to-your-ultimaker.

PCB Heatbed [WWW]. [Cited 24.02.2014]. Available at: http://reprap.org/wiki/PCB_Heatbed_MK2.

PLA Silver-Grey [WWW]. [Cited 11.02.2014]. Available at: https://www.ultimaker.com/products/pla-silver-grey.

Showa Denko K.K. [WWW]. [Cited 08.05.2014]. Available at: http://www.showadenko.com/fileadmin/template/img/Bionolle/Bionolle_2013_20131205_reduced_size_PDF.pdf.

UltiController Kit [WWW]. [Cited 04.03.2014]. Available at: https://www.ultimaker.com/products/ulticontroller.

Ultimaker Axis End Cap [WWW]. [Cited 28.01.2014]. Available at: http://www.thingiverse.com/thing:54075.

Ultimaker Belt Tensioner [WWW]. [Cited 28.01.2014]. Available at: http://www.thingiverse.com/thing:32044.

Ultimaker Extruder Gear Upgrade [WWW]. [Cited 28.01.2014]. Available at: http://www.thingiverse.com/thing:151642.

Ultimaker Fan-Duct [WWW]. [Cited 28.01.2014]. Available at: http://www.thingiverse.com/thing:25611.

Ultimaker Original [WWW]. [Cited 13.12.2013]. Available at: https://www.ultimaker.com/products/ultimaker-original.

Ultimaker Quick Connect Shim [WWW]. [Cited 28.01.2014]. Available at: http://www.thingiverse.com/thing:22851.

Ultimaker Quiet Retraction [WWW]. [Cited 28.01.2014]. Available at: http://www.thingiverse.com/thing:53690.

Ultimaker Reel Holder [WWW]. [Cited 28.01.2014]. Available at: http://www.thingiverse.com/thing:33495.

Ultimaker rev.4 assembly: Z-stage [WWW]. [Cited 24.02.2014]. Available at: http://wiki.ultimaker.com/Ultimaker_rev.4_assembly:_Z-stage.

Ultimaker specs and features [WWW]. [Cited 25.06.2013]. Available at: http://wiki.ultimaker.com/Ultimaker_Introduction#Specifications.

Ultimaker Strong Foot [WWW]. [Cited 28.01.2014]. Available at: http://www.thingiverse.com/thing:25351.

Ultimaker wiki [WWW]. [Cited 25.06.2013]. Available at: http://wiki.ultimaker.com/Main_Page.

UM 1.5.7 Heatbed Firmware [WWW]. [Cited 24.02.2014]. Available at: https://dl.dropboxusercontent.com/u/1911369/Shared%20Files/UM_1.5.7_with_heatbed_firmware.zip.

V9 Brass Extruder Nozzle .25 mm [WWW]. [Cited 04.02.2014]. Available at: http://store.qu-bd.com/product.php?id_product=114.

What is Additive Manufacturing? [WWW]. [Cited 24.06.2013]. Available at: http://additivemanufacturing.com/basics/.

Agarwala, M.K., Jamalabad, V.R., Langrana, N.A., Safari, A., Whalen, P.J. & Danforth, S.C. 1996. Structural quality of parts processed by fused deposition. Rapid Prototyping Journal 2, 4, pp. 4-19.

Ahn, K., Wessels, B.W. & Sampath, S. 2005. Spinel humidity sensors prepared by thermal spray direct writing. Sensors and Actuators B: Chemical 107, 1, pp. 342-346.

Ahn, S., Montero, M., Odell, D., Roundy, S. & Wright, P.K. 2002. Anisotropic material properties of fused deposition modeling ABS. Rapid Prototyping Journal 8, 4, pp. 248-257.

Antonov, E.N., Bagratashvili, V.N., Whitaker, M.J., Barry, J.J., Shakesheff, K.M., Konovalov, A.N., Popov, V.K. & Howdle, S.M. 2005. Three-Dimensional Bioactive and Biodegradable Scaffolds Fabricated by Surface-Selective Laser Sintering. Advanced Materials 17, 3, pp. 327-330.

Armillotta, A. 2006. Assessment of surface quality on textured FDM prototypes. Rapid Prototyping Journal 12, 1, pp. 35-41.

Auras, R., Harte, B. & Selke, S. 2004. An overview of polylactides as packaging materials. Macromolecular bioscience 4, 9, pp. 835-864.

Bansal, R. 2011. Improving dimensional accuracy of fused deposition modelling (FDM) parts using response surface methodology. Bachelor's Thesis. Rourkela. National Institute of Technology, Rourkela. 32 p.

Brady, G.A. & Halloran, J.W. 1997. Stereolithography of ceramic suspensions. Rapid Prototyping Journal 3, 2, pp. 61-65.

Bullen, D., Chung, S., Wang, X., Zou, J., Mirkin, C.A. & Liu, C. 2004. Parallel dip-pen nanolithography with arrays of individually addressable cantilevers. Applied Physics Letters 84, 5, pp. 789-791.

Chartier, T., Chaput, C., Doreau, F. & Loiseau, M. 2002. Stereolithography of structural complex ceramic parts. Journal of Materials Science 37, 15, pp. 3141-3147.

Chim, H., Hutmacher, D., Chou, A., Oliveira, A., Reis, R., Lim, T.C. & Schantz, J. 2006. A comparative analysis of scaffold material modifications for load-bearing applications in bone tissue engineering. International journal of oral and maxillofacial surgery 35, 10, pp. 928-934.

Chua, C.K., Chou, S.M. & Wong, T.S. 1998. A study of the state-of-the-art rapid prototyping technologies. The International Journal of Advanced Manufacturing Technology 14, 2, pp. 146-152.

Dimitrov, D., Schreve, K. & De Beer, N. 2006. Advances in three dimensional printing - state of the art and future perspectives. Rapid Prototyping Journal 12, 3, pp. 136-147.

Drummer, D., Cifuentes-Cuéllar, S. & Rietzel, D. 2012. Suitability of PLA/TCP for fused deposition modeling. Rapid Prototyping Journal 18, 6, pp. 500-507.

Gibson, I., Cheung, L., Chow, S., Cheung, W., Beh, S., Savalani, M. & Lee, S. 2006. The use of rapid prototyping to assist medical applications. Rapid Prototyping Journal 12, 1, pp. 53-58.

Gibson, I., Rosen, D.W. & Stucker, B. 2010. Additive manufacturing technologies: rapid prototyping to direct digital manufacturing. Springer. 484 p.

Guo, N. & Leu, M.C. 2013. Additive manufacturing: technology, applications and research needs. Frontiers of Mechanical Engineering 8, 3, pp. 215-243.

He, Z., Zhou, J.G. & Tseng, A.A. 2000. Feasibility study of chemical liquid deposition based solid freeform fabrication. Materials & Design 21, 2, pp. 83-92.

Hutmacher, D.W., Sittinger, M. & Risbud, M.V. 2004. Scaffold-based tissue engineering: rationale for computer-aided design and solid free-form fabrication systems. Trends in biotechnology 22, 7, pp. 354-362.

Jamshidian, M., Tehrany, E.A., Imran, M., Jacquot, M. & Desobry, S. 2010. Poly-Lactic Acid: Production, Applications, Nanocomposites, and Release Studies. Comprehensive Reviews in Food Science and Food Safety 9, 5, pp. 552-571.

Kadekar, V., WEIYA, F. & Liou, F. 2004. Deposition technologies for micromanufacturing: a review. Journal of manufacturing science and engineering 126, 4, pp. 787-795.

Korpela, J., Kokkari, A., Korhonen, H., Malin, M., Närhi, T. & Seppälä, J. 2013. Biodegradable and bioactive porous scaffold structures prepared using fused deposition modeling. Journal of Biomedical Materials Research Part B: Applied Biomaterials 101, 4, pp. 610-619.

Kruth, J., Mercelis, P., Van Vaerenbergh, J., Froyen, L. & Rombouts, M. 2005. Binding mechanisms in selective laser sintering and selective laser melting. Rapid Prototyping Journal 11, 1, pp. 26-36.

Landers, R., Pfister, A., Hübner, U., John, H., Schmelzeisen, R. & Mülhaupt, R. 2002. Fabrication of soft tissue engineering scaffolds by means of rapid prototyping techniques. Journal of Materials Science 37, 15, pp. 3107-3116.

Lee, K., Kim, R.H., Yang, D. & Park, S.H. 2008. Advances in 3D nano/microfabrication using two-photon initiated polymerization. Progress in Polymer Science 33, 6, pp. 631-681.

Levy, G.N., Schindel, R. & Kruth, J. 2003. Rapid manufacturing and rapid tooling with layer manufacturing (LM) technologies, state of the art and future perspectives. CIRP Annals-Manufacturing Technology 52, 2, pp. 589-609.

Lewis, J.A. & Gratson, G.M. 2004. Direct writing in three dimensions. Materials today 7, 7, pp. 32-39.

Melchels, F.P., Feijen, J. & Grijpma, D.W. 2010. A review on stereolithography and its applications in biomedical engineering. Biomaterials 31, 24, pp. 6121-6130.

Mette, A., Richter, P.L., Hörteis, M. & Glunz, S.W. 2007. Metal aerosol jet printing for solar cell metallization. Progress in Photovoltaics: Research and Applications 15, 7, pp. 621-627.

Peltola, S.M., Melchels, F.P., Grijpma, D.W. & Kellomäki, M. 2008. A review of rapid prototyping techniques for tissue engineering purposes. Annals of Medicine 40, 4, pp. 268-280.

Pham, D. & Gault, R. 1998. A comparison of rapid prototyping technologies. International Journal of Machine Tools and Manufacture 38, 10-11, pp. 1257-1287.

Sin, L.T., Rahmat, A.R. & Rahman, W.A.W.A. 2012. Polylactic acid : PLA biopolymer technology and applications. Oxford, William Andrew. 341 p.

Spangenberg, A., Hobeika, N., Stehlin, F., Malval, J., Wieder, F., Prabhakaran, P., Baldeck, P. & Soppera, O. 2013. Recent Advances in Two-Photon Stereolithography. In: Hosaka, S. (ed.). Updates in Advanced Lithography. InTech. pp. 35-63.

Sun, C., Fang, N., Wu, D. & Zhang, X. 2005. Projection micro-stereolithography using digital micro-mirror dynamic mask. Sensors and Actuators A: Physical 121, 1, pp. 113-120.

Upcraft, S. & Fletcher, R. 2003. The rapid prototyping technologies. Assembly Automation 23, 4, pp. 318-330.

Wang, J., Ye, M., Liu, Z. & Wang, C. 2009. Precision of cortical bone reconstruction based on 3D CT scans. Computerized Medical Imaging and Graphics 33, 3, pp. 235-241.

Wimpenny, D.I., Bryden, B. & Pashby, I.R. 2003. Rapid laminated tooling. Journal of Materials Processing Technology 138, 1, pp. 214-218.

Winder, J. & Bibb, R. 2005. Medical rapid prototyping technologies: state of the art and current limitations for application in oral and maxillofacial surgery. Journal of Oral and Maxillofacial Surgery 63, 7, pp. 1006-1015.

Yan, X. & Gu, P. 1996. A review of rapid prototyping technologies and systems. Computer-Aided Design 28, 4, pp. 307-318.

Yang, S., Leong, K., Du, Z. & Chua, C. 2002. The design of scaffolds for use in tissue engineering. Part II. Rapid prototyping techniques. Tissue engineering 8, 1, pp. 1-11.

Zein, I., Hutmacher, D.W., Tan, K.C. & Teoh, S.H. 2002. Fused deposition modeling of novel scaffold architectures for tissue engineering applications. Biomaterials 23, 4, pp. 1169-1185.

de Gans, B., Duineveld, P. & Schubert, U. 2004. Inkjet printing of polymers: state of the art and future developments. Advanced Materials 16, 3, pp. 203-213.

## APPENDIX 1: SAMPLE MODELS, MATERIALS AND CHARACTERIZATION METHODS

| Model | Materials | Characterization methods |
|---|---|---|
| **Sample A**  | PLA silver grey<br>PLA 70/30<br>PLA 96/4<br>Bionolle 1020 MD | - Tensile testing<br>- Inherent viscosity measurements<br>- DSC analysis |
| **Sample B** 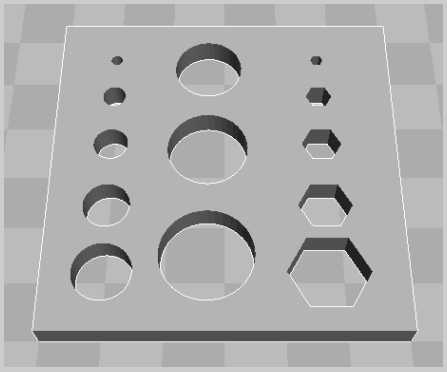 | PLA silver grey | - MicroCT imaging<br>- Circularity measurements |
| **Sample C** 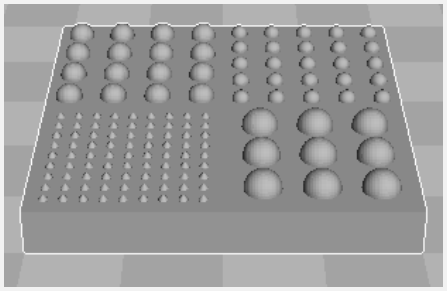 | PLA silver grey | - Visual inspection |
| **Sample D** 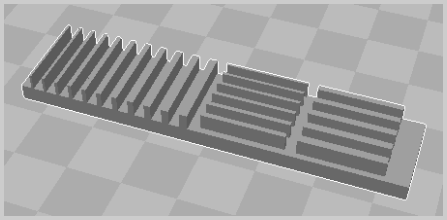 | PLA silver grey | - MicroCT imaging<br>- Visual inspection |
| **Sample E** 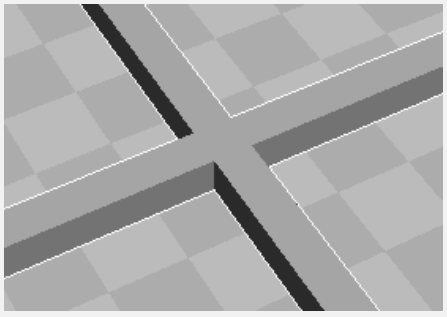 | PLA silver grey | - Dimensional stability measurements |

| | | |
|---|---|---|
| **Sample F**<br> 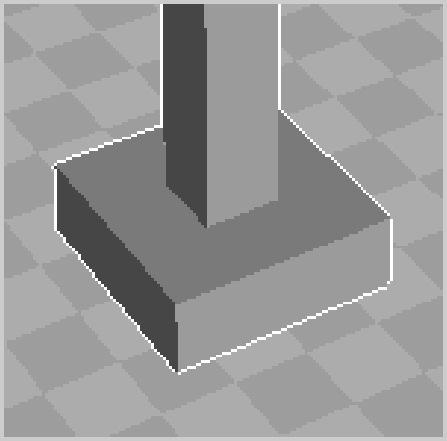 | PLA silver grey | - Dimensional stability measurements |
| **Sample G**<br> 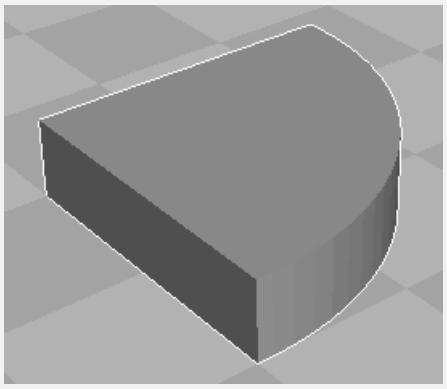 | PLA silver grey | - MicroCT imaging<br>- Visual inspection |

# APPENDIX 2: CURA SETTINGS FOR SAMPLES PRINTING

## Sample A

| **Material** | PLA silver grey | PLA 70/30 | PLA 96/4 | Bionolle 1020 MD |
|---|---|---|---|---|
| **Cura version** | 13.06.5 | 13.06.5 | 13.06.5 | 13.06.5 |
| **BASIC SETTINGS** | | | | |
| **Quality** | | | | |
| Layer height (mm) | 0.1 | 0.1 | 0.1 | 0.1 |
| Shell thickness (mm) | 0.5/0.8 | 0.8 | 0.8 | 0.8 |
| Enable retraction | True | True | True | True |
| **Fill** | | | | |
| Bottom/Top thickness (mm) | 0.3 | 0.3 | 0.3 | 0.3 |
| Fill density (%) | 100 | 100 | 100 | 100 |
| **Speed & Temperature** | | | | |
| Print speed (mm/s) | 50/100 | 50 | 50 | 50 |
| Printing temperature (°C) | 190/200/210/220 | 220/230/240/250 | 230/240 | 200/220 |
| Bed temperature (°C) | 0 | 0 | 0 | 0 |
| **Support** | | | | |
| Support type | None | None | None | None |
| Platform adhesion type | None | None | None | None |
| **Filament** | | | | |
| Diameter (mm) | 2.85 | 2.85 | 2.85 | 2.85 |
| Flow (%) | 100 | 100 | 100 | 100 |
| **ADVANCED SETTINGS** | | | | |
| **Machine** | | | | |
| Nozzle size (mm) | 0.25/0.4 | 0.4 | 0.4 | 0.4 |
| **Retraction** | | | | |
| Speed (mm/s) | 40 | 40 | 40 | 40 |
| Distance (mm) | 4.5 | 4.5 | 4.5 | 4.5 |
| **Quality** | | | | |
| Initial layer thickness (mm) | 0 | 0 | 0 | 0 |
| Cut off object bottom (mm) | 0 | 0 | 0 | 0 |
| Dual extrusion overlap (mm) | 0.2 | 0.2 | 0.2 | 0.2 |
| **Speed** | | | | |
| Travel speed (mm/s) | 150 | 150 | 150 | 150 |
| Bottom layer speed (mm/s) | 30 | 30 | 30 | 30 |
| Infill speed (mm/s) | 0 | 0 | 0 | 0 |
| **Cool** | | | | |
| Minimal layer time (s) | 5 | 5 | 5 | 5 |
| Enable cooling fan | True | True | True | True |
| **EXPERT SETTINGS** | | | | |
| **Infill** | | | | |
| Infill overlap (%) | 20 | 20 | 20 | 20 |

| | Sample B | Sample C | Sample D | Sample E | Sample F | Sample G |
|---|---|---|---|---|---|---|
| **Cura version** | 13.06.5 | 13.06.5 | 13.04 | 13.04 | 13.04 | 13.04 |
| **BASIC SETTINGS** | | | | | | |
| **Quality** | | | | | | |
| Layer height (mm) | 0.1 | 0.1 | 0.1 | 0.2 | 0.2 | 0.1 |
| Shell thickness (mm) | 0.5 | 0.5 | 0.5 | 0.8 | 0.8 | 0.25 |
| Enable retraction | True | True | True | True | True | True |
| **Fill** | | | | | | |
| Bottom/Top thickness (mm) | 0.3 | 0.3 | 0.3 | 0.6 | 0.6 | 0.25 |
| Fill density (%) | 100 | 100 | 100 | 20 | 20 | 100 |
| **Speed & Temperature** | | | | | | |
| Print speed (mm/s) | 50 | 50 | 50 | 70 | 70 | 30 |
| Printing temperature (°C) | 220 | 220 | 220 | 220 | 220 | 220 |
| Bed temperature (°C) | 0 | 0 | 0 | 0 | 0 | 0 |
| **Support** | | | | | | |
| Support type | None | None | None | None | None | None |
| Platform adhesion type | None | None | None | None | None | None |
| **Filament** | | | | | | |
| Diameter (mm) | 2.85 | 2.85 | 2.85 | 2.89 | 2.89 | 2.89 |
| Flow (%) | 100 | 100 | 100 | 100 | 100 | 100 |
| **ADVANCED SETTINGS** | | | | | | |
| **Machine** | | | | | | |
| Nozzle size (mm) | 0.25 | 0.25 | 0.25 | 0.4 | 0.4 | 0.25 |
| **Retraction** | | | | | | |
| Speed (mm/s) | 40 | 40 | 40 | 40 | 40 | 40 |
| Distance (mm) | 4.5 | 4.5 | 4.5 | 4.5 | 4.5 | 4.5 |
| **Quality** | | | | | | |
| Initial layer thickness (mm) | 0 | 0 | 0 | 0.3 | 0.3 | 0.3 |
| Cut off object bottom (mm) | 0 | 0 | 0 | 0 | 0 | 0 |
| Dual extrusion overlap (mm) | 0.2 | 0.2 | 0.2 | 0.2 | 0.2 | 0.2 |
| **Speed** | | | | | | |
| Travel speed (mm/s) | 150 | 150 | 150 | 100 | 100 | 100 |
| Bottom layer speed (mm/s) | 30 | 30 | 30 | 50 | 50 | 30 |
| Infill speed (mm/s) | 0 | 0 | 0 | 0 | 0 | 0 |
| **Cool** | | | | | | |
| Minimal layer time (s) | 5 | 5 | 5 | 5 | 5 | 5 |
| Enable cooling fan | True | True | True | True | True | True |
| **EXPERT SETTINGS** | | | | | | |
| **Infill** | | | | | | |
| Infill overlap (%) | 20 | 20 | 20 | 20 | 20 | 20 |

# APPENDIX 3: DEVICE FOLDER – ULTIMAKER 3D PRINTER

TAMPEREEN TEKNILLINEN YLIOPISTO
TAMPERE UNIVERSITY OF TECHNOLOGY

**Folder name:** **Device folder – Ultimaker 3D printer**

| | |
|---|---|
| **Instruction type:** | **Work instruction** |
| **Version:** | **TYO-140514** |
| **Author(s):** | **Mikael Virta** |
| **Acceptor:** | **Ville Ellä** |

# 1. Intended use of the device

The Ultimaker 3D printer is used for fabricating three-dimensional parts from certain polymer materials by using extrusion. Polymer material is fed into the printer as a thin filament. The polymer is heated up into a semi-solid state during extrusion and solidified afterwards.

# 2. Device register information

**Hardware:**

| | |
|---|---|
| **Name of the device** | Ultimaker 3D Printer |
| **Manufacturer** | Ultimaking LTD |
| **Serial number** | - |
| **Type** | - |
| **Device register number** | - |
| **Purchase year** | 2012 |

**Software:**

| | |
|---|---|
| **Name of the program** | Cura |
| **Version** | 13.04 |
| **Type** | Open-source software |

# 3. Qualifications required for the usage of the device

The operating instructions and operation of the device should be familiarized carefully. The guidance of the person in charge of the device is required when using the device for the first time.

# 4. Responsibilities

**Person in charge: -**

**Researcher in charge: -**

**Responsibilities of the person in charge of the device:**
- device usage guidance
- functionality of the device as well as maintenance and repair operations

**Responsibilities of the operator:**
- appropriate usage of the device and compliance of the operating instructions
- cleaning of the working environment after usage
- informing the person in charge about breakage or malfunction of the device
- filling up the usage log

# 5. Application information

## 5.1. The principle of 3D printing

The first step in producing the 3D part is to create the 3D model with the CAD software and convert the model file into the file format that includes all the information the printer needs for fabricating the part.

Fused deposition modeling (FDM) is an additive manufacturing technique. With FDM it is possible to fabricate polymer parts layer by layer from bottom to top via extrusion. The extrusion means that the build material is forced out through the nozzle by using pressure and elevated temperatures. The material that is being extruded is heated up into a semi-solid state. After the extrusion, the material is quickly solidified in order to remain its shape. During the extrusion, the preceding material bonds with material that has already been extruded. Bonding occurs when the extrusion head supplies enough heat energy and activates the surfaces of the previous layers. After the layer is completed, the build platform (printing bed) moves downwards by one layer thickness and the next layer is built. During printing the build platform moves vertically downwards and the extrusion head moves horizontally. In FDM a polymer material is fed into the extrusion head as a continuous filament. A schematic of the FDM system can be seen in Figure 1.

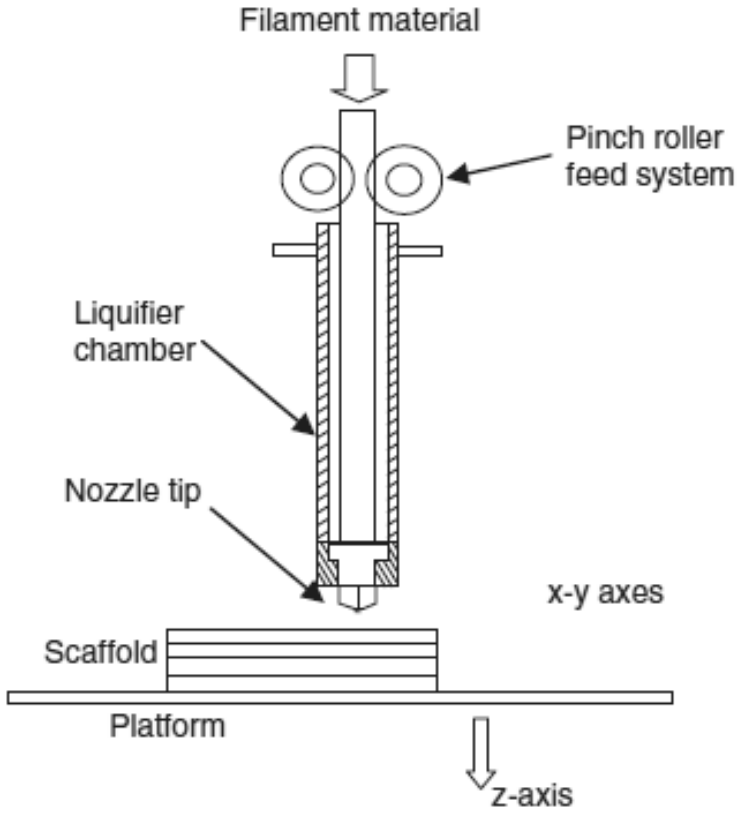


***Figure 1.*** *A schematic of the fused deposition modeling system.*

Several thermoplastic polymers can be used as build materials with FDM. Polymers should be rather amorphous in nature (proper viscosity behavior) than highly crystalline.

## 5.2. Ultimaker

The Ultimaker 3D printer utilizes the FDM technique. Ultimaker is an open-source printer. Physical part upgrades are released online for free and they can be printed with Ultimaker. Also software upgrades are free. Ultimaker supports two filament materials; polylactide (PLA) and acrylonitrile butadiene styrene (ABS). However, the printer is not limited to use only these two polymer materials. It is possible to adjust the printer to work also with several other polymers. The Ultimaker 3D printer is shown in Figure 2.

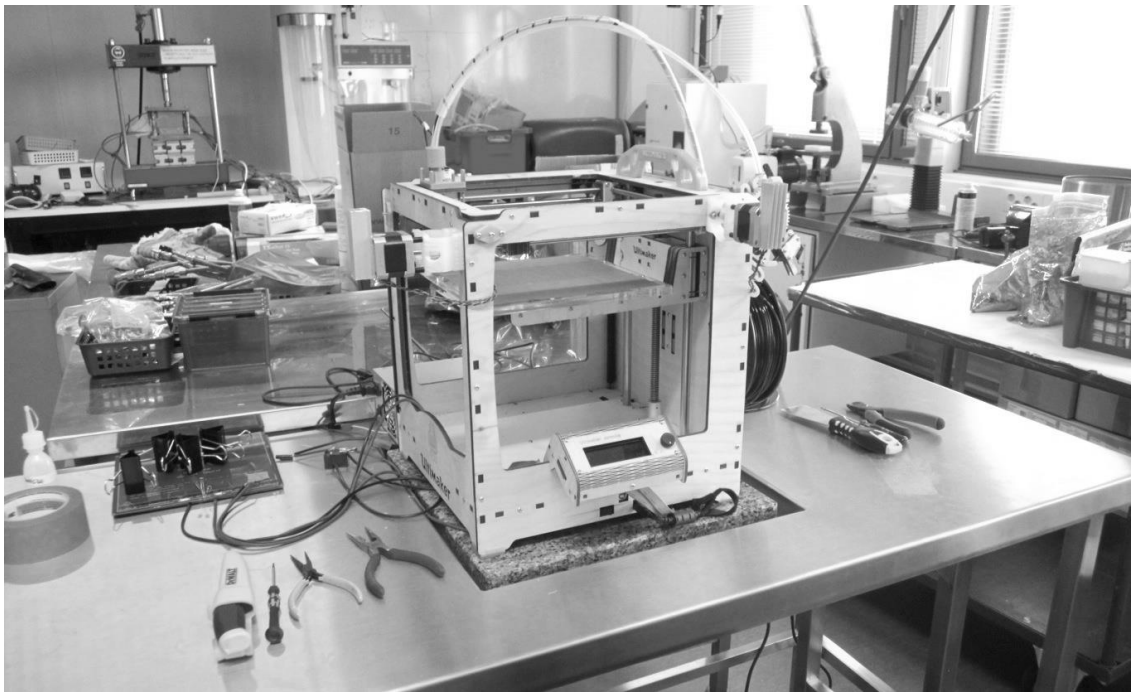

***Figure 2.*** *The Ultimaker 3D printer.*

The printer is made of birch plywood. The polymer filament comes in a reel. The build platform is made of acrylic glass. The hot-end heats up to the printing temperature within two minutes. The shape of the extrusion nozzle is conical and the hole of the nozzle is round. There are two different nozzle sizes available; 0.25 mm and 0.4 mm. The printer can be controlled via UltiController or computer.

## 5.3. Cura - slicing software

Cura is an open-source slicing program and developed for Ultimaker. Cura includes everything that is needed for preparing the 3D model for printing. It converts a model file (.stl file) into a .gcode file format which includes all the information the printer needs for building the part (Figure 3). The part can be printed either directly after converting via USB connection or by copying the .gcode file onto the SD card which goes into UltiController. Also the calibration of Ultimaker can be executed with Cura.

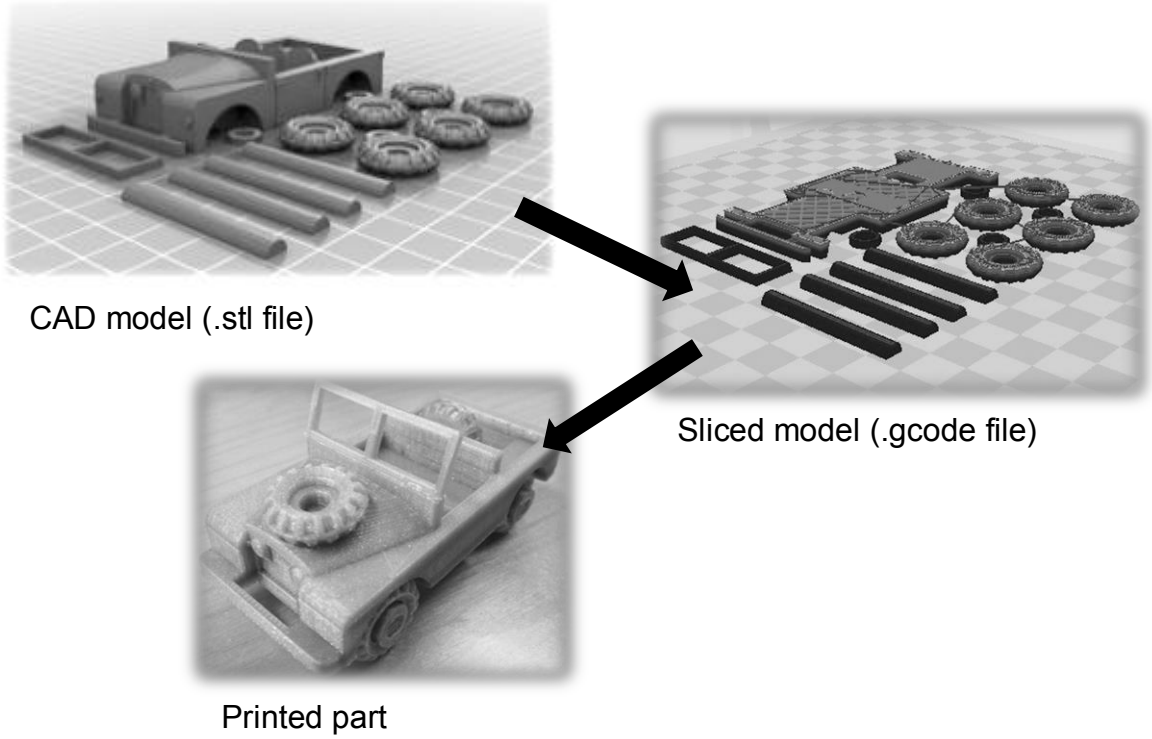


***Figure 3.*** *The .stl file modeled with the CAD software, the .gcode file sliced with the printing software and the printed part.*

# 6. Operating instructions

## 6.1. Measures before printing

### 6.1.1. Changing the filament reel (if necessary)

- Switch on Ultimaker.
  - The power switch is located on the bottom right side of the device (Figure 4).

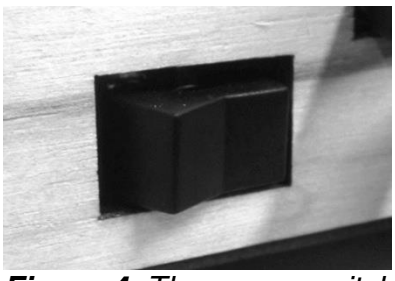

***Figure 4.*** *The power switch.*

- Open the filament feeder if it is not already open (Figure 5).

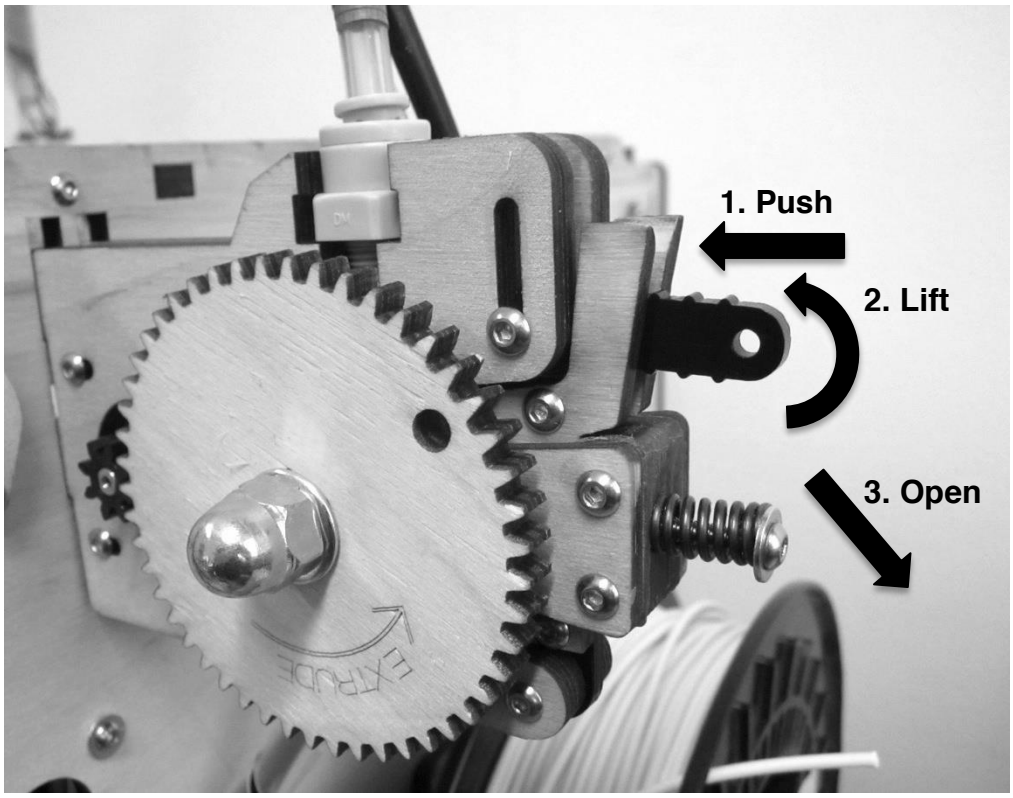


***Figure 5.*** *Opening the filament feeder (front view).*

***N.B.*** *The extrusion head must be preheated close to the melting temperature of the filament material before the filament can be pulled out from the tube (PLA: 210°C, ABS: 250°C).*

- Preheat the extrusion head by using UltiController (UltiController instructions in Chapter 10).
    - Main menu → Prepare → Preheat PLA/Preheat ABS
- Pull out the filament by hand after the target temperature has been reached.
- Cut off the melted head of the filament with pliers at the point where there is no signs of the melting anymore.
- Roll the filament around the reel and put the head of the filament through the hole at the reel wall in order to prevent the filament from unraveling.
- Place the new filament reel on the filament holder (filament rotation direction shown in Figure 6).

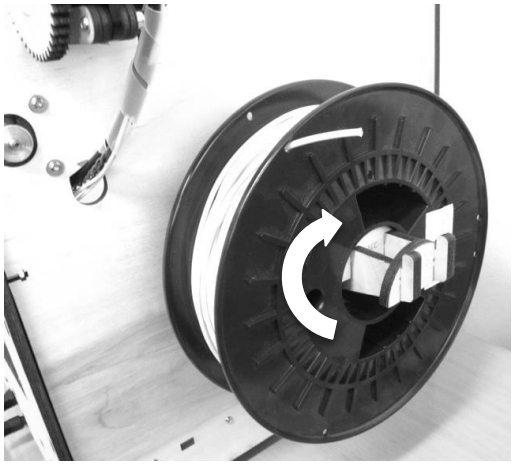

***Figure 6.*** *The filament reel on the filament holder.*

- Feed the filament into the filament feeder (Figure 7) by hand and through the transparent tube into the extrusion head until the filament does not move forward anymore.

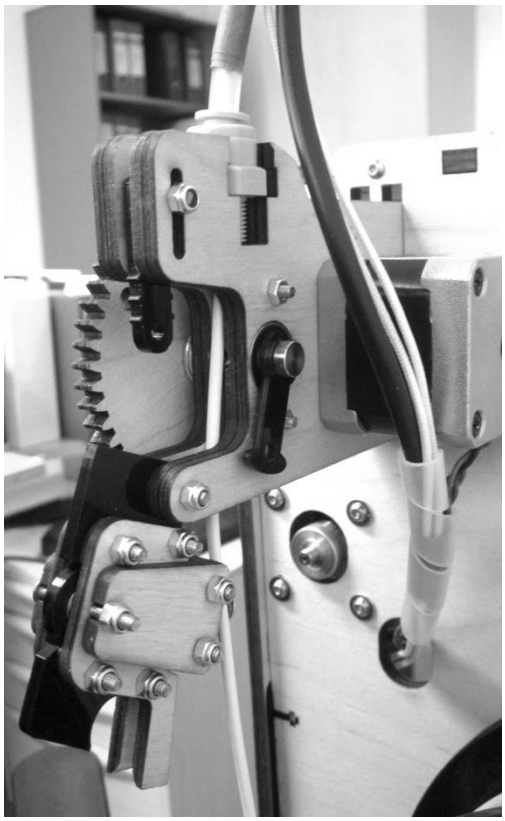

***Figure 7.*** *The filament feeder (back view).*

- Close the filament feeder (Figure 8).

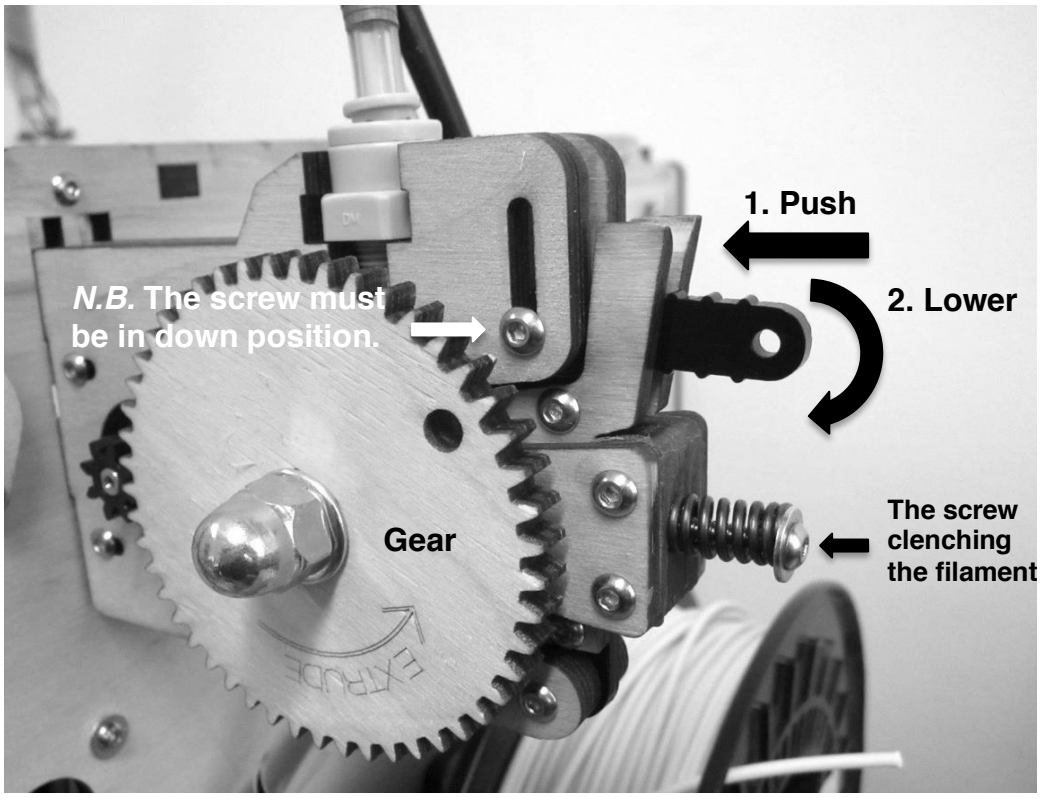


***Figure 8.*** *Closing the filament feeder (front view).*

- Adjust the screw which is clenching the filament (Figure 8) with screwdriver until the screw does not tighten anymore without excessive force.
- Feed the filament into the extrusion head by turning the gear (Figure 8) by hand until the molten filament starts coming out from the nozzle.
- Stop heating the extrusion head.
    - Main menu → Prepare → Cooldown
- Clean up the filament from the nozzle and the printing bed with trowel. Pay attention not to scratch the nozzle or the printing bed.

***N.B.*** *In case the new filament material or color differs from the previous one, feed the filament into the extrusion head until the previous filament has completely become replaced by the new filament.*

### 6.1.2. Taping the printing bed

- Use the 3M Scotch-Blue tape.
- Wipe the acrylic printing bed with 2-propanol before taping.
- Tape the bed thoroughly (the area inside the carved scale) (Figure 9).
    - Edges of the tapes should touch each other.
    - There may not be gaps between tapes and tapes may not be on top of each other.

***Figure 9.*** *Taping the printing bed.*

- Cut off the excessive tape with a sharp knife along the carved scale.
- Clean the taped printing bed with 2-propanol if desired.

***N.B.*** *Cleaning the taped printing bed with 2-propanol makes the printed part to stick better onto the bed but also makes the removal of the part harder.*

### 6.1.3. Calibration of the printing bed

***N.B.*** *During the calibration, the printer must be connected to the computer by USB cable.*

- Turn on the computer.
- Switch on Ultimaker.
    - The power switch is located on the bottom right side of the device (Figure 10).

***Figure 10.*** *The power switch.*

- Open the Cura program on the computer (Figure 11).


***Figure 11.*** *Cura shortcut.*

- Launch the bed leveling wizard (Figure 12).
    - Menu → Expert → Run bed leveling wizard


***Figure 12.*** *The bed leveling wizard.*

- Select ”Connect to printer”.
- Adjust the front left screw of the bed so that the regular piece of paper barely fits between the nozzle and bed (slight friction is desirable) (Figure 13).

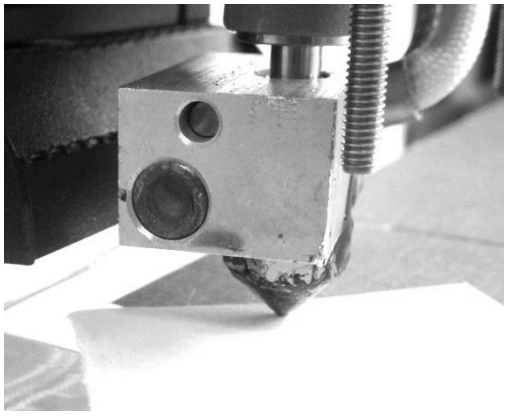

***Figure 13.*** *Calibrating the printing bed.*

- Select ”Resume”.
- Adjust also the remaining three screws in the same way (notice that the nozzle is just on the edge of the tape when adjusting the third and fourth screw).
- Next the printer heats up to the default temperature and prints two squares on the printing bed.
    - The squares on the bed should slightly touch each other and the print trail should remain constant in all sections. (If not, repeat the calibration.)
- Select ”Finish”.
- Remove the squares from the printing bed.

## 6.2. Printing

***N.B.*** *This work instruction covers printing using quick print settings. The usage of full settings requires printing experience and knowledge of filament materials. More information about full settings can be found in Chapter 9.*

- Open the Cura program from the computer.
  - Cura start up screen is shown in Figure 14

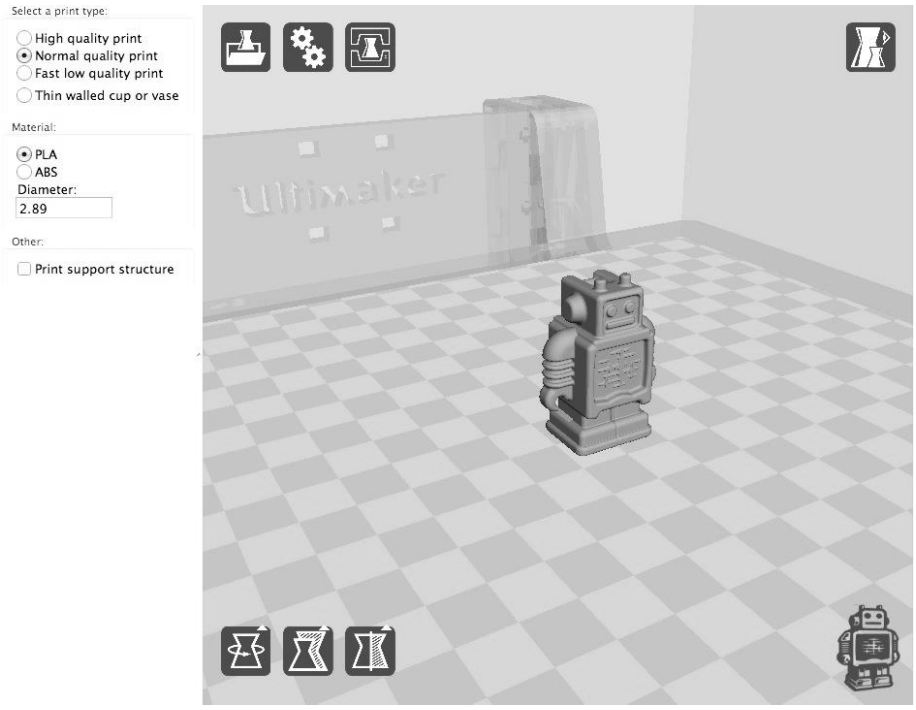


***Figure 14.*** *Cura start up screen.*

- Check that "quickprint" settings are selected.
  - Menu → Tools → Switch to quickprint
- Load the 3D model (the .stl file) to the Cura program.
  - Menu → File → Load model file
- Select the print type from the column at the left (high quality print / normal quality print / fast low quality print).
- Select the correct filament material (PLA / ABS).
- Prepare the model for printing.
  - Menu → File → Prepare print
  - Preparation progress can be seen from the bar at the bottom (Figure 15)


***Figure 15.*** *Preparation progress bar.*

***N.B.*** *Printing can be carried out by using either Cura or UltiController. UltiController enables more possibilities to affect the printing parameters during printing than Cura does. Printing with both Cura and UltiController is explained next.*

**Cura**

- Start printing after the model is prepared.
  - Menu → File → Print
- The printing window shows up (Figure 16).

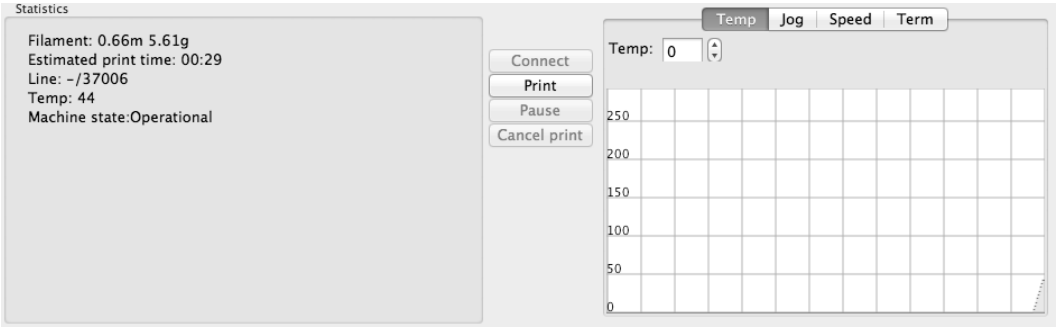


***Figure 16.*** *The printing window.*

- Wait until the ”Print” button becomes available and press it.
- The printer warms up to the printing temperature and prints the part.

***N.B.*** *Extrude a small amount of filament from the nozzle by turning the gear just before the nozzle temperature has reached the printing temperature in order to ensure that the nozzle is filled with filament.*

***N.B.*** *If some problems occur during printing, press the ”Cancel print” button, disable the stepper motors (UltiController: Menu → Prepare → Disable steppers), lower the printing bed a few centimeters by turning the lead screw by hand, and clean up the filament from the nozzle and the printing bed with trowel. Start printing from beginning if necessary.*

- After printing wait a moment (~20 seconds) and let the part to cool down.
- Remove the part from the printing bed by using the thin steel trowel.
- Close the printing window.

**UltiController**

- Insert the SD memory card from UltiController into the card reader of the computer. The memory card locates on the left side of the UltiController.
- Copy the prepared model file made with Cura in the memory card.
  - The prepared model file (.gcode) is saved in the same folder with original file (.stl).
- Insert the memory card back into Ulticontroller.
- Start printing.
  - UltiController: Menu → Card Menu → Select the correct file

***N.B.*** *Extrude a small amount of filament from the nozzle by turning the gear just before the nozzle temperature has reached the printing temperature in order to ensure that the nozzle is filled with filament.*

***N.B.*** *If some problems occur during printing, select Menu → Stop Print, disable the stepper motors by selecting Menu → Prepare → Disable steppers, lower the printing bed a few centimeters by turning the lead screw by hand, and clean up the filament from the nozzle and the printing bed with trowel. Start printing from beginning if necessary.*

***N.B.*** *The usage of UltiController is explained in more detail in Chapter 10.*

## 6.3. Measures after printing

- The filament reel can be either left on the printer or removed if necessary (see Chapter 6.1.1).
- Close the Cura program.
- Remove damaged/dirty tapes and replace them with new ones (see Chapter 6.1.2).
- Open the material feeder.
- Turn off Ultimaker.
- Turn off the computer.
- Clean the working environment.

# 7. Maintenance

- Functionality check of the printer weekly.
- Calibration of the printer monthly (Chapter 8).
- Ordering of spare parts when needed and installation.

***N.B.*** *The assembly guide for Ultimaker can be found online from http://wiki.ultimaker.com/Mechanics_build_guide*

# 8. Calibration

***N.B.*** *More information about the calibration can be found online from http://wiki.ultimaker.com/Calibrate*

**Aligning the axes**

Lower the printing bed until there is a couple of centimeters of space between the nozzle and the bed. When the axis are aligned correctly, the extrusion head can be moved manually by pushing/pulling the two sliding blocks of each axle separately. (Sliding blocks are at the end of the x- and y-axis). If there is a lot of resistance, the axis are not probably aligned correctly. Alignment can also be checked by measuring the distances between the axis and the frame. The axis should have equal distances from the frame on the both ends and the axes should have aligned like a cross (+). That means that when the left sliding block moves, the right sliding block moves in the exact same position but on the opposite end of the axle.

If alignment is necessary, loosen all eight belt tensioners attached on the sliding blocks. Loosen also the screws on the sliding blocks that are tightening the timing belts. Loosen then the pulleys that have the timing belts around themselves. The best way to align the axis is to use some sort of a rigid tool or object that can be held between the axis and the frame. This should be done on the both sides of the axis (left and right or front and back). Tighten the pulleys without moving them or the axis out of place. Tighten the screws on the sliding blocks. Tighten the timing belts with belt tensioners (see the section Belt tensioning). Also a small amount of very fine oil can be added on the axes around the frame. The x- and y-axes are self lubricating and do not need any oil.

**Belt tensioning**

The timing belts can be tensioned with belt tensioners attached on the both sides of the sliding blocks. The tension is correct when there is an 4-6 mm opening between the both sides of the belt when trying to make the sides touch each other.

**End stops**

The end stops (or limit switches) are meant to give a signal to the extrusion head when it has reached the end of the printing bed. Some sliding blocks have a lever that triggers these end stops. The end stops for x- and y-axis are aligned correctly during the Ultimaker assembly and only the screw tightness of those end stops should be checked time to time.

The top z-switch has to be adjusted if a different kind of nozzle is installed. This switch is for homing the bed until it is elevated to the home position. The home position means that there is no distance anymore between the bed and the nozzle. The top z-switch is located in the left back side inside Ultimaker.

Loosen the two bolts slightly so the end stop can be moved up and down. Turn the lead screw to elevate the printing bed until the nozzle almost touches the printing bed. Adjust the end stop so that the switch clicks and fasten the two bolts. Recheck the z-position by manually moving the bed up and down. The switch should click just before the nozzle touches the bed.

**Bed leveling**

Bed leveling is explained in the Chapter 6.1.3.

# 9. Cura 13.04 instructions

## 9.1. General use

In the main window of Cura there are several buttons that can be selected:

By pressing Load button it is possible to select a file wished to be printed (the .stl file format). The selected file shows up on the platform. Loading of the file may take a while depending on the size of the file.

By pressing Prepare button a model is prepared by the software into a toolpath before it can be printed. This toolpath contains the actual instructions for the machine. Depending on the model and settings the preparation process can take from seconds up to several minutes.

By pressing Print button it is possible to print the prepared model if the printer is connected to the computer with the USB cable. Pressing this button opens up the printing window (see also Chapter 6.2).

Cura has different 3D view modes. Normal view displays the model in a solid color with nothing special. This is the default view. Transparent view allows to inspect the internals of the model. X-Ray view displays the model in blue, except for holes or extra faces inside the model. The red parts indicate errors in the model. Overhang view displays the model the same way as the normal view, except for the parts that have a steep angle. These parts are shown in red and require support during printing. Layers view displays the actual toolpath that will be printed by Ultimaker. The toolpath can be inspected layer by layer by moving the white square up and down along the grey bar located on the right corner of the main window.

It is possible to rotate the object in three different directions when this button is selected. Those directions are displayed as round lines and can be moved by keeping the left mouse button pressed down on top of the line. Lay flat button turns the object so that the part section touching the printing bed is flat. Orientation of the object can also be reset with Reset button.

By selecting Scale button it is possible to change the model dimensions in x-, y- and z-directions. The model can be scaled by percentage or length. When the padlock is closed, all the values will change in relation to each other. When the padlock is opened, values can be changed separately. By pressing To max button the object is scaled up as large as possible. Scaling can also be reset with Reset button.

By selecting Mirror button, the x-, y-, and z-axis of the object can be mirrored.

## 9.2. Quickprint settings mode

Quickprint settings mode can be selected by choosing Tools → Switch to quickprint. These settings are explained in Chapter 6.2.

## 9.3. Full settings mode

Full settings mode can be selected by choosing Tools → Switch to full settings. There are four settings tabs: Basic, Advanced, Plugins, Start/End-GCode.

***N.B.*** *Also by placing the mouse cursor on top of the setting it is possible to get information about that setting.*

**Basic tab**

Basic settings have the most impact on the end result and printing quality.

- *Layer height:* The thickness of each layer. This is the most important setting for the printing quality and printing time. 0.2 mm is for a low quality print and 0.1 mm for a high quality print. Also thinner layers can be printed when the printer is calibrated perfectly.

- *Wall thickness:* The thickness of the outside walls. The thickness of 0.8 mm gives good results, but for small prints 0.4 mm is better. Increasing the thickness improves the strength of the part. The wall thickness should be a multiply of the nozzle size.

- *Enable retraction:* The retraction means pulling the filament back when moving over a gap in the print. This reduces the amount of thin lines between printed sections of the part. These thin lines are called strings. The retraction should be always enabled, unless a material does not allow the retraction.

- *Bottom/Top thickness:* Controls the outer shell thicknesses of the top and bottom surfaces (how many layers are fully filled). Setting it higher gives a stronger part, setting it lower gives a weaker part. 0.6 mm gives strong enough parts without holes. This value has meaning only when printing porous parts (not fully solid parts).

- *Fill density:* Cura fills the internal parts of the model with a specific structure. The amount of infill is influenced by this setting. More infill produces stronger parts that take longer to print and vice versa. If high strength is not a requirement, this setting can be put on 20%.

- *Print speed:* Controls how fast the printer prints. The default of 50 mm/s is a decent speed for Ultimaker and gives good quality prints. For very small and detailed parts even lower speeds should be used. Even speeds over 100 mm/s can be attained with the well calibrated and tuned machine.

- *Printing temperature:* This setting has a lot of impact on the print. The printing temperature depends on the printing speed and filament material. The faster the speed, the higher the temperature. The default value for PLA is 220°C and for ABS 260°C. Lower temperatures reduce the stringing effect.

- *Support type:* Supports are structures printed around and inside of the prints to support areas that would otherwise collapse. Supports need to be removed after printing.

  There are three options: None, Exterior only, Everywhere. None does not do any support. Exterior only creates support where the support structure will touch the printing bed. Everywhere creates support even on the insides of the model.

- *Add raft:* A raft is a few layers of crossing lines printed below the part. A raft helps keeping the part attached on the printing bed and thus prevents warping. For PLA, a raft is not usually needed. For ABS, it is almost always required.

- *Filament diameter:* The diameter of the filament up to two decimals. Correct diameter improves the printing quality. The Ultimaker filament has an average diameter of 2.89 mm.

- *Packing density:* Some filaments compress or lose material during printing. The packing density is a correction factor for the filament. For PLA the correct value is 1.00 and for ABS 0.85.

**Advanced tab**

Advanced settings are usually changed only when there are special needs that do not match with the default settings.

- *Nozzle size:* The size of the nozzle hole. The default Ultimaker nozzle is 0.4 mm.

- *Skirt:* The skirt is the line(s) printed around the part before the first layer of the part is printed. The skirt helps to prime the extruder by filling the nozzle with filament. It also helps in detecting if the printing bed is out of level. Line count setting defines the amount of lines printed around the part. Setting this to 0 will disable the skirt. Start distance setting defines the distance between the skirt and the first layer.

- *Retraction:* Speed setting defines the speed at which the filament is retracted (pulled back) when the extrusion head moves over holes. A higher speed works better, but a very high speed can lead to filament grinding. Distance setting defines the amount of the filament in mm that is retracted. With PLA 4.5 mm gives good results. Other materials may need different retraction settings.

- *Travel speed:* The speed at which the printer moves when it is not printing. The default value is 150 mm/s. With a well calibrated and tuned Ultimaker travel speed of 300 mm/s can be achieved. Too high travel speed may cause the machine miss steps.

- *Bottom layer speed:* Print speed for the bottom layer. The first layer sticks better to the printing bed when it is printed with slower speed.

- *Minimal layer time:* The minimum time spent on printing a single layer. This ensures that a layer is cooled down and solid enough before the next layer is put on top.

- *Enable cooling fan:* For PLA the cooling fan should be enabled to improve the printing quality. For some other materials the cooling fan can be disabled.

- *Initial layer thickness:* The thickness of the first layer. The default value is 0.3 mm. A 0.3 mm layer makes sticking to the printing bed easier. When set to 0.0 the initial layer thickness will be the same as the other layers.

**Plugins**

Plugins are addons for Cura that can add features that are otherwise missing. By default Cura comes with a plugin to set a pause at a certain height. More plugins can be found at the CuraPlugin web page.

**Start/End-Gcode**

Start-Gcode and End-Gcode are pieces of code that influence the start and end procedures of printing. This code can be customized, but editing requires knowledge of Gcode.

# 10. UltiController instructions

UltiController (Figure 17) has a LCD screen and a black navigation button. Scrolling up and down in the menus happens by turning the button. Selecting and switching between the menus happens by pushing the button.

**Watch menu**


***Figure 17.*** *UltiController.*

There are two temperature values in the first row. The first value is the actual temperature of the nozzle. The second value is the temperature Ultimaker is aiming to.

x-, y- and z-positions in mm can be seen in the second row. When the printer head is in the home position, all the values are zeros.

The first thing in the third row is FR, feed rate. The default value is always 100%. By turning the button, feed rate either increases or decreases. This involves all speeds; perimeter, infill and minimal layer speed. The faster the print speed is the faster the filament will be extruded from the nozzle. The second thing on the third row is SD---% and it keeps track of how far the print is. This indication is not based on time, but on the amount of layers. The third thing is time spent on a current print.

***N.B****. If the print speed is increased, also the printing temperature should be increased and vice versa.*

The fourth row tells a state of the printer. When Ultimaker is turned on there is a note “Ultimaker Ready”. When the SD card is inserted there is a note “Card inserted”, and when it is removed there is a note “Card removed”.

**Main menu**

The main menu can be accessed by pressing the button once. By selecting “Watch” it is possible to return to the watch menu. In the main menu there are three submenus: Prepare, Control, Card Menu.

**Prepare menu**

*Disable steppers:* With this function the stepper motors can be disabled. It allows moving the extrusion head and printing bed without resistance from the motors.

*Auto home:* Auto home sends the extrusion head to the auto home position. The home position is in the front left corner of the printing bed.

*Preheat PLA:* The hot end will heat up to 210°C.

*Preheat ABS:* The hot end will heat up to 250°C.

*Cooldown:* Temperature drops to room temperature. This may take a while.

*Move Axis:* Selecting “Move axis” opens another sub-menu which allows moving the axis around. By moving 10 mm at a time it is possible to move x- and y-axis. By moving 1 mm or 0.1 mm at a time it is possible to move x-, y-, and z-axis as well as extrude filament either 1 mm or 0.1 mm. (Extrusion will only work when the printer head is heated at least to 180°C.)

**Control menu**

*Temperature menu:*

> *Nozzle:* A desired temperature can be set for the nozzle.
>
> *Fan speed:* The speed of the fan can be changed (0-255).
>
> *Preheat PLA Conf / Preheat ABS Conf:* Preheat settings for PLA and ABS can be configured. These include the fan speed and nozzle temperature. Changes can also be saved.

*Motion menu:* In this menu it is possible to change acceleration, speed, and accuracy settings of the x-, y- and z-motors.

*Store memory:* With Store memory it is possible to save changed settings.

*Load memory:* With Load memory it is possible to load saved settings.

*Restore failsafe:* Restore failsafe will reset UltiController to its original settings.

*Firmware version:* Tells the current firmware version of Ultimaker.

**Card Menu**

In the card menu all the .gcode files on the SD card will be visible. By selecting a file, printing will start. At first the hot end will heat up to the printing temperature.

**Tune Menu**

When the print has been initiated, one option in the main menu will change. Instead of “Prepare” there will be “Tune”. In the tune menu it is possible to live tune the printer during printing.

*Speed:* Changing this has a same effect than turning the button in the watch menu (changing FR).

*Nozzle:* The temperature of the hot end can be changed.

*Fan Speed:* The speed of the fan can be changed.

*Flow:* Flow allows increasing or decreasing the amount of filament that is being extruded from the nozzle. This may be useful when there is either over- or underextrusion with current settings.

***N.B.*** *Over- or underextrusion usually indicates to hardware problems and/or that there is something wrong with the initial printing settings.*

There are also two other new options in the main menu: With ”Pause Print” the printing can be stopped temporarily at a certain point. With ”Stop Print” the printing will be stopped and cancelled.

***N.B****. ”Stop Print” only stops printing. The cooling fan will continue cooling and the hot end temperature will remain at the printing temperature. For that reason, the printer should be restarted if something is not printed immediately after stopping the print.*